CORROSION BEHAVIOR INVESTIGATION OF MARINE GRADE MILD STEELS IN THE BAY OF BENGAL WATER ENVIRONMENT

KHALID AHMED (SN. 0420240007)

A Thesis Submitted in Partial Fulfillment of the Requirements for the Degree of Master of Science in Department of Naval Architecture and Marine Engineering

DEPARTMENT OF NAVAL ARCHITECTURE AND MARINE ENGINEERING
MILITARY INSTITUTE OF SCIENCE AND TECHNOLOGY
DHAKA, BANGLADESH

DECEMBER 2024

CORROSION BEHAVIOR INVESTIGATION OF MARINE GRADE MILD STEELS IN THE BAY OF BENGAL WATER ENVIRONMENT

M.Sc Engineering Thesis

By

KHALID AHMED (SN. 0420240007)

Approved as to style and content by the Board of Examination on 07 December 2024.

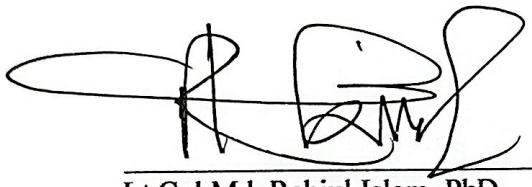

Lt Col Md. Rabiul Islam, PhD
Associate Professor of Naval Architecture and Marine Engineering Department, MIST, Dhaka

Chairman (Supervisor)
Board of Examination

Dr. Md. Shahidul Islam
Professor of Bangladesh University of Engineering and Technology (BUET), Dhaka

Member (External)
Board of Examination

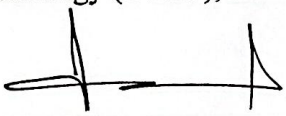

Dr. S M Ikhtiar Mahmud
Assistant Professor of Naval Architecture and Marine Engineering Department, MIST, Dhaka

Member
Board of Examination

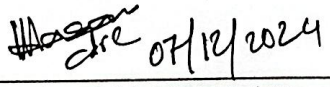

Commodore Md. Mohidul Hasan
Senior Instructor of Naval Architecture and Marine Engineering Department, MIST, Dhaka

Head of Department
Member (Ex-Officio)

Department of Naval Architecture and Marine Engineering, MIST, Dhaka

CORROSION BEHAVIOR INVESTIGATION OF MARINE GRADE MILD STEELS IN THE BAY OF BENGAL WATER ENVIRONMENT

DECLARATION

I hereby declare that the study reported in this thesis entitled as above is my original work and has not been submitted before anywhere for any degree or other purposes. Further I certify that the intellectual content of this thesis is the product of my own work and that all the assistance received in preparing this thesis and sources have been acknowledged and/or cited in the reference Section.

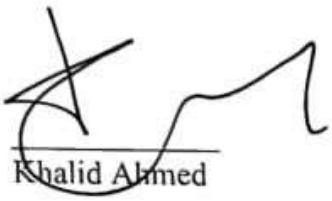

Khalid Ahmed

Department of Naval Architecture and Marine Engineering
Military Institute of Science and Technology (MIST), Dhaka

CORROSION BEHAVIOR INVESTIGATION OF MARINE GRADE MILD STEELS IN THE BAY OF BENGAL WATER ENVIRONMENT

A Thesis

By

Khalid Ahmed

DEDICATION

In memory of Commodore M Muzibur Rahman (E), psc, PhD, BN (Retd),
my teacher and initial supervisor, without whose wisdom and guidance the completion of this thesis and my MSc in Engineering would not have been possible.
This work stands as a tribute to his legacy.

ABSTRACT

CORROSION BEHAVIOR INVESTIGATION OF MARINE GRADE MILD STEELS IN THE BAY OF BENGAL WATER ENVIRONMENT

The corrosion behavior of marine-grade mild steels in seawater environments is a critical factor influencing the maintenance and longevity of marine structures such as vessels, offshore platforms, and coastal installations. Despite extensive research in various oceanic regions, the specific challenges posed by the Bay of Bengal (BoB) have not been fully explored, particularly for marine-grade steels. These steels, distinct in their alloying elements, may exhibit unique corrosion behaviors in the BoB's dynamic and chemically complex environment. This study aims to address this gap by investigating the corrosion behavior of two types of marine-grade mild steels, Grade A and Grade 907, under both static and dynamic conditions. The research employed laboratory-based experiments using gravimetric and electrochemical methods to measure corrosion rates of seamless and welded steel samples. These samples were immersed in seawater collected from multiple BoB locations, with exposure times ranging from initial immersion to extended submersion. Additionally, mechanical testing, including tensile strength and hardness assessments, was conducted to evaluate the degradation in material properties due to corrosion. Microstructural analysis using Optical and Scanning Electron Microscopy (SEM) revealed significant changes in the crystalline structure of the steel samples, indicating the extent of corrosion damage. Results indicate that dynamic conditions significantly accelerate corrosion rates, especially in deeper regions of the BoB, where the corrosion activity was higher than in coastal areas. Welded samples exhibited greater susceptibility to localized corrosion, suggesting a need for enhanced protective measures in these areas. The mechanical tests revealed a measurable reduction in hardness and more pronounced corrosion-induced damage in welded joints, highlighting the need for enhanced protection strategies in these marine areas. These findings highlight the necessity for region-specific corrosion protection strategies tailored to the unique environmental conditions of the BoB. By concentrating on the water composition of the Bay of Bengal, solutions to reduce corrosion in marine-grade mild steels particularly in this region can be developed. Also, a wider understanding of corrosion behavior in marine environments will come out.

সারসংক্ষেপ

CORROSION BEHAVIOR INVESTIGATION OF MARINE GRADE MILD STEELS IN THE BAY OF BENGAL WATER ENVIRONMENT

বিভিন্ন ধরনের মেরিন স্ট্রাকচার যেমনঃ জাহাজ, অফশোর ও উপকূলীয় স্থাপনাদি ইত্যাদির দীর্ঘস্থায়িত্বের উপরে, সমুদ্রের পানিতে মেরিন গ্রেড মাইল্ড স্টিলের মরিচার প্রকৃতি ও বৈশিষ্ট্যের গুরুত্বপূর্ণ প্রভাব রয়েছে। এ বিষয়ে বিভিন্ন সাগর-মহাসাগরীয় অঞ্চলে বিশদ গবেষণা করা হলেও বঙ্গোপসাগরে এর প্রকৃতি কেমন, বিশেষত মেরিন গ্রেড এর ক্ষেত্রে তা কেমন এটি এখনো কোন গবেষণার মাধ্যমে বের করা হয়নি। সংকর ধাতু হিসেবে মেরিন গ্রেড মাইল্ড স্টিলের গঠনগত উপাদান ভিন্ন ও স্বতন্ত্র। বঙ্গোপসাগরের গতিশীল ও রাসায়নিকভাবে মিশ্র পরিবেশে এ ধরনের ধাতু একদমই ভিন্ন ও স্বতন্ত্র ধরনের মরিচার প্রকৃতি ও বৈশিষ্ট্য প্রদর্শন করার সম্ভবনা রয়েছে। এ কারণে বর্ণিত বিষয়ে গবেষণার বর্ণিত ঘাটতি দূর করাই এই গবেষণাটির মূল লক্ষ্য। এটি করার জন্য এই গবেষণা সমুদ্রের পানির স্থীর ও গতিশীল উভয় পরিস্থিতিতে মেরিন গ্রেড মাইল্ড স্টিলের ০২ (দুই) টি ধরণ- এমএস গ্রেড 'এ' ও এমএস গ্রেড '৯০৭' কী ধরনের মরিচার প্রকৃতি প্রদর্শন করে তা নির্ণয়ের চেষ্টা করেছে। এই গবেষণায় গবেষণাগার ভিত্তিক ২ ধরনের পরীক্ষা, ওজনভিত্তিক ও তড়িৎ রাসায়নিক পদ্ধতির প্রয়োগ করা হয়েছে। এর দ্বারা ওয়েল্ডিং জয়েন্টসহ ও ওয়েল্ডিং জয়েন্ট ছাড়া এই উভয় ধরনের নমুনায় মরিচার ধরন পরীক্ষা করা হয়েছে। বঙ্গোপসাগরের বিভিন্ন স্থান হতে সংগৃহীত সমুদ্রের পানিতে নমুনা স্টিলগুলো নিমজ্জিত করে রাখা হয়েছিল। সমুদ্রের পানিতে স্টিলগুলো প্রারম্ভিক নিমজ্জনকাল থেকে শুরু করে দীর্ঘমেয়াদী সময় পর্যন্ত নিমজ্জিত রাখা ছিল। এছাড়াও মরিচার কারণে স্টিলের নমুনাগুলোর পদার্থগত বৈশিষ্ট্যের কী ধরনের ক্ষয় হয়েছে তা নির্ণয়ে বিভিন্ন মেকানিক্যাল টেস্টিং যেমনঃ প্রসার্য দৃঢ়তা, কঠোরতা ইত্যাদি ব্যবহৃত হয়েছে। সাধারণ অপটিক্যাল ও স্ক্যানিং ইলেকট্রন এ উভয় ধরনের মাইক্রোস্কোপ ব্যবহার করে পদার্থের আণুবীক্ষণিক বিশ্লেষণ করা হয়েছে। এতে স্টীলের নমুনাগুলোর কেলাস বিন্যাসের লক্ষনীয় পরিবর্তন দেখা গিয়েছে। যার মাধ্যমে মরিচার মাত্রা সম্পর্কে ধারণা পাওয়া যায়। এছাড়াও পরীক্ষার ফলাফলে সমুদ্রের পানির গতিশীল অবস্থাকে মরিচা ধরার হারকে বিশেষভাবে ত্বরান্বিত করতে দেখা গিয়েছে। বিশেষত, উপকূলীয় অঞ্চল এর তুলনায় গভীর সমুদ্রের যে স্থানে মরিচার সক্রিয়তা বেশি সেই ধরনের স্থানে পূর্বে বর্ণিত বিষয়টি অধিক মাত্রায় সক্রিয় ছিল। ওয়েল্ডেড নমুনাগুলো স্থানীয় মরিচার ক্ষেত্রে অধিক সংবেদনশীলতা প্রদর্শন করেছে এবং এর মাধ্যমে এ ধরনের ক্ষেত্রে অধিকতর সংরক্ষণমূলক ব্যবস্থা গ্রহণের প্রয়োজনীয়তা অনুভূত হয়েছে। ওয়েল্ডিং জয়েন্টগুলোর মেকানিক্যাল টেস্টে লক্ষণীয় মাত্রায় কঠোরতার হ্রাস এবং মরিচাজনিত সুস্পষ্ট ক্ষয় দেখা গিয়েছে। যা এ ধরনের মেরিন এলাকাতে আরো ভাল মরিচারোধী ব্যবস্থার প্রয়োজনীয়তার জানান দেয়। বঙ্গোপসাগরের অনন্য প্রাকৃতিক পরিবেশের জন্য আলাদাভাবে এই ফলাফলসমূহ এলাকা-ভিত্তিক মরিচারোধী কৌশল প্রণয়নের উপরে গুরুত্বারোপ করে। বঙ্গোপসাগরের পানির উপাদানসমূহ পর্যালোচনা করে এই এলাকাতে মেরিন গ্রেড মাইল্ড স্টিলের মরিচা রোধে কী করণীয় তা নির্ধারণ করা সম্ভব হবে। এছাড়াও এই গবেষণার ফলাফল দ্বারা মেরিন পরিবেশে মরিচার প্রকৃতি সম্পর্কেও একটি বিশদ ধারণা পাওয়া যাবে।

ACKNOWLEDGEMENTS

I am deeply thankful to Almighty Allah for His blessings , which have been the driving force behind the completion of this research. I am grateful to late Commodore M. Muzibur Rahman, my initial supervisor, whose invaluable guidance and support significantly contributed to this work. I am also deeply thankful to Commodore M Mohidul Hasan, Head of the Department of Naval Architecture and Marine Engineering, MIST, for his unwavering support. I would like to express my profound appreciation to my supervisor, Lieutenant Colonel Rabiul Islam, whose constant supervision, motivation and insightful advice were crucial to the completion of this thesis.

I am also indebted to the Bangladesh Navy for providing vital resources, including laboratory facilities and seawater collection support. I would like to express my sincere gratitude to Commodore A B M Shamsul Alam for his invaluable encouragement and support, which greatly contributed to the successful completion of this research.

I am grateful to Lieutenant Commander Mohammad Nazmul Basher, Lieutenant Commander Md Hasanuzzaman, Lieutenant Commander Md Imran Sarker and Lieutenant Commander Samiul Islam for their assistance throughout the research.

I would like to acknowledge the technicians of the Ship Instrument and Ship Structure Lab of the NAME Department—Mr. Nahid Hasan Shuvo, Mr. Minhajur Rahman and Mr. Jaber Hossain along with Mr. Md. Shafiqur Rahman, the technician of the Materials Lab of ME Department, for their expert technical support and invaluable help during my research.

Lastly, I owe immense gratitude to my wife and sons for their unyielding sacrifice, patience, and unwavering support, which enabled me to focus on my research.

TABLE OF CONTENTS

LIST OF FIGURE

LIST OF TABLE

LIST OF SYMBOL/NOTATION

Symbol	Description	Units
A	Exposed surface area of the specimen	cm^2
ΔW	Weight loss of the specimen	g
CR	Corrosion rate	mm/year
ρ	Density of the material	g/cm^3
T	Immersion time	hours
Icorr	Corrosion current density	$\mu A/cm^2$
Ecorr	Corrosion potential	V
K	Unit conversion factor	Dimensionless
pH	Acidity/alkalinity level	--
DO	Dissolved oxygen concentration	mg/L
Cl^-	Chloride ion concentration	mg/L
SO_4^{2-}	Sulfate ion concentration	mg/L
TDS	Total Dissolved Solids	g/L
TSS	Total Suspended Solids	mg/L
HV	Vickers Hardness	--
BHN	Brinell Hardness Number	--
UTS	Ultimate Tensile Strength	MPa
W_o	Initial weight of the specimen	g
W_f	Final weight after immersion	g
θ	Contact angle	Degrees
σ	Stress	MPa
ε	Strain	--
P	Load applied during tensile testing	N
D	Diameter of indenter (Brinell Hardness Test)	mm
t	Time duration of exposure	seconds
F	Force applied	N
V	Voltage	Volt
OEM	Optical Electron Microscope	--
SEM	Scanning Electron Microscope	--

CHAPTER ONE
INTRODUCTION

1.1 Preamble

Material degradation is a significant contributor to system failures, with surface degradation, particularly corrosion, being a major reason. While precise global statistics can vary, it is widely acknowledged that corrosion alone causes substantial economic losses annually. By understanding the mechanisms and impacts of material degradation, engineers and scientists can develop effective strategies to mitigate these failures and improve the reliability of systems. This research aims to explore the intricacies of material degradation, focusing on the role of surface phenomena and corrosion processes.

Metals are usually extracted as ores from mine. But pure metals are brittle and tend to return to chemically stable forms. This causes materials to degrade over time because of chemical or electrochemical reactions and corrosion.

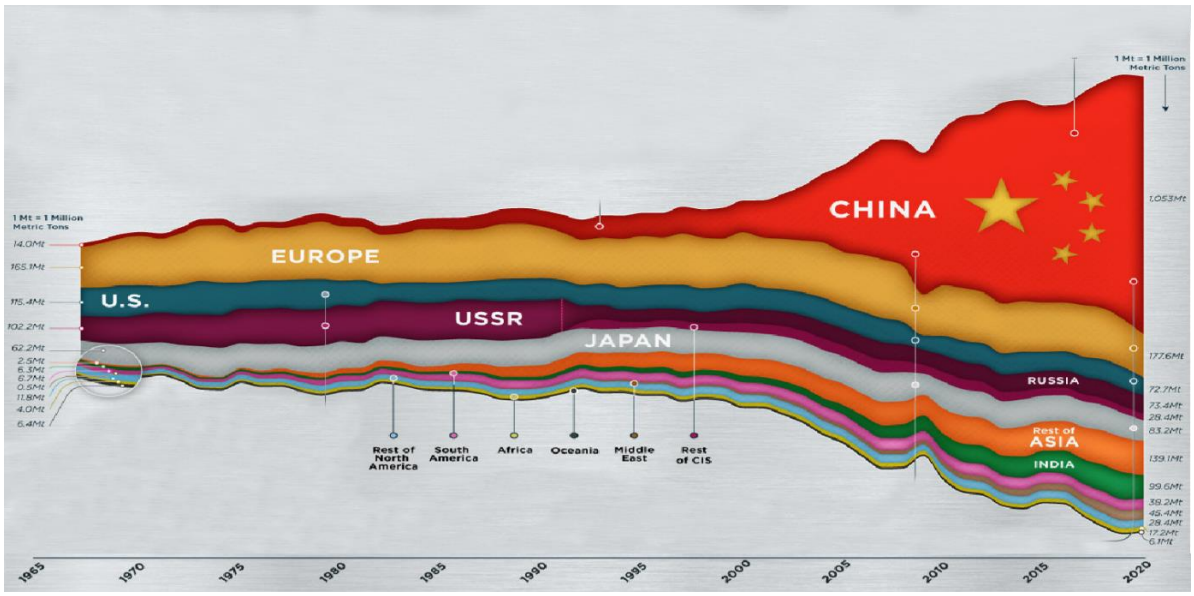

Figure 1.1: Worldwide iron production from the year 1965-2020.

Iron has played a pivotal role in civilization since it replaced bronze, marking the beginning of the Iron Age. Iron is the most commonly used metal in the world and, from an economic standpoint, is the most valuable metal due to its high demand, surpassing that of gold and diamonds. Being the most abundant element on our planet, it is widely recycled. It also helps in the production of blood in human bodies.

The above infographic (Figure 1.1) shows worldwide iron production from the year 1965-2020 (Dyczko, 2023). The largest iron ore mine in the world is the Kiruna mine in Sweden, which produces more than 950 million tonnes of iron ore. Carbon steel or stainless steel usually contains up to 2% carbon, and small amounts of manganese, sulfur, phosphorus and silicon. Alloys containing varying amounts of other metals are used in special applications depending on the composition of the alloy.

Corrosion is the gradual deterioration of materials, particularly metals, due to chemical interactions with their environment. This process weakens structures such as bridges, buildings and vehicles which can lead to catastrophic failures resulting in a loss of life or injury. Corrosion has a significant economic impact because it requires constant maintenance, repair and replacement of the affected materials leading to heavy financial losses. Besides, corrosion can be very dangerous as it causes accidents such as pipeline leaks or even structural collapses that put both human lives and the natural environment at risk. It also reduces machinery efficiency by causing friction, blockage or malfunctioning equipment. Beyond these practical concerns, corrosion can damage the aesthetic appeal of surfaces further stressing the importance of preventing and managing this pervasive problem.

The grade of steel refers to a classification system that defines the properties and composition of different types of steel. It is a specification to which the characteristics of strength, hardness, ductility, and chemical makeup are specified, for the application it's intended for, and with it, the grade of steel. Many times, steel grades are arranged by organizations that control standards, one example being ASTM, ISO, or EN, in regard to a combination of letters and numbers. These names provide information on alloying material, mechanical properties, and the purpose of the material. For instance, the grade designations in carbon steel could be related to the carbon content of the alloy, while the classification of stainless steel grades generally will be with respect to the chrome and nickel content of the alloy that adds to corrosion-resistant properties. Knowing steel grade assists the selection processes in terms of construction, manufacturing, and engineering.

Marine-grade steel is specifically designed for use in ships and offshore structures due to its high corrosion resistance. These steels are classified under various standards, such as "AH36" or "EH36" in the American Bureau of Shipping (ABS) or Lloyd's Register, which are commonly used for shipbuilding and other marine applications. Seawater, a

strong electrolytic solution, varies in composition across different oceans, leading to varying corrosion behaviors of marine-grade metals in different parts of the world.

1.2 Background

Since ancient times, people have been working to utilize sea and steel. The use of steel hull vessels in seawater began approximately 200 years ago (Hillstrom, 2005). During the last two centuries, many developments have occurred in the construction of ships, and the mild use of steel has taken a major share worldwide (Warren, 1998). However, one of the major challenges in maintaining hulls and machinery is material degradation due to corrosion in contact with seawater. Overall, marine corrosion affects the lifetime of steel plates and, subsequently, various marine vessels and structures. Therefore, it has a significant economic impact on the maritime world.

According to the chemical composition, many grades of mild steel plates are available for the construction of ships. On the other hand, welding is the modern and commonly used method for joining the steel plates to build any structure. Therefore, the effect of marine corrosion on mild steel varies from unwelded to welded steel. In addition, the seawater composition varies from sea to sea, which affects the corrosion rate of mild steel plates in various ways (Valdez et al., 2016). The impact of local conditions on marine corrosion is significant. Factors such as ship type and ships' location also influence the geometry and rate of marine corrosion.

In recent decades, the use and importance of sea-based activities has increased significantly due to the growing demand for marine resources, global trade, and the strategic importance of maritime routes. Additionally, advancements in technology have enabled more efficient exploration and exploitation of ocean resources (Rahman, 2017). Owing to the mechanical strength, high machinability, weldability, and reasonable cost, mild steel is commonly used in seawater, especially as a structural material for marine vessels, offshore drilling towers, piling for piers and docks, etc. However, mild steel is highly corrosive to seawater (Chuka et al., 2014). This affects the life expectancy and maintenance of marine vessels. The underwater hull of marine vessels and other marine platforms is the most vulnerable part to corrosion, as it is supplied with a good amount of O_2. The factors that affect the rate of corrosion in seawater are physical, mechanical, chemical, or biological owing to seawater content, relative velocity, temperature

variation, etc. Seawater content, such as salinity, dissolved O_2, sulfate, and chloride, varies from ocean to ocean, which causes variations in corrosion behavior (Rahman, Ahmed and Kaiser, 2020a).

Various types of corrosion occur in marine structures, vessels, and objects that are composed of mild steels exposed to seawater. Corrosion can manifest in various forms depending on the environment and material involved. Some common types include: uniform corrosion, pitting corrosion, galvanic corrosion, crevice corrosion, intergranular corrosion, stress corrosion cracking etc. General attack is a form of corrosion which is the most common type of corrosion and sometimes called uniform corrosion. In this type of corrosion, all exposed areas are attacked more or less at the same rate, but the loss of metal is rarely completely uniform over the surface. In this research, this uniform type of corrosion, which can be called general attack also, has been emphasized.

Various studies have been carried out worldwide to evaluate the corrosion behavior of steels, taking into account specific seawater environments, such as the Arabian Sea, multiple locations of the Indonesian Sea territory, coast of South India, and coastal area of Nigeria. In addition, research on the measurement of the corrosion rate of metal alloys and the corrosion behavior of copper alloys in the Bay of Bengal (BoB) environment has also been conducted (Sawant, venkat and Wagh, 1993; Rahman, Ahmed and Kaiser, 2020a). All of these studies have provided distinct findings and observations.

Nevertheless, there is a research gap in the investigation of the corrosion behavior of marine-grade mild steel in BoB water environment. It may be mentioned that marine-grade mild steel contains slightly more alloying elements than its ASTM counterparts. As such, an effort to study the corrosion behavior of marine-grade mild steels in a BoB water environment is considered paramount.

1.3 Motivation

The purpose of this study is to investigate how marine-grade mild steels behave when these are subjected to seawater environment. These steels are suitable for the use in the Bay of Bengal region both safely and economically. Because of the highly corrosion nature of the oceans, improper handling of marine structures may result in high repair expenses, potential hazards, and pollution of the surrounding ecosystem. With the help of

an understanding of the behavior of mild steels in the Bay of Bengal, it is possible to build more durable maritime structures and maintain them properly.

Previous researches have a great contribution to our understanding of the mechanisms and parameters which are keeping their impact on corrosion rates in maritime environments. In their investigation on corrosion behavior of mild steel in saltwater environments, Sundjono et al. (2018) and Malik et al. (1999) highlighted crucial factors that affect the corrosion behavior. Rahman, Ahmed and Kaiser (2022) highlighted the importance of material-specific correlations in this region by investigating the corrosion behavior of solder-affected copper in the Bay of Bengal.

Li, Li and Hou (2000) examined how various offshore seabed sediments affected steel corrosion, showing how the environment, including the makeup of the seabed, affects corrosion processes. This is very important in the Bay of Bengal as it has some unique environmental characteristics. Zhu et al. (2008) provided insights into the long-term corrosion characteristics of metallic materials in marine environments. These are crucial for understanding the durability of materials exposed to these conditions.

The behavior of corrosion in the Bay of Bengal is significantly influenced by a number of environmental parameters such as salinity gradients, monsoon dynamics, and river discharge. In their studies, Vinayachandran et al. (2012) emphasized the critical role of freshwater outflow, salinity gradients, and ocean dynamics in shaping the environmental characteristics of the Bay of Bengal. These factors indirectly influence the corrosion processes by altering the chemical composition of seawater, thereby affecting the corrosion behavior of materials in this region.

A thorough understanding of these environmental parameters is needed for an accurate assessment of the corrosion behavior of mild steels in this region. In another study, Li et al. (2022) highlighted the necessity of assessing the resistance of marine steel to corrosion in different types of exposure conditions. This study emphasized the significance of specific research for particular maritime environments.

Through research on marine atmospheric corrosion of carbon steel, Alcántara et al. (2017) highlighted the advancements in scientific knowledge and the development of new materials with enhanced corrosion resistance in marine environments.

This study provides insight into the necessary maintenance and life-span of marine-grade mild steels. Therefore, this study is essential because of usage of marine-grade mild steels in the equipment, vessels, and structures exposed to corrosive conditions in the Bay of Bengal. These findings will be beneficial for the infrastructure and industries in this particular region. Combining the results from relevant researches and keeping concentration on the unique obstacles presented by the Bay of Bengal marine atmosphere, researchers can advance the understanding of corrosion mechanisms for mild steels of marine grade, thereby enhancing the endurance and efficiency of steel constructions in this area.

1.4 Literature Review

Driven by a strong interest in the topic and a clear realization of the research gap, numerous scientific articles on the topic were thoroughly reviewed. Scientists have explored how different metals corrode in various water settings. The results of their research are documented in numerous academic publications.

Studies show copper and its alloys, including those affected by SnPb solder resist corrosion in sea-related uses. SnPb solder in copper alloys speeds up corrosion. It boosts the corrosion rate of work-hardened copper by 14% in environments with changing pH levels. Acid solutions at pH1 caused the most damage, while alkaline pH13 environments came second. Rahman also investigated copper corrosion in the Bay of Bengal and discovered that SnPb solder-affected copper exhibits better corrosion resistance than commercial alloys, emphasizing the importance of corrosion allowance for copper products in marine applications (Rahman, Ahmed and Kaiser, 2022).

Comparisons of the corrosion rates of different steels, such as 440C and M50, in artificial seawater by Venkatesh et al. (2022) highlighted the impact of Cl ions on corrosion rates. The role of Cr in enhancing the corrosion resistance of ferrite-pearlite steels in acidic environments has also been reported with emphasis on the formation of protective oxides that will reduce galvanic corrosion effects (Hao et al., 2023). Malik et al. (1999) studied the corrosion behavior of steels in the Gulf seawater environment and found low corrosion rates under severe conditions, thus establishing that protective measures such as coating and cathodic protection are necessary for mild steels.

Muntazir et al. (2019) found that cupronickel alloys and mild steel corrode faster in salty warm seawater due to environmental and microbiological factors. Priyotomo et al. (2019) examined mild steel corrosion in West Java's seawater and noted that corrosion resistance dropped in Karangsong and Eretan seawater, as chloride ions blocked passive film formation. In another study, Usman, Tukur and Usman (2019) compared mild steel corrosion in different water samples and found that seawater caused the most corrosion, followed by effluent and freshwater. Time, temperature, and other physical and chemical factors play a big role in mild steel corrosion. Mild steel corrosion happens when the metal reacts with its surroundings, creating iron oxide (Oluwaseun and Simeon, 2015). Sundjono

Sundjono et al. (2018) exposed mild steel to seawater from Java and Bali and reported uniform corrosion with a resistance that decreased with time. There have always been critical factors, such as dissolved oxygen and chloride ions, inducing risks for corrosion. Few works have been done on the corrosion performance of mild steel in subtropical and tropical regions; these few published studies mainly highlighted the effects of dissolved oxygen, salinity, and temperature effects on its corrosion performance (Al-Moubaraki, Al-Judaibi and Asiri, 2015). Wan Nik et al. (2011) reported that the variation in temperature and salinity affects the corrosion behavior of mild steel in the coastal areas of Kuala Terengganu.

Khan et al. (2020) studied the role of aluminum and zirconium in improving the corrosion resistance of bell metal and obtained results that the alloys formed by mixing these elements in the base alloy improved the corrosion resistance compared to the base alloy. Rahman, Ahmed and Kaiser (2020b) evaluated temperature and flow velocity as variables for corrosion rates; it was found out that an increase in temperature along with flow velocity increased corrosion rate considerably and also proved that corrosion in seawater is three times higher than in river water.

Shikshak et al. (2015) investigated the flow velocity dependence of the corrosion behavior of low-carbon steel in seawater and observed that corrosion rates increased at higher flow velocities until they reached a peak, after which they decreased at high speeds. Apparently, the same study also went ahead to examine changes in corrosion rates correlated with various seawater compositions and identified iron oxide/hydroxide as the significant corrosion products. Li et al. (2019) examined the corrosion behavior of X65

steel in various hydrostatic pressures and showed that with an increase in pressure, there is an increase in the corrosion rate as a result of changes in the corrosion products.

Fujiwara et al. (2020) evaluated the performance of sodium nitrite and sodium metaborate as inhibitors in reducing carbon steel corrosion in seawater and determined the corrosion rate to be reduced by the additions of both components. Moreover, electrical conductivity reduction and flow velocity increase also reduced the corrosion rates. Paul (2010) utilized genetic algorithms for the prediction of corrosion rate of steel under marine conditions, which, therefore, could give insights for life estimation of marine structures. Valdez et al. (2016) proposed paints and coatings for the protection of marine assets from corrosion and also urged that regulations to avert degradation be developed.

Mild steel is one of the most used engineering, construction, and infrastructure materials because of mechanical strength, formability, weldability, availability, and cost (Adetoro, 2011). It however, easily corrodes in corrosive media, so it needs to be protected either by coating or cathodic protection. Exposure studies by Mariappan et al. (2008) on the corrosion of metals in an industrial marine environment present an investigation into different corrosion behaviors of metals due to marine industrial atmospheres. The corrosion rates for metals depend on variables such as chloride, SO_2, and humidity.

Rahman et al. (2022) studied the tensile properties of welding joints of marine-grade mild steel and concluded that welding reduces the tensile strength and fracture strain; the welded samples were found to fail brittle whereas the seamless samples showed ductile failure. Chuka et al. (2014) conducted experiments on the corrosion of mild steel in five different environments, including acidic and atmospheric conditions, by measuring weight loss and concluded that mild steel is unsuitable for acidic environments but is recommended for atmospheric conditions. Coatings in saltwater of mild steel will retard corrosion in various media; hence, for material screening only, the laboratory immersion test is best at this stage.

Ting, Potty and Liew (2012) investigated marine corrosion of mild steel using the weight loss method. His work was done in Lumut, Malaysia, and looked into the corrosion behavior, models, and environmental parameters. Okpaga (2021) studied the efficiency of the Moringa oleifera extracts on mild steel corrosion in acid. He used weight loss and polarization techniques for corrosion analysis and found that corrosion rates were reduced

by 83% in 1.0M HCl and 78% in NaOH. Eddy et al. (2008) found that Sparfloxacin is an effective inhibitor of mild steel corrosion in HCl. High efficiency was shown by this compound and Sparfloxacin was recommended as an inhibitor for mild steel corrosion.

For estimating corrosion resistance, mild steel was subjected to different methods—which Dorothy et al. (2021) did—including weight loss, polarization, and AC impedance. This research represented the coating on hull plates as protective barrier film, which shifts the corrosion potential and increases the hardness of oil-coated mild steel. Therefore, oil-coated mild steel exhibited better corrosion resistance in seawater. In another work, Rajendran et al. (2022) tested various inhibitors for their corrosion inhibition performance in a marine environment. The obtained results showed that the use of some inhibitor systems increased the resistance of mild steel corrosion. In this work, the natural product inhibitor used is the extract of sandalwood oil, which was found to inhibit the corrosion of mild steel in seawater.

Larrabee (1958) evaluated the corrosion resistance of six steels containing different amounts of nickel, copper, and phosphorous exposed to seawater for one, two, and five years. Ni-Cu-P steels showed greater corrosion resistance when compared with structural carbon steel as a standard material in high-tide conditions. The five-year exposure tests indicated that the steel containing 0.5 percent Ni, 0.5 percent Cu and 0.12 percent P had the greatest resistance of the steels tested. Below low tide, corrosion attack was relatively slight and little affected by steel composition, while pitting corrosion was severe but localized.

The weight loss method quantifies corrosion by measuring the reduction in specimen mass after immersion. Priyotomo et al. (2019) analyzed mild steel corrosion in Indonesian seawater, linking chloride content to corrosion rate. Usman et al. (2019) compared corrosion in seawater, freshwater, and industrial effluents, finding seawater most aggressive. Rahman, Ahmed and Kaiser (2020a) studied Sn-Pb solder-affected copper alloys across pH ranges, showing highest corrosion rates in acidic and basic conditions due to chloride ions. These studies highlight the method’s versatility in diverse environments.

The potentiodynamic polarization technique is a widely used electrochemical method to analyze corrosion behavior and kinetics. Świątkowski et al. (2024) studied thermally

treated activated carbon, highlighting its impact on anodic and cathodic polarization characteristics. Yuan et al. (2024) applied this method to assess corrosion resistance in high-strength steel reinforcement under simulated service conditions, focusing on key parameters such as corrosion potential (*Ecorr*) and current density (*Icorr*). Both studies demonstrate the effectiveness of this method in understanding corrosion processes and material performance.

Seawater is a complex chemical system, and its properties depend on a wide range of factors, including dissolved oxygen, salinity, concentration of minor ions, biological activity, and pollutants (Al-Moubaraki, Al-Judaibi and Asiri, 2015). In its genuine form, the coast and its adjacent areas onshore and offshore are an integral part of the local ecosystems which form gulfs, bays, and estuaries; it sometimes mixes fresh and salty waters (Valdez et al. 2016). All these factors are very important to understand for the corrosion resistance of materials used in marine environments and the implementation of effective protective measures.

These studies provide a pointer toward the corrosion behavior of dissimilar metals under varied-aqua conditions and highlight alloy composition and environmental conditions as significant factors controlling corrosion resistance.

1.5 Objectives and Scopes of this Research

The objectives and scopes of this research are as follows:

(i) To investigate the rate of corrosion (C_R) of marine grade steels in the Bay of Bengal water environment.

(ii) To evaluate the effect of arc welding joints on corrosion of marine Grade A and 907 mild steel.

(iii) To analyze the changes in physical and mechanical behavior of marine grade mild steel due to prolonged immersion in seawater corrosive environment.

1.6 Thesis Outline

A research project that is organized using a framework flow in a methodical manner makes it simple to follow from start to finish. The research comprises seven chapters with each of them looking at different sides of the investigation:

Chapter 1 consists an introduction that has a broad background which includes an in-depth review of literature that helps to connect this study to other existing knowledge. It also describes why the study is being carried out, it's aims, and what influences such a study as well as its importance and possible effects.

Chapter 2 describes the materials and methods used in the study, focusing on MS Grade A and MS Grade 907 steels. It covers sample preparation, seawater collection, and key environmental factors like pH and chloride levels. The chapter outlines the corrosion testing setup and methods for analyzing hardness and microstructure. Equipment and procedures are described to ensure replicability.

Chapter 3 presents the results of corrosion testing on marine-grade mild steels in both static and dynamic seawater conditions. It details the experimental setup for laboratory-based tests, using seawater from the Bay of Bengal and compares corrosion rates between static and dynamic environments. The chapter also covers on-site testing in coastal and deep-sea locations, providing real-world findings of the experimental data.

Chapter 4 explores the mechanical behavior of marine-grade mild steels, focusing on their performance under the corrosive environment of the Bay of Bengal. The investigations include microstructure analysis using OEM and SEM, EDX for elemental composition, chemical composition testing by OES method and mechanical assessments such as hardness and tensile tests. The results reveal the material's reliability and suitability for high-stress applications in marine and industrial sectors.

Chapter 5 investigates the effect of pH variations on the corrosion of marine-grade mild steels. The study examines material performance under acidic, neutral, and alkaline conditions. This provides a detailed understanding of corrosion rates and their implications. This chapter provides valuable information about the durability of the material in diverse marine environments.

Chapter 6 shows the findings from Potentiodynamic Polarization test, including Tafel plots, to determine corrosion parameters such as Icorr, Ecorr and rate of corrosion. The chapter compares corrosion behavior across different time periods (0-day, 1-day, and 3-day), and between welded and unwelded samples, highlighting trends like higher corrosion rates in welded samples and discussing their implications.

Chapter 7 compares experimental results with findings from a real-world case study, providing practical validation of the research. By analyzing real-world applications, this chapter contextualizes laboratory data and highlights the relevance of the findings in marine industry scenarios.

Chapter 8, the final chapter of the work, gives the conclusions that emerged while conducting the study. The chapter provides a comprehensive review of the major findings arising out of the research and provides a concluding section of the work. Recommendations for future research are also provided, highlighting areas that need further study and mentioned the areas of limitaions of the work.

CHAPTER TWO
MATERIALS AND METHODS

2.1 Preamble

This chapter provides a detailed account of the practical steps and compounds used in this research work. All the procedures were normally carried out in such a manner that it could be easily reproduced by other researchers to confirm the result that was arrived at. Due to the given research questions of the present study, the given methodologies were chosen and optimized considering previous advancements and pilot trials.

An explanation of the materials employed in the investigation is provided with regard to properties, source, actual model number, and characteristics that can influence the results of the experiment. The specific information about the materials contributes to the elimination of mistypes and helps to reproduce the experiments. The processes that have been followed during the experiments are also outlined, such as how the experiments were designed as well as methods of preparing the samples for data gathering and analysis.

2.2 Materials

MS or mild steel is a material that is used for the construction of ships across the world and in Bangladesh owing to its cheap, ready availability and good mechanical properties. This material is universal as it fulfills many aspects of shipbuilding starting from structural to functional.

Mild steel consists of various grades, each of which is used to fulfil specific construction requirements. These grades possess unique properties that make them appropriate for different parts of a ship's construction. MS Grade A and MS Grade 907 are widely recognized and commonly used in the maritime industry, with a significant presence in shipbuilding and other marine-related activities. These grades, in particular, have seen extensive use in Bangladesh, where they are favoured for their reliability and performance in the construction of various marine vessels and structures. MS Grade A is used for general construction, particularly in ship construction since it strikes a middle ground between high tensile strength and elongation. On the other hand, MS Grade 907 is preferred for its higher strength and strong operational reliability, for use in the critical

components of vessels. This work focuses on investigating the mechanical and corrosion properties of MS grade A and MS grade 907 to assess their applicability in shipbuilding, especially considering the BoB as an area of operation.

Butt welding holds significant importance in ship construction and is widely employed for the welding of steel plates and sections. Joints formed by butt welding are pivotal components contributing to the structural integrity and longevity of ships. This comprehensive study also investigates the characteristics of butt-welding joints in both MS Grade A and MS Grade 907 materials. The chemical compositions of those areas are shown in table 2.1. It encompasses a thorough assessment of the welding process, the integrity of the welds and the durability of such joint under diverse operational conditions.

Therefore, in this study the mechanical properties of the selected Mild steel grades have been analyzed. After that, the characteristics of the welded joints formed from this material were investigated to evaluate their performance on the operational conditions. The research aims to identify potential improvements in the performance characteristics of various mild steel grades and welding methods, offering valuable information on their effects on the overall durability and structural quality of marine vessels.

Table 2.1 Chemical composition of samples (mass fraction %)

Serial	Elements	MS- Grade A (mass fraction %)	MS- Grade 907 (mass fraction %)
1.	Iron (Fe)	96.9	95.1
2.	Carbon (C)	0.15	0.07
3.	Silicon (Si)	0.15	0.34
4.	Manganese (Mn)	0.26	0.43
5.	Tantalum (Ta)	>0.58	>0.8
6.	Cerium (Ce)	0.24	0.26
7.	Cobalt (Co)	0.13	0.18
8.	Molybdenum (Mo)	0.17	0.18

The material selection process is pivotal to this research as it determines the effectiveness of the mild steel grades and welding methods under the specific conditions of the Bay of Bengal. This study evaluates how different steel grades and welded joints perform in the

corrosive marine environment, aiming to identify the most suitable materials for marine in applications. By analyzing the corrosion resistance, mechanical properties and durability of various mild steel grades, the research will provide recommendations for selecting materials that enhance ship performance and longevity. These findings will guide the selection of materials and welding techniques and support more effective corrosion management, streamline maintenance efforts, and ensure longer-lasting performance of marine vessels in the Bay of Bengal's challenging waters.

2.3 Experimental Details

The study focused on examining the corrosion behavior of the marine grade mild steel immersed in the water of the Bay of Bengal, including both steels with and without butt-welded joints. Since these steels are used widely in marine applications, it is important to know their corrosion behavior in actual marine environments. The operational research techniques used in the research include sample preparation activities, collection of seawater and analysis of the content of seawater as well as methods of corrosion assessment. Following such an elaborate set of experimental procedures, the study seeks to develop a clear picture on the corrosion trend of marine grade mild steels within the Bay of Bengal water environment.

2.3.1 Sample Preparation

MS plates, measuring 6 meters in length and 1 meter in width, were sourced from the local market in the form of metal ingots. These metal ingots were further processed to create the test sample necessary for this study, ensuring the material met the fixed percentage composition required for correction testing. In the initial step, the ingots were carefully cut down to the desired dimensions: 60 mm in length, 15 mm in width and 6 mm in thickness. The precise cutting process took place at the Bangladesh Navy Dockyard in Chattogram.

Figure 2.1: Cutting and sizing of the coupons in BN Dockyard Shop: (a) sample cutting, (b) butt welding of the samples, (c) cutting of welded metals

The process involved a two-step approach: firstly, the plates were cut to rough dimensions in the Platter & Welding Shop. Figure 2.1 illustrates the initial stage, where raw mild steel sheets were cut into standard-sized coupons and the butt welding of the metals were done. After the cutting the metal pieces were refined to the final required size using a CNC cutting machine located in the machine shop of the same dockyard, shown in Figure 2.2.

Figure 2.2: Machining of the coupons in the CNC Cutting Machine of BN Dockyard.

Following the cutting process, the mild steel coupons underwent a detailed polishing procedure at the Metallurgical Laboratory of the Mechanical Engineering Department at MIST (Fig 2.3). This step was essential to create a smooth, uniform surface, ensuring accurate microscopic examination and consistent corrosion testing. Dry polishing was performed first, utilizing silicon carbide (SiC) emery papers provided by the lab, with grit sizes progressing in sequence— 60, 120, 600, 800, 1000, 1200, and 1500. This systematic approach allowed for effective material removal and the creation of a uniform surface finish on the steel coupons. The incremental polishing process ensured that any surface irregularities were eliminated, providing an ideal surface condition for accurate and reliable microscopic examination and corrosion analysis

Once dry polishing was complete, the samples were subjected to wet polishing using alumina paste which further enhanced the surface quality, bringing it to a near mirror-like condition. This final stage of polishing is essential, as a highly polished surface is required for accurate and consistent corrosion testing. Upon completion of the wet polishing, the steel samples were carefully rinsed and dried in the same Metallurgical Laboratory at room temperature, utilizing natural convection. Special care was taken to avoid contamination or oxidation of the freshly polished surface during the drying process; A thorough and meticulous record of each prepared sample was maintained for reference during the subsequent stages of experimental investigation, ensuring all samples were in prime condition for detailed corrosion behavior analysis.

Figure 2.3: Polishing of the Metal Samples.

The finalized samples, polished and dimensioned for uniformity, are presented in Figure 2.4. To ensure accurate identification and tracking of the various metal samples used in this study, a systematic coding system was implemented. Each sample was assigned a unique code that clearly indicated its grade, welding status, and set number. The following methods were adopted:

(i) Grade Designation. The initial letter or numbers in the code represented the grade of the steel. "A" denoted MS Grade A, while "907" or "N" indicated MS Grade 907. This distinction was crucial as it allowed for direct comparison between the two grades and their respective corrosion behavior.

(ii) Welding Status: The letter "W" was appended to the code for welded samples, indicating that they had undergone a welding process. This parameter was essential for investigating the potential influence of welding on corrosion susceptibility.

(iii) Set Number: A numerical suffix, such as "-1," "-2," or "-3," was added to each code to identify the specific set to which the sample belonged. This designation was necessary to track the progress of multiple tests conducted simultaneously and to facilitate data analysis and comparison.

(iv) By adhering to this coding system, it was possible to maintain a clear and organized record of all metal samples used in the study. This ensured that each sample could be easily_identified and referenced throughout the research process, thereby enhancing the accuracy and reliability of the experimental data obtained. For example, the code "AW-2" would represent a sample from the second set, made of MS Grade A steel, and subjected to a welding process.

Figure 2.4: Prepared Sample. Coupons. Dimension: ’60 mm x 15 mm x 6 mm’ following the ASTM guidelines.

2.3.2 Seawater Collection and Analysis

For this corrosion behavior study, about 600 liters of seawater were carefully and hygienically taken from the Bay of Bengal. Figure 2.5 shows the seawater collection process, highlighting the use of clean containers to ensure that the natural properties of the seawater were preserved for the experiments.While collecting the samples, precautions were taken so that the collected water samples would be typical of the marine environment in the region. This large amount of seawater was vital in constantly and

adequately supplying an unlike platform for the immersion of several steel samples for a long period without changing the experimental conditions as they would be in actual field conditions.

Figure 2.5: Collection and Storing of Seawater from Bay of Bengal

After the seawater was collected, its key properties were thoroughly analyzed, as they are crucial for understanding the corrosion processes in marine environments. Several important variables were measured, including pH, Total Dissolved Solids (TDS), Total Suspended Solids (TSS), and Dissolved Oxygen (DO), all of which have a direct impact on the rate and nature of corrosion. The pH level indicates the acidity or alkalinity of seawater, a factor known to significantly influence corrosion rates. TDS quantifies the amount of dissolved substances in the water, while TSS measures the solids suspended in the solution, both of which can affect the electrochemical reactions occurring on the surface of the metal. Dissolved oxygen was also measured, given its vital role in the formation of_rust and other corrosion products. By analyzing these variables, a clear understanding of the environmental conditions affecting the mild steel samples was established, enabling accurate evaluation of the corrosion trends observed throughout the study.

The key parameters studied and their effects on corrosion are as follows:

(i) Dissolved Oxygen (DO). Promotes oxidation, accelerating rust formation and increasing the overall corrosion rate.

(ii) pH. Dictates the acidity or alkalinity of the environment, with lower pH levels typically accelerating corrosion.

(iii) Electrical Conductivity (EC). Reflects the ionic strength of the water, influencing the electrochemical reactions that drive corrosion.

(iv) Total Dissolved Solids (TDS). Indicates the concentration of dissolved salts and minerals, which can increase the corrosion rate by enhancing conductivity.

(v) Total Suspended Solids (TSS). Refers to the solid particles in water that may cause localized corrosion through abrasion or by affecting electrochemical reactions.

(vi) Chloride (Cl): Chloride ions are highly corrosive and can penetrate protective oxide layers on metals, causing pitting and crevice corrosion.

(vii) Sulfate (SO_4^{2-}). Sulfate ions can influence the rate and type of corrosion, often accelerating the process, especially in combination with chloride.

The results of the tests of contents of the collected seawaters are shown in Table 2.2. The study measured several critical parameters essential for understanding the marine water environment's impact on corrosion. The dissolved oxygen (DO) levels recorded at Outer Anchorage, Fairway Buoy, and St. Martin's Anchorage Point were 7.36 mg/L, 7.21 mg/L, and 7.49 mg/L, respectively. These values fall comfortably within the Bangladesh Inland Surface Water standard range of 4.5 to 8 mg/L, indicating that the waters are well-aerated, which is crucial for maintaining healthy aquatic ecosystems. Furthermore, the pH levels at these sites were found to be 7.26, 7.31, and 7.41, respectively, showing slightly alkaline conditions. These values fall within the Bangladesh inland surface water standard of ≤6 to 9, suggesting the waters are chemically balanced and safe for both marine life and industrial activities. Slightly alkaline conditions are often favorable in preventing overly aggressive corrosion, thus relevant for understanding how the selected mild steel samples will react in this marine environment.

The electrical conductivity (EC) recorded was higher than Bangladesh inland surface water standard of ≤ 1. 2 mS/cm, to be precise, the values were recorded as 43.9 mS/cm at Outer Anchorage and Fairway Buoy and 45.1 mS/cm at St Martins anchorage. The value of Total Dissolved Solids (TDS) that was obtained 27.2 gm/L at Outer Anchorage and Fairway Buoy. On the other hand, the value of TDS of St Martins was 27 gm/L which is slightly lower than other two locations. Overall, these values are lower than the Bangladesh inland water standard of ≤1000 mg/L. Total Suspended Solid (TSS) was low with 11 mg/L at the Outer Anchorage, 13 mg/L at the Fairway Buoy, while 9 mg/L at St.

Martins and thus did not exceed the permissible limit of 150 mg/L of Bangladesh Standard for Inland Surface Water. Chloride levels were much higher than the inland surface water standard of ≤600 mg/L, with measurements of 25000 mg/L at the Outer Anchorage, 24750 mg/L at the Fairway Buoy, and 25250 mg/L at St Martins, which is typical for seawater because of its salt content. The sulfate concentrations were the highest and ranged between 2500 mg/L at the Outer Anchorage and 2400 mg/L at St Martins with the Fairway Buoy having slightly higher value of 2600 mg/L; all of which are typical for seawater.

Table 2.2: Contents of the Collected Seawaters

Parameter	Unit	Outer Anchorage, Chattogram	Fairway Buoy, Maheshkhali	St Martins Anchorage Point	Bangladesh Standard for Inland Surface Water (ECR,1997)
Dissolved Oxygen (DO)	**mg/L**	***7.36***	***7.21***	***7.49***	4.5-8
pH	--	7.26	7.31	7.41	≤6-9
Electrical Conductivity (EC)	mS/cm	43.9	43.9	45.1	≤1.2
Total Dissolved Solids (TDS)	gm/L	27.2	27.2	27	≤1000
Total Suspended Solid (TSS)	mg/L	11	13	09	≤150
Chloride (Cl)	**mg/L**	**25000**	**24750**	**25250**	≤600
Sulfate (SO_4^{2-})	mg/L	2500	2600	2400	---

In conclusion, the analyzed parameters from the water samples collected from the designated locations in the Bay of Bengal indicate a high salinity environment, as reflected in the elevated levels of dissolved solids and chloride concentrations, typical of marine water. The moderate alkaline pH and adequate dissolved oxygen content suggest conditions conducive to corrosion processes. These environmental characteristics- high chloride levels, significant sulfate presence, and elevated electrical conductivity-

collectively highlight the aggressive nature of the marine environment. Such factors play a pivotal role in accelerating the corrosion of mild steel structures. This detailed assessment of the water chemistry provides a comprehensive understanding of the harsh conditions that the mild steel samples will face, allowing for a more accurate analysis of their corrosion behavior in these waters.

2.3.3 Experimental Setup

The collected seawater was carefully divided into three separate barrels to establish distinct testing conditions for the mild steel coupons. Each barrel was securely sealed to prevent evaporation and protected from external contamination, such as dust, which could potentially alter the seawater's composition. Special precautions were taken to ensure the quality of the seawater remained consistent throughout the experiment. This control was essential to replicate natural marine conditions as closely as possible while minimizing the influence of external factors that could interfere with the corrosion process.

It is important to note that the prepared mild steel (MS) coupons were fully submerged in the seawater-filled barrels and kept at room temperature for the entire duration of the analysis. As shown in Figure 2.6, the coupons were immersed completely to avoid partial submersion, which could lead to uneven corrosion patterns and compromise the integrity of the results. Additionally, to prevent contact between the coupons and the barrel walls—thus avoiding contamination or other factors that could influence corrosion—the samples were suspended in the middle of each barrel. This arrangement ensured uniform exposure to seawater, enabling a controlled study that could be generalized to reflect the conditions found in the Bay of Bengal.

Figure 2.6: Immersion of the metal specimens in the stored seawater for gravimetric analysis

The extensive procedures and precautionary measures adopted were essential for conducting reliable experiments aimed at determining the corrosion characteristics of marine-grade mild steels in a controlled seawater environment.

2.3.4 Initial Examination

Prior to the immersion process, the prepared mild steel samples underwent microstructural analysis using the Optical Electron Microscope (OEM) (Model: MM 500T) available at the Metallurgical Lab of MIST, shown in Figure 2.7. This advanced microscope, equipped with a computer interface, enabled detailed investigation of the samples' microstructure and surface topography. Conducting this analysis was essential to establish the initial state and condition of the samples before subjecting them to the corrosive effects of seawater.

Figure 2.7: Optical Electron Microscope (Model: MM 500T)

Following the microstructural examination, the precise weight of each sample was measured using a 'RADWAG Precision Measurement Analytical Balance,' showin in Figure 2.8, renowned for its exceptional accuracy. This analytical instrument can measure weights with a precision ranging from 0.0001 to 0.00001 grams. By carefully recording the initial weight of each sample, the study ensured that any weight changes resulting from corrosion during the immersion period could be monitored with a high degree of accuracy, allowing for precise quantification of corrosion effects.

Figure 2.8: RADWAG Precision Weighing Machine with accuracy of 0.00001g

2.3.5 Immersion and Periodic Analysis

The experiment involved immersing mild steel coupons in seawater to analyze their corrosion behavior. The research meticulously measured various properties, including weight, dimensions, Vickers hardness, and microstructural characteristics over a structured timeline. Initial readings were taken after 24 hours to establish a baseline for early changes caused by exposure to seawater. Subsequent measurements were taken at intervals of 3, 6, 12, 18, 24, 30, 36, and 48 days. Each time, the samples were carefully removed, immediately measured, and then returned to the seawater to minimize the impact of air exposure, which could potentially alter the corrosion process (Fig 2.9).

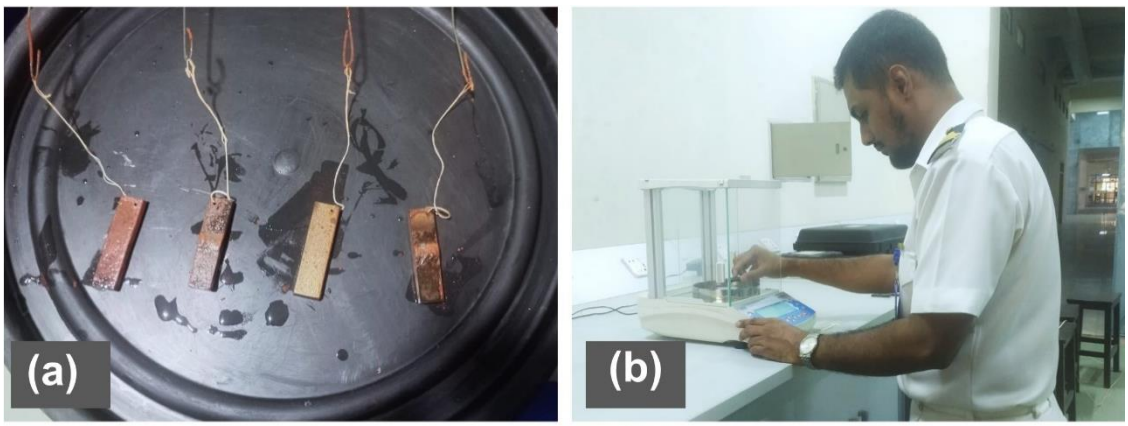

Figure 2.9: Weight taking of the corroded specimens: (a) A set of sample corroded from lab based test immersion, (b) Weight taking of the corroded specimens

The systematic measurements provided a comprehensive evaluation of the extent and progression of corrosion over the designated period. Weight measurements were important in assessing mass loss as a result of corrosion, while dimensional tests helped confirm any physical alterations to the coupons. The mechanical property changes were evaluated using a Vickers hardness tester, with results indicating that the surface of mild steel became prone to hardening or roughening as the corrosion process progressed. Detailed microstructural analysis, including digital scans and examinations through optical electronic microscopy, revealed significant changes in the microstructure, surface hydration, and any surface alterations that occurred throughout the test period. The data collected through this rigorous and methodical approach provided invaluable insights into the corrosion behavior of marine-grade mild steels exposed to the specific conditions of the Bay of Bengal marine environment.

In many cases, as corrosion progresses, the metal surface may develop a thin protective layer of corrosion products (such as oxides or hydroxides). This layer can partially or completely cover the surface, slowing down the corrosion rate because it acts as a barrier, reducing the contact between the metal and the corrosive environment (seawater, in your case). Once this protective layer is formed, the corrosion rate often stabilizes and reaches a steady state.

Corrosion is an electrochemical process involving anodic (oxidation) and cathodic (reduction) reactions. Over time, as the material corrodes, these reactions often reach equilibrium, and the corrosion current (Icorr) stabilizes. This steady-state behavior is typically observed when the anodic dissolution of the metal and the cathodic reduction (e.g., oxygen reduction) reach a constant rate.

2.3.6 Hardness Testing

Thus, to determine the effects of corrosion on the mechanical properties of the mild steel samples, a comprehensive mechanical condition test was conducted by measuring micro-hardness values before and after the experiments in the corrosive seawater environment. The Digital Micro-Vickers Hardness Tester TMHV-1000DTe, illustrated in Figure 2.10 was employed, using a force of 5 kg with a holding time of 10 seconds. This testing method assesses the material's resistance to indentation, providing insights into surface hardness alterations due to corrosion processes.

Figure 2.10: Micro-Vickers Hardness Tester (TMHV-1000DTe)

Pre-immersion examinations of mechanical properties were conducted on mild steel coupons through micro-hardness tests. These initial values served as benchmarks for subsequent measurements taken at various intervals during and after immersion to monitor the degree of hardness loss caused by corrosion over time. While Vickers hardness testing offers valuable localized insights, its micro-indentations are often too small to capture the broader effects of corrosion fully. Since corrosion impacts larger areas of the material surface, relying solely on micro-hardness may overlook significant changes in mechanical properties.

For this reason, Brinell hardness testing was also employed to provide a more comprehensive understanding of the material's overall resistance to deformation post-corrosion. Brinell tests, conducted using an applied load of 187.5 kgf for 20 seconds, offer larger indentations that reflect the general hardness of the material surface. Figure 2.11 illustrates the process of measuring the indentations created during Brinell hardness testing

This method is beneficial for understanding how corrosion affects the bulk properties of marine-grade mild steel, making it a more suitable approach for evaluating the mechanical weakening of materials exposed to seawater. Ten readings were taken for each sample, with the average recorded, ensuring a robust and reliable analysis of corrosion-induced hardness loss.

Figure 2.11: Brinell Hardness Testing

This combination of hardness testing methods enhances the accuracy and depth of the analysis, providing critical insights into the mechanical durability of the steel in marine environments.

2.4 Lab/Workshop Facilities Used

The following laboratory and workshop facilities were utilized for this research:

Table 2.3: List of Laboratory and Workshop Facilities Utilized for the Research

Ser	Name of Organization	Lab/Workshop Facilities
1.	BN Dockyard, Chattogram	Platter and Welding Shop
		Machine Shop
		Material Testing Lab
		Battery Shop
2.	ME Dept, MIST	Metallurgical Laboratory
		Applied Mechanics Lab
3.	NAME Dept, MIST	Ship Instrument Lab
4.	EWCE Dept, MIST	Environmental Engineering Lab
5.	Science & Hum Dept, MIST	Chemistry Lab
6.	IPE Dept, MIST	SEM Lab
7.	BCSIR, Dhaka	Industrial Physics Lab
		Fuel Research and Development Lab

CHAPTER THREE
CORROSION BEHAVIOR INVESTIGATION THROUGH GRAVIMETRIC ANALYSIS

3.1 Preamble

Corrosion behavior is pivotal in determining critical structures and components' safety, reliability and lifespan especially in marine environments. The degradation caused by corrosion can lead to failures if not properly understood and managed. Therefore, investigating corrosion behavior is a key area within materials science and engineering. By thorough understanding how and why materials corrode, effective mitigation strategies can be developed, ensuring the integrity of these materials and significantly extending their service life.

This chapter presents various experimental methods and investigations to analyze corrosion behavior in different conditions. The methodologies described will comprehensively understand the corrosion mechanisms affecting marine-grade mild steels. The following tests will be discussed in this chapter in detail:

(i) Seawater Laboratory Test (Static Condition). Analyzes corrosion in stagnant or near-stagnant seawater environments.

(ii) Seawater Laboratory Test (Dynamic Condition). Explores the effects of water flow or velocity on corrosion rates.

(iii) On-Site Corrosion Testing. Evaluates real-world corrosion behavior by exposing samples to actual marine environments.

These tests aim to provide a deeper understanding of how different environmental factors influence the corrosion of marine-grade materials and how this knowledge can be applied to improve durability and performance.

3.2 Electrochemical Basis of Aqueous Corrosion

Corrosion that occurs in aqueous solutions such as sea water at ordinary temperatures is electrochecmical in nature and is similar to that occuring in an electrochemical cell. This process involves two primary electrochemical reactions: anodic and cathodic reactions.An

electrochemical cell is depicted in Figure 3.1. The cell is conssists of 2 electrodes immersed in an electrolyte , i.e. a liquid tha conducts electricity and joined by an wire as conductor. The andoe is the electrode from which positive electric current flows to the solution or where electrons flow through the external circuit in the reverse direction. Generally the oxidation (corrosion) occurs at the anode. Conversely, the cathode is the electrode which receives a positive current from the solution or where electrons flow in the reverse direction. During this process the electrons liberated by the oxidation reaction at the anode are transferred through the wire to the cathode.

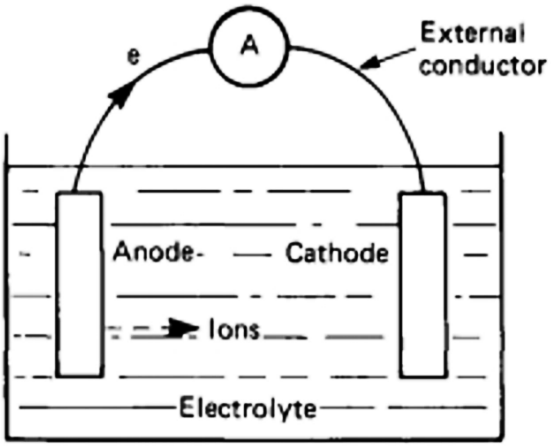

Figure 3.1: Simple Electrochemical Cell

At the anodic site, metal atoms undergo oxidation, losing electrons and entering the electrolyte as metal cations:

$$Fe \rightarrow Fe^{2+} + 2e^{-}$$

Simultaneously, at the cathodic site, electrons are gained by an oxidizing agent from the electrolyte solution. The reduction reactions can occur in various forms:

Hydrogen Evolution: $2H^{+} + 2e^{-} \rightarrow H_2$ (in acidic solutions)

Oxygen Reduction: $O_2 + 2H_2O + 4e^{-} \rightarrow 4OH^{-}$ (in neutral or alkaline solutions)

3.3 Static Testing in Laboratory

Gravimetric analysis was conducted on seawater collected from the Bay of Bengal in a indoor atmosphere under static conditions. At first water was collected from three

different locations. The locations of seawater collection are shown in Figure 3.2. The water collection points are:

(i) Outer Anchorage, Chattogram

(ii) Fairway Buoy, Maheshkhali, Chattogram

(iii)St. Martins Point Anchorage, St Martins, Teknaf

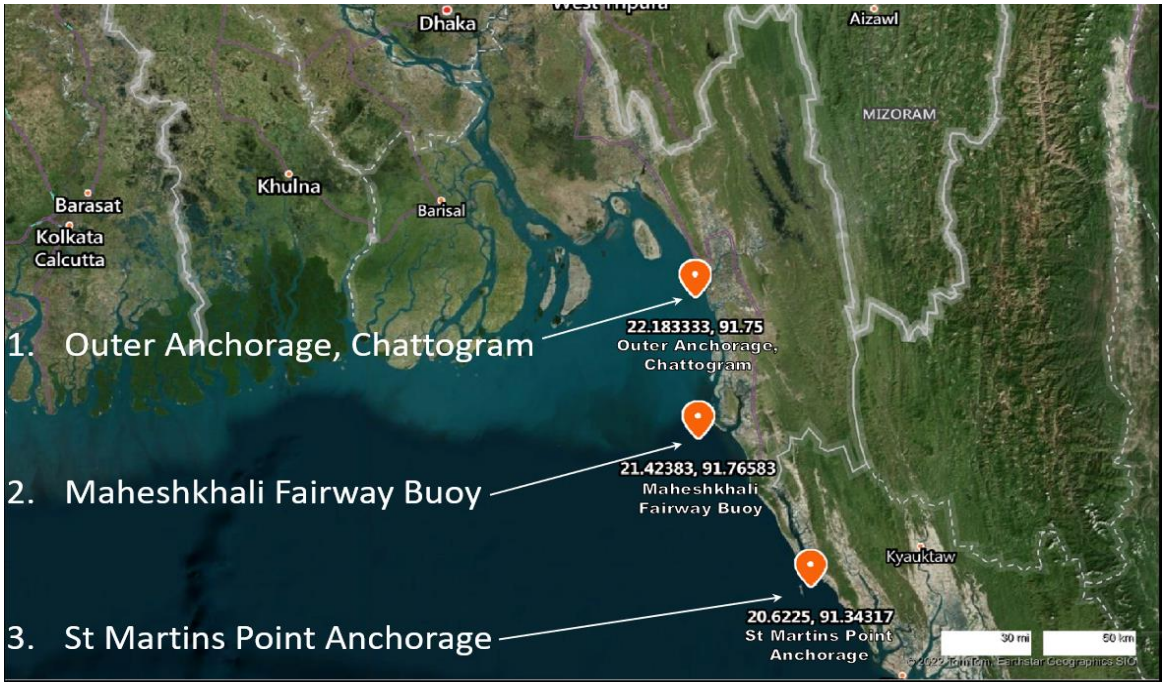

Figure 3.2: Three different locations of collection of seawater at Bay of Bengal

3.3.1 Experimental Setup

Then, samples were weighed, measured, and identified by marking. The samples were then immersed in the waters of each location. Figure 3.3 depicts the preparation and experimental process for corrosion testing of seamless and welded samples. In (a), two sets of seamless and welded samples are shown, prepared for immersion. Image (b) displays the samples being suspended on a wooden frame to ensure uniform exposure during immersion. The setup for immersing the samples in a large container filled with seawater is shown in (c), simulating the marine environment. Finally, (d) illustrates the samples after removal from seawater, visibly affected by corrosion.

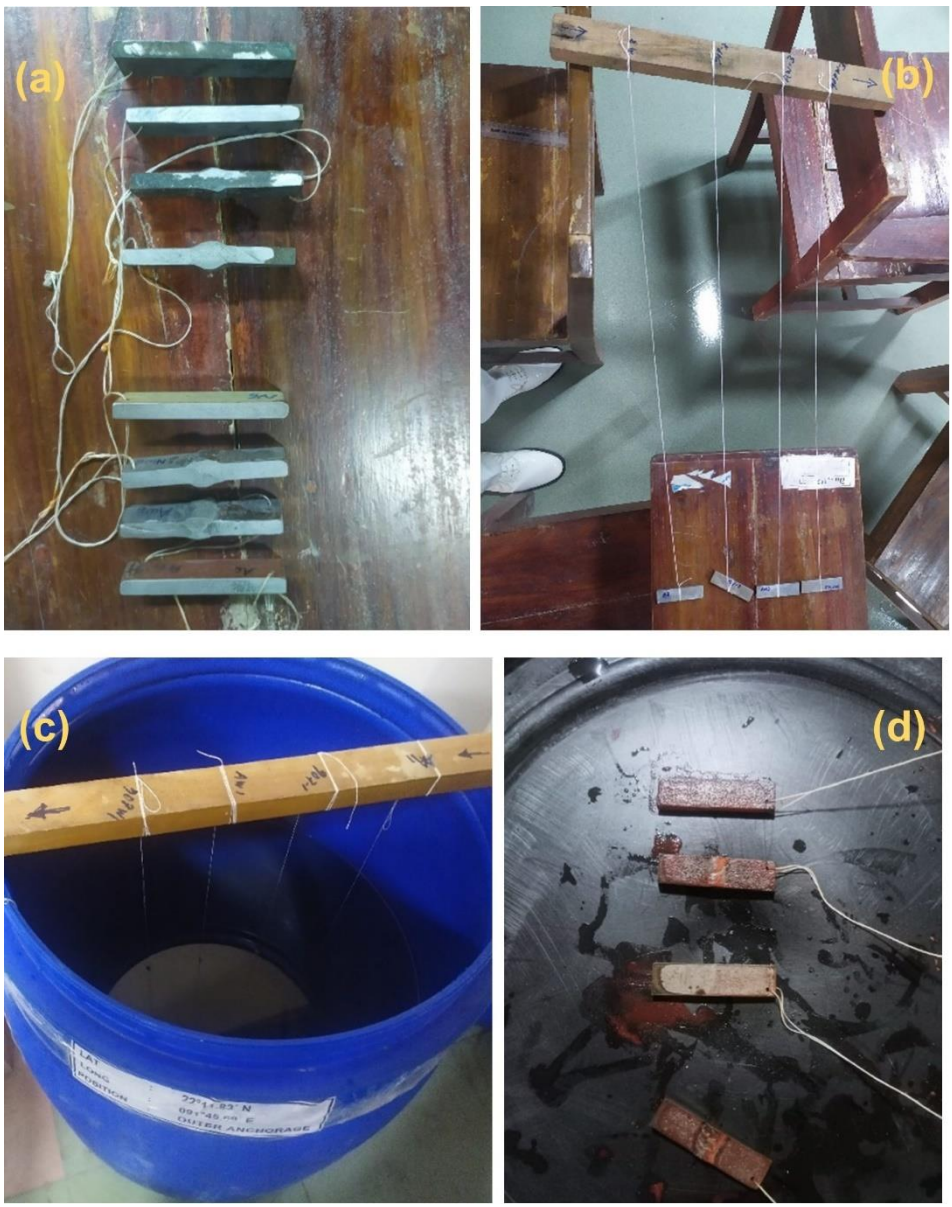

Figure 3.3: Sample Immersion Setup: (a) Seamless and welded samples, multiple sets prepared for testing; (b) Samples being prepared for hanging on a wooden frame; (c) Samples immersed in seawater within a large container; (d) Samples after removal from seawater, showing corrosion effects.

3.3.2 Formula Used for Gravimetric Analysis

Formula used for gravimetric analysis is as follows:

Mass degradation of material,

$$\Delta W = \frac{(W_o - W_f)}{A} \quad (3.1)$$

The rate of corrosion,

$$R_{corr} = \frac{(K \times \Delta W)}{(\rho \times T)} \quad (3.2)$$

Where,

ΔW = Mass degradation per exposed surface area (gm/cm^2),

W_o = Initial mass (gm),

W_f = Mass after designated submerged period (gm),

A = Surface area exposed in the media (cm^2),

R_{corr} = Rate of corrosion (mm/year),

K = Unit conversion factor = 87.6 x 10^3 for corrosion rate in mmpy,

ρ = Density of material (gm/cm^3),

T = Exposed duration (hour).

3.3.3 Results and Discussion

3.3.3.1 Outer Anchorage Seawater

In the outer anchorage water, all samples exhibited significant corrosion. While the corrosion rates varied across samples, their overall patterns were quite similar. The results in Figure 3.4 demonstrate that initially the corrosion rate was high, but it decreased as the test progressed. However, this reduction was non-linear. Eventually, the rate of corrosion stabilized, showing no further decline towards the end. Due to this stabilization, the test period was not extended, as continued testing would likely yield a constant corrosion rate.

From Table 3.1 and Figure 3.4, it is evident that the highest corrosion rate was observed in the MS Grade 907 sample. The welded MS Grade 907 specimen exhibited the second-

highest corrosion rate, followed by the MS Grade A specimen and the welded MS Grade A specimen, respectively.

Table 3.1: Highest and Lowest Corrosion Rate against Materials

Materials	Highest Corrosion Rate (mmpy)	Lowest Corrosion Rate (mmpy)
MS Grade A	0.11374	0.06823
MS Grade A (Welded)	0.10749	0.07052
MS Grade 907	0.12743	0.05776
MS Grade 907 (Welded)	0.12052	0.05408

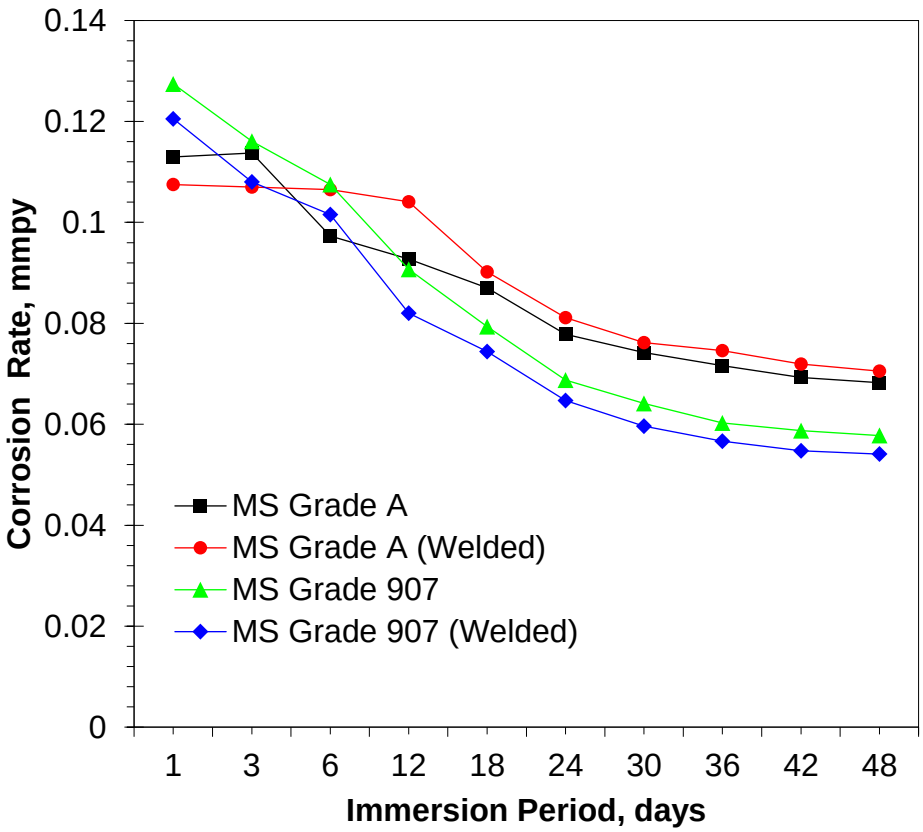

Figure 3.4: Corrosion Rate vs Immersion Period curve for Outer Anchorage Seawater

3.3.3.2 Maheshkhali Fairway Buoy Seawater

Figure 3.5 shows that like the previous, in Maheskhali also, the peak corrosion values dropped sharply after the initial attack period. Eventually, the rate stabilized, with no further decline in the later stages of the test.

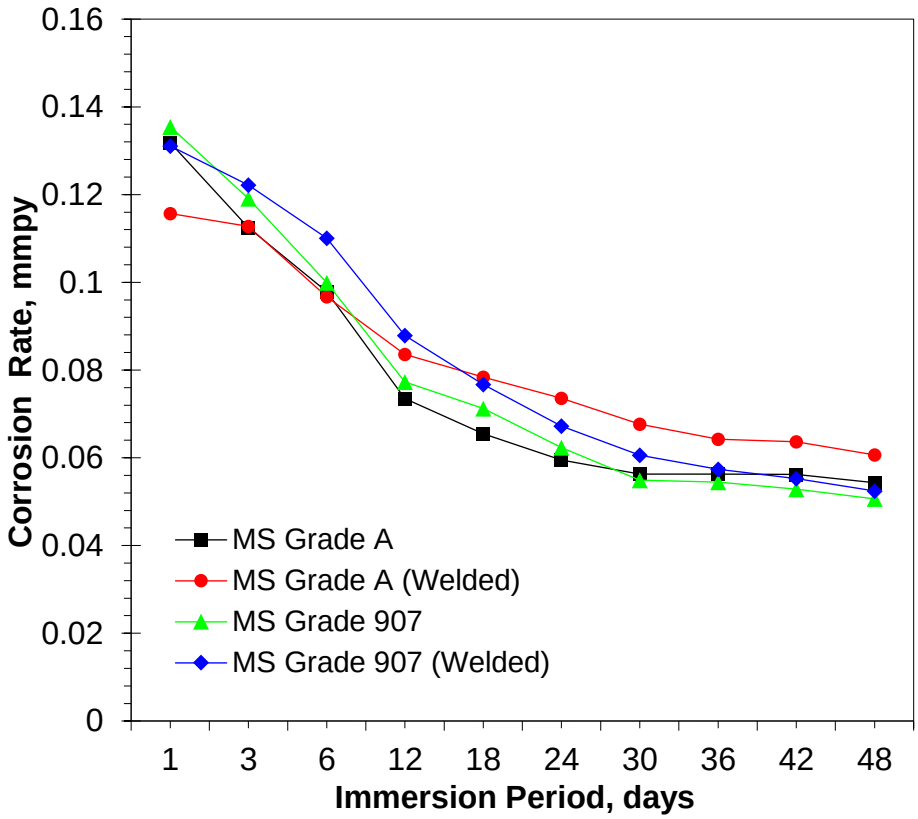

Figure 3.5: Corrosion rate vs Immersion period curve for Maheshkhali Seawater

Table 3.2: Highest and Lowest Corrosion Rate against Materials for Maheshkhali Seawater

Material	Highest Corrosion Rate (mmpy)	Lowest Corrosion Rate (mmpy)
MS Grade A	0.13182	0.05432
MS Grade A (Welded)	0.11568	0.06065
MS Grade 907	0.13548	0.05063
MS Grade 907 (Welded)	0.13109	0.05244

Table 3.2 shows that the highest corrosion rate occurred in the MS Grade 907 sample, consistent with the results from the outer anchorage seawater. However, the MS Grade A

specimen exhibited the second-highest corrosion rate in this case, followed by the welded MS Grade 907 and welded MS Grade A specimens, respectively. In both scenarios, the lowest corrosion rate was observed in the welded MS Grade A specimen.

3.3.3.3 Saint Martins Point Anchorage Seawater

Figure 3.6 shows that in St. Martin's, the corrosion rates are notably different and more significant. As in previous cases, the initial corrosion rate was higher, followed by a decrease in the later stages. However, this reduction was again non-linear. Eventually, the rate stabilized, with no further decline towards the end of the test period. As a result, the testing period was not extended.

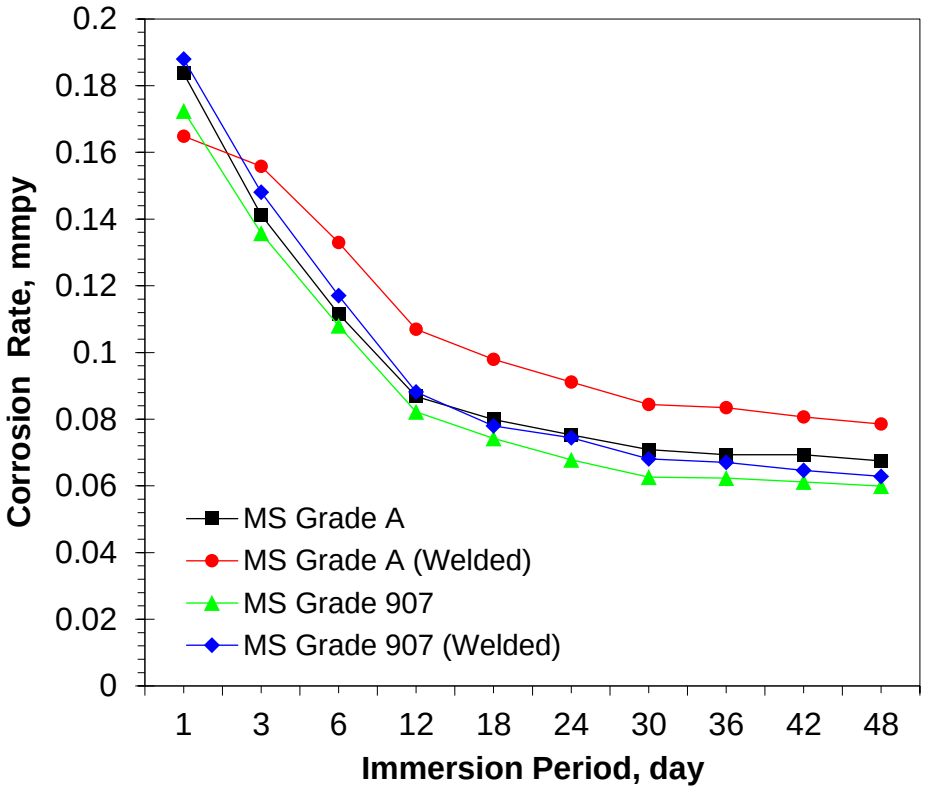

Figure 3.6: Corrosion rate vs Immersion period curve for Saint Martin Point Seawater

From Table 3.3 and Figure 3.6, the highest corrosion rate occurred in the welded MS Grade 907 sample, which contrasts with the other locations. In this case, the MS Grade A specimen exhibited the second-highest corrosion rate, similar to the Maheshkhali fairway buoy seawater results. This was followed by the MS Grade 907 and welded MS Grade A

specimens, respectively. Across all scenarios, the welded MS Grade A showed the lowest corrosion rate.

Table 3.3: Highest and Lowest Corrosion Rate against Materials for Saint Martin Point Seawater

Material	Highest Corrosion Rate (mmpy)	Lowest Corrosion Rate (mmpy)
MS Grade A	0.18365	0.06748
MS Grade A (Welded)	0.16486	0.07853
MS Grade 907	0.17243	0.05991
MS Grade 907 (Welded)	0.18796	0.06284

3.3.3.4 Comparison of Average Corrosion Rate of Three Locations

Figure 3.7 compares the corrosion rate trends across the three seawater locations for all sample types, illustrating the influence of site-specific environmental factors on corrosion rates. A relation between the corrosion rates in different seawater samples and their chemical contents can be seen. The releveant factors behind the observed trends are explained below:

(i) **Chloride Content:** Chloride ions (Cl^-) play a significant role in accelerating corrosion, especially for marine-grade steels. According to Table 2.2, the chloride content is highest in the St. Martin's seawater (25,250 mg/L), followed by outer anchorage (25,000 mg/L), and lowest in Maheshkhali (24,750 mg/L). The higher the chloride content, the more aggressive the seawater will promote corrosion through processes.

Correlation: The highest corrosion rate in St. Martin's can be attributed to the highest chloride concentration, while Maheshkhali, with the lowest chloride content, exhibited the lowest corrosion rate.

(ii) **Dissolved Oxygen (DO):** Dissolved oxygen is another important factor in corrosion, as oxygen is required for the cathodic reaction during the corrosion process. The dissolved oxygen levels in St. Martin’s are slightly higher (7.49 mg/L) compared to outer anchorage (7.36 mg/L) and Maheshkhali (7.21 mg/L).

Correlation: Higher dissolved oxygen in St. Martin's may have also contributed to the elevated corrosion rate, facilitating the oxygen reduction reaction that drives corrosion.

(iii) **Electrical Conductivity (EC):** Electrical conductivity indicates the seawater's ability to carry ionic current, which is essential for electrochemical corrosion. St. Martin's has the highest electrical conductivity (45.1 mS/cm), followed by outer anchorage and Maheshkhali (both around 43.9 mS/cm).

Correlation: Higher conductivity in St. Martin's means it can support faster electrochemical reactions, contributing to the higher corrosion rate.

(iv) **pH:** pH affects the stability of the passive oxide layer on steel surfaces. In slightly acidic conditions (lower pH), this protective layer can break down more easily. However, all three locations have pH values within a neutral to slightly alkaline range (7.26 - 7.41), which is less aggressive towards corrosion.

Correlation: Since the pH values are quite similar, the pH doesn't seem to play a major role in the differing corrosion rates.

(v) **Sulfate (SO_4^{2-}):** Sulfate ions are less corrosive than chloride ions, but when combined with chloride, they can affect the corrosion process. The sulfate content is highest in Maheshkhali (2,600 mg/L), followed by outer anchorage (2,500 mg/L), and lowest in St. Martin's (2,400 mg/L).

Correlation: Since sulfate concentrations are reasonably similar, they likely play a minimal role in the corrosion rate variations across the locations.

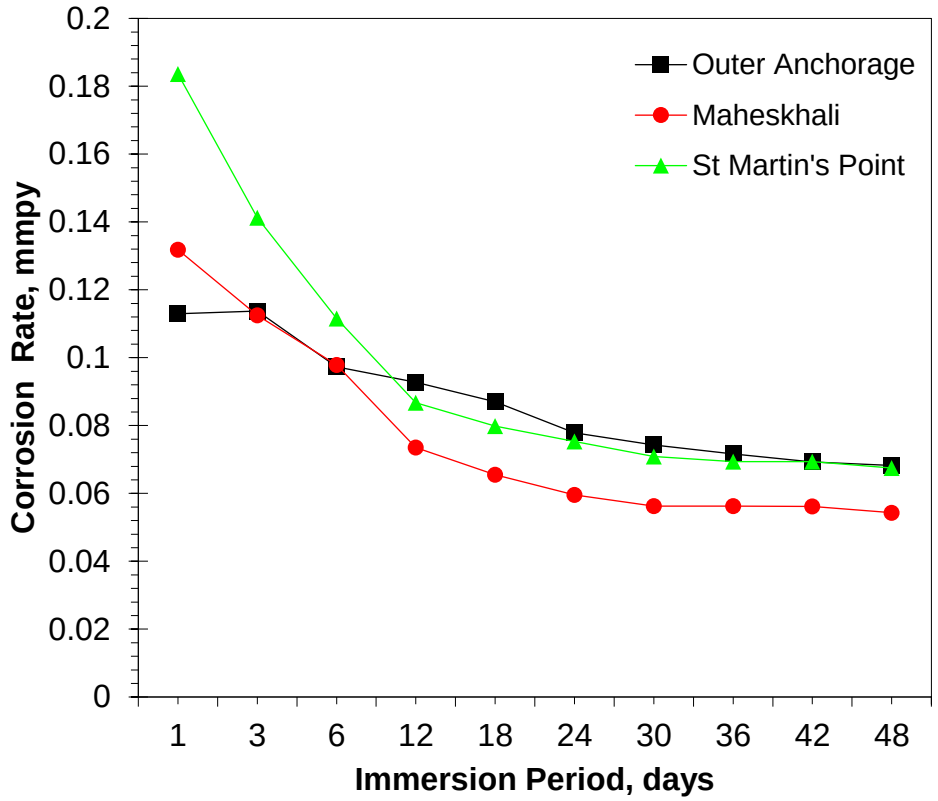
Outer Anchorage
Maheskhali
St Martin's Point
Corrosion Rate, mmpy
Immersion Period, days
0.2
0.18
0.16
0.14
0.12
0.1
0.08
0.06
0.04
0.02
0
1
3
6
12
18
24
30
36
42
48

(a)

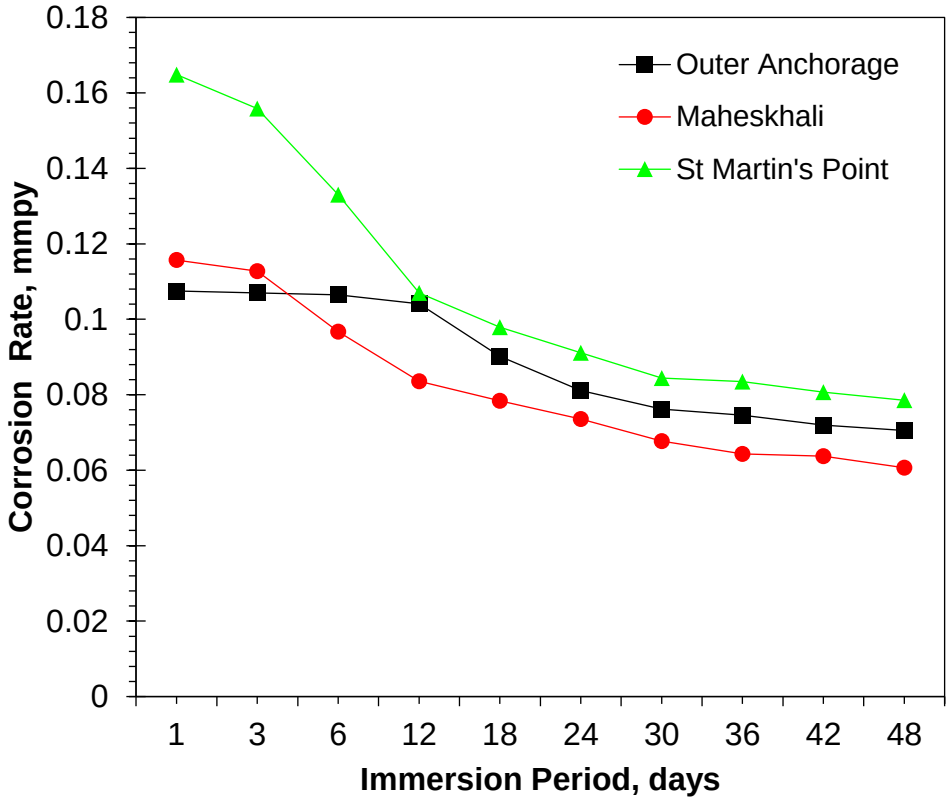
Outer Anchorage
Maheskhali
St Martin's Point
Corrosion Rate, mmpy
Immersion Period, days
0.18
0.16
0.14
0.12
0.1
0.08
0.06
0.04
0.02
0
1
3
6
12
18
24
30
36
42
48

(b)

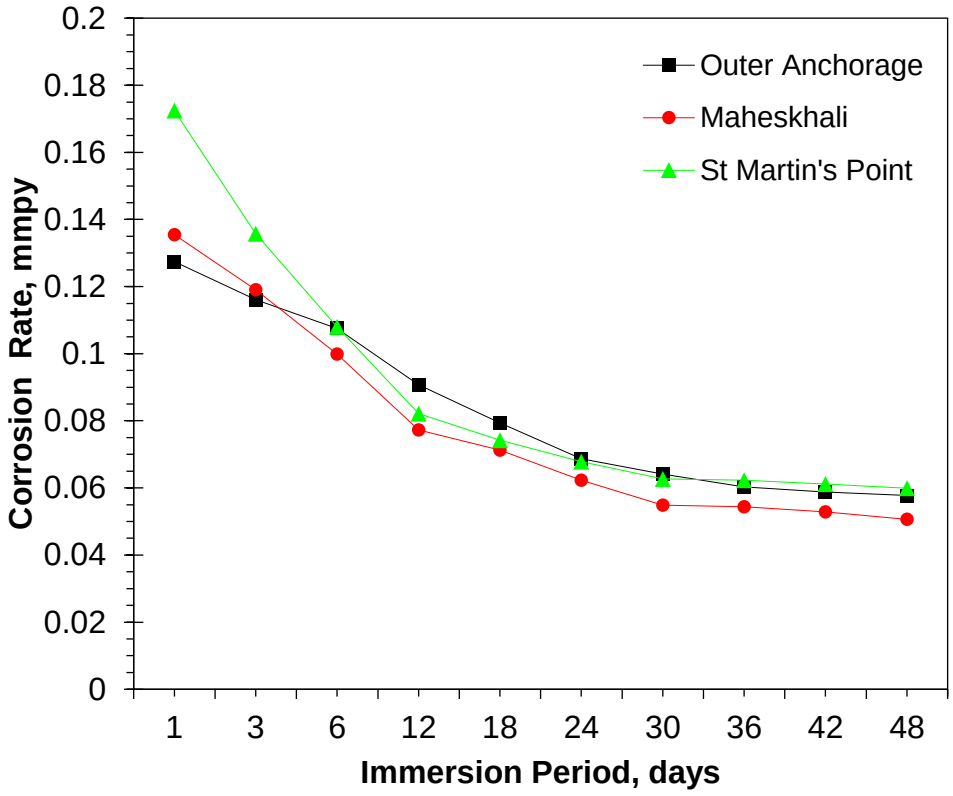

(c)

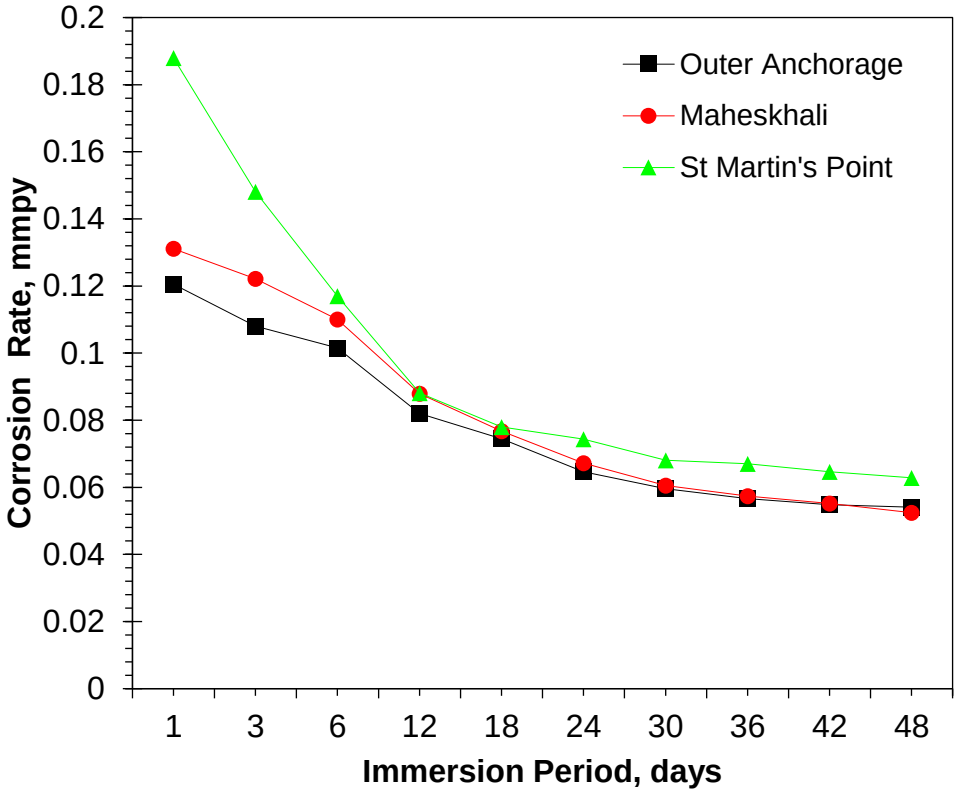

(d)

Figure 3.7: Corrosion rate vs Immersion period curve (a) MS Grade A, (b) MS Grade A (Welded), (c) MS Grade 907 and (d) MS Grade 907 (Welded)

3.3.4 Summary of Reuslts

St. Martin's, having the highest chloride concentration, dissolved oxygen, and electrical conductivity, exhibited the most significant corrosion rate, while Maheshkhali, with the lowest values, showed the least corrosion. The outer anchorage seawater had 2nd highest values for these parameters, corresponding with its intermediate corrosion rate. Furthermore, MS Grade 907 demonstrated a lower corrosion rate than MS Grade A, indicating better resistance to corrosion. This indicates that the lower carbon and manganese levels in MS Grade A's composition directly reduce its corrosion resistance.

3.4 Dynamic Testing in Laboratory

The dynamic test was conducted in St. Martin's water, as it exhibited the highest corrosion rate among the samples evaluated.

3.4.1 Experimental Setup

Based on the results of static experiment- dynamic test was carried out for the highest corrosive seawater. The setup shown in the Figure 3.8 was used to conduct the test. Relative velocity of 2 ms^{-1} was maintained while the propeller was rotating in the seawater with the hanging samples.

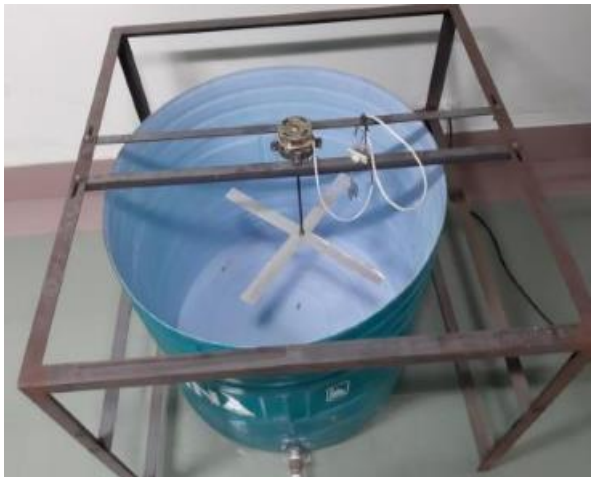

Figure 3.8: Experimental setup for the seawater dynamic lab test.

3.4.2 Results and Discussion for Dynamic Test

The results in the Figure 3.9 demonstrates that like the static tests, the corrosion rate was initially higher, then continued to decrease and became steady. The pattern is the same for all samples.

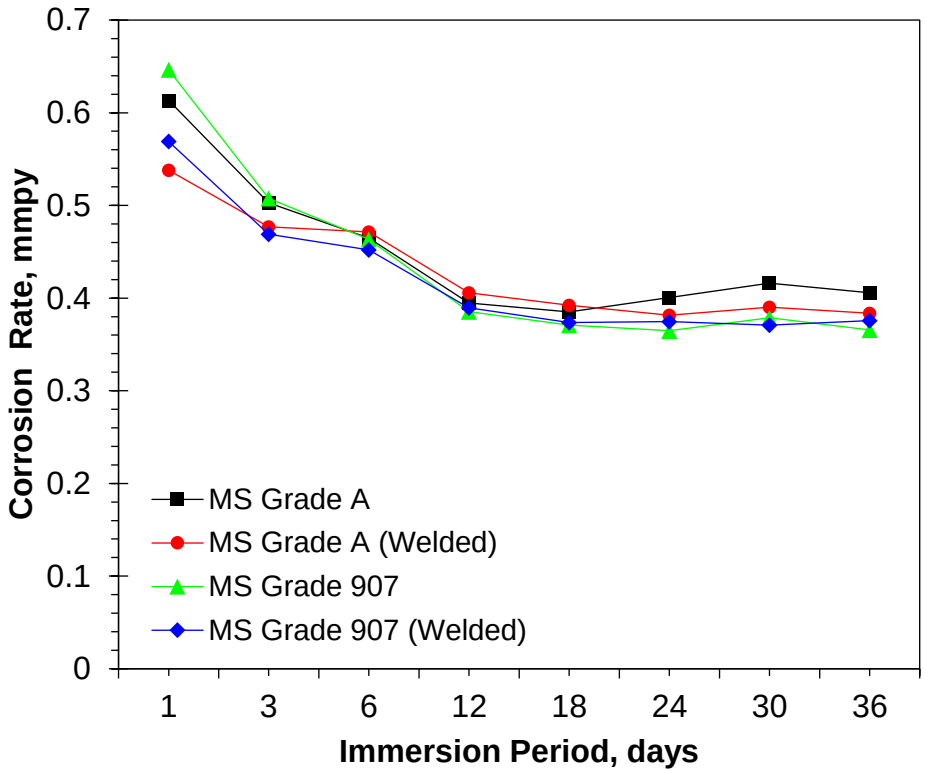

Figure 3.9: Corrosion rate vs Immersion period curve for Saint Martin Point Seawater of Dynamic method

Table 3.4: Highest and Lowest Corrosion Rate against Materials for St Martin's Water (Dynamic Method)

Material	Highest Corrosion Rate (mmpy)	Lowest Corrosion Rate (mmpy)
MS Grade A	0.6134	0.40576
MS Grade A (Welded)	0.6464	0.36566
MS Grade 907	0.53797	0.38359
MS Grade 907 (Welded)	0.56899	0.37567

3.5 Static and Dynamic Corrosion Rate Comparison of St. Martin's Anchorage

Figure 3.10 illustrates the difference in averaged corrosion rates between static and dynamic conditions. In the dynamic environment, where the water velocity was

maintained to simulate conditions found in real marine situations, the corrosion rate was significantly higher compared to the static condition. This could be primarily due to the water velocity, which facilitated the faster transport of corrosive ions, such as chloride and sulfate, to the surface of the mild steel specimens. As a result, the increased ion flow might have led to a more aggressive corrosion process, continuously attacking the exposed steel.

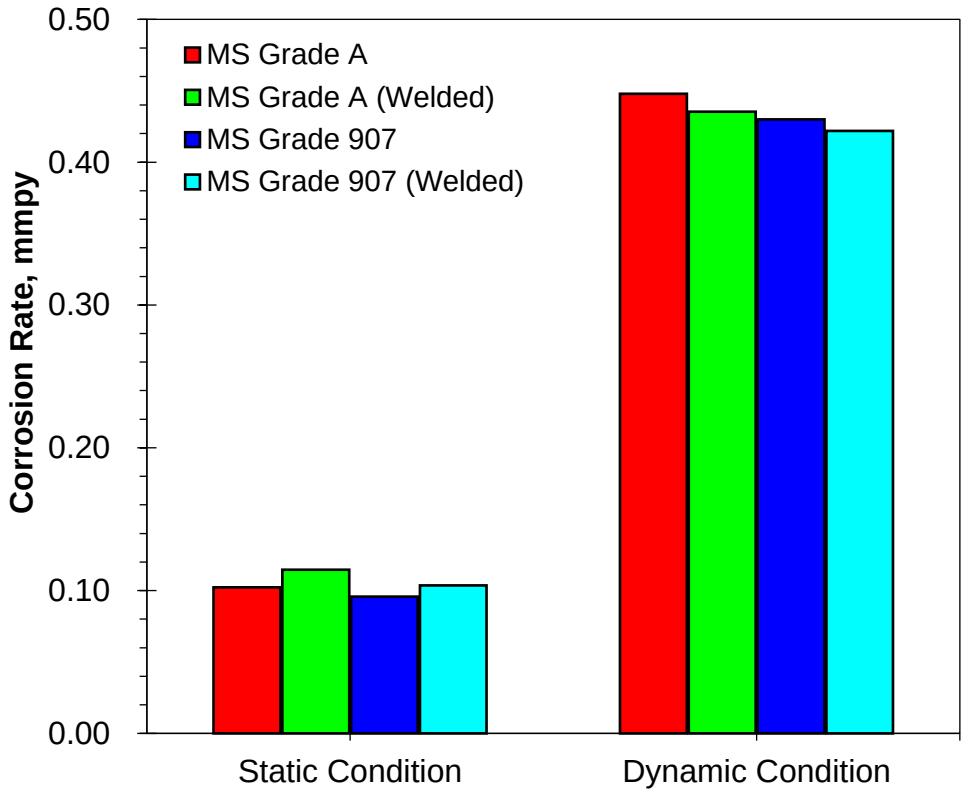

Figure 3.10: Comparison of Average Corrosion Rate of Static and Dynamic Condition of St Martins Anchorage Water

3.6 On-site Test

On-site corrosion tests were carried out in two different regions of the Bay of Bengal: one in the inner coastal region and another in the outer deep-sea region.

3.6.1 Experimental Setup

Experimental coupons were deployed on two vessels operating in distinct regions to evaluate the differential impact of marine environments on corrosion. One ship navigated in an inner area characterized by sheltered waters, while the other traversed the outer

region, exposed to the full force of ocean conditions. After a 90-day immersion period, the corrosion rates of the coupons were meticulously examined to assess the effects of these varying environments on metal degradation.

3.6.2 Results and Discussion for On-site Test

The results of the on-site tests carried out with the assistance of BN ships, shown in Figure 3.11 depicts that the average corrosion rate in the deep-sea region is 1.8 times higher than in the coastal region. From the chart, it was obtained that increment of corrosion rate in from coastal region to deep sea for-

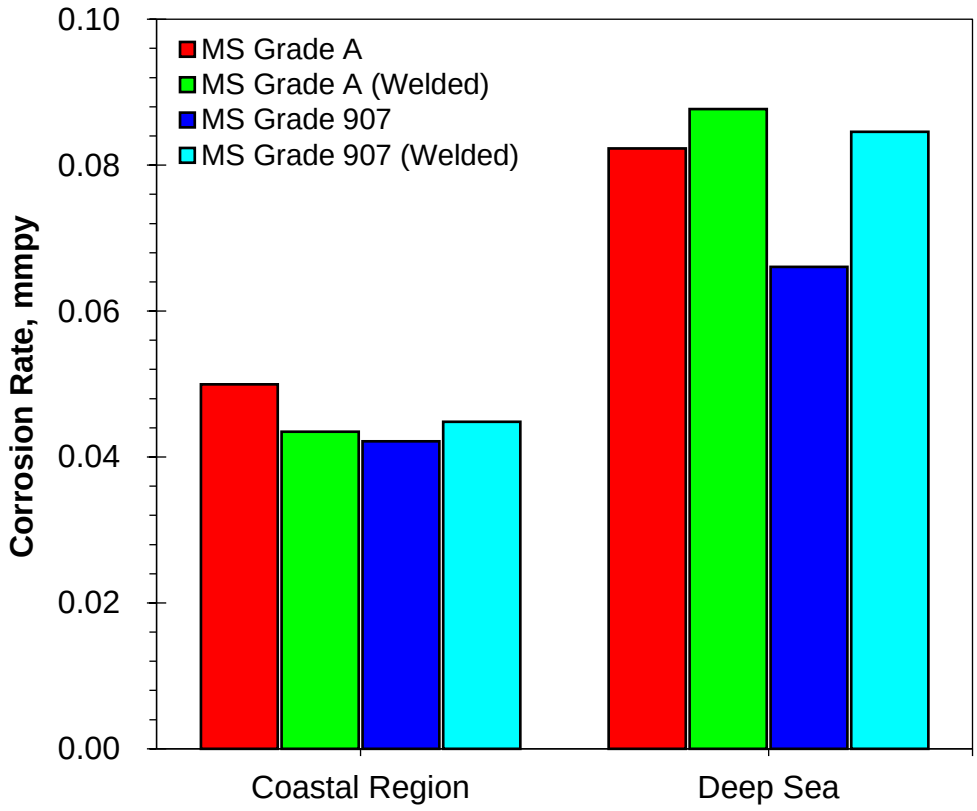

Figure 3.11: Comparison of Corrosion rates between deep sea and coastal region.

3.7 Summary

This chapter investigated the corrosion behavior of marine-grade mild steels in both static and dynamic seawater conditions, focusing on MS Grade A and MS Grade 907, as well as seamless and welded samples. The results exhibited significant differences in corrosion rates based on environmental conditions, material composition, and sample preparation methods.

Dynamic conditions consistently demonstrated significantly higher corrosion rates than static conditions, with an average increase of more than 300%, indicating the substantial influence of environmental motion in accelerating corrosion. Among the three seawater locations studied, St. Martin's Anchorage showed the most corrosive behavior, attributed to its higher salinity and dissolved oxygen levels in comparison to rest locations studied. Moreover, MS Grade A showed lower corrosion resistance than MS Grade 907, particularly in dynamic environments.

Furthermore, the study revealed that corrosion rates were highest at the initial stages of immersion and gradually decreased to a steady value, indicating a time-dependent steadiness. Welded samples displayed slightly better corrosion resistance than seamless samples across all conditions, likely due to localized structural modifications introduced during the welding process.

CHAPTER FOUR
INVESTIGATION OF MECHANICAL BEHAVIOR

4.1 Preamble

The study of mechanical properties, or the response of a material or structure under applied loads, is fundamental for predicting how it will behave under specific conditions. This investigation typically involves the execution of several tests and analytical procedures. They are aimed at understanding the material's behavior when exposed to various mechanical forces. These tests not only evaluate the strength and resilience of the material but also provide deeper insights into its structural integrity under stress.

Through these investigations, key characteristics, capabilities, and potential failure modes of the material can be ascertained. This knowledge is helpful for designing safer and more reliable products. A thorough understanding of mechanical behavior is particularly important in industries where material quality and durability are paramount, such as offshore, aerospace, automotive, and construction sectors. In these fields, materials are subjected to extreme conditions of temperature, pressure, and environmental factors, necessitating compliance with strict safety and performance standards.

This chapter focuses on the comprehensive investigation of the mechanical behavior of marine-grade mild steels. It considers the influence of the corrosive environment of the Bay of Bengal on their structural and mechanical properties. Examination of these properties provides a clearer understanding of the effects of such conditions on material performance and their long-term viability in marine applications.

Therefore, in this chapter, various investigations into the mechanical behavior will be described:

(i) Microstructure Inspection: OEM

(ii) Microstructure Inspection: SEM

(iii) EDX

(iv) Chemical Composition Test

(v) Experimental Investigation of Hardness

(vi) Tensile Testing

4.2 Microstructure Inspection: OEM

The microstructural investigation conducted with an Optical Electron Microscope (OEM) gives vital understandings into the physical and chemical processes taking place within materials at the microscopic level. This method enables the observation and analysis of the surface morphology and grain structure of mild steel both prior to and following exposure to corrosive environments. By examining these microstructures, important information regarding the material's performance, corrosion effects, and any irregularities in grain structure can be determined, ensuring a thorough evaluation of corrosion-related degradation.

The OEM analysis gives a detailed examination of the material's microstructure, revealing the arrangement and size of grains, as well as any defects or imperfections. This information is essential for understanding the underlying mechanisms of corrosion, such as pitting, crevice corrosion, or intergranular corrosion. By comparing the microstructures of mild steel samples before and after exposure to seawater, it is possible to identify the specific changes caused by corrosion and assess the material's susceptibility to degradation. Also, the OEM can be used to study the effects of different factors on corrosion, such as the presence of impurities, the influence of welding, or the impact of environmental conditions.

4.2.1 Experimental Setup for OEM

The steel samples were prepared for corrosion testing by first grinding them with silicon carbide (SiC) emery papers of varying grit sizes: 60, 120, 600, 800, 1000, 1200, and 1500. This process removed any surface contaminants and created a smooth surface for the subsequent polishing step.

After grinding, the samples were polished using a Nano 2000T Grinder-Polisher machine. This machine used alumina (Al_2O_3) powder to further refine the surface and produce a mirror-like finish. Some samples were then etched, which means they were treated with a chemical solution to reveal their microstructure. Other samples were left un-etched.

Figure 4.1: Microstructure Inspection by OEM

Finally, micrographs of the samples were taken using an Optical Electronic Microscope (OEM) model MM 500T at magnifications of 160x, 320x, 800x, and 1600x. These images provided a detailed view of the surface and microstructure of the steel samples. The microstructure inspection setup using an Optical Electron Microscope (OEM) is depicted in Figure 4.1, showcasing the equipment and methodology used for observing grain structure and surface morphology of the steel samples.

4.2.2 Results and Discussion for OEM

The Optical Electronic Microscope (OEM) images provide information about the microstructural changes took placr in the mild steel samples before and after exposure to the corrosive environment of the Bay of Bengal seawater. At a magnification of 320X, the OEM images clearly depicted the initial grain structure across all four samples before and after corrosion. The observed differences for the pre and post corrosion condition are discussed here separately for each type of sample.

4.2.2.1 MS Grade A (Seamless)

Before corrosion, the OEM image of the MS Grade A seamless sample (Fig. 4.2(a)) reveals a well-defined and uniform microstructure, with smooth grain boundaries that indicate an intact surface. After corrosion (Fig. 4.2(c)), the sample exhibits clear signs of degradation, with localized pitting and roughened surface features becoming prominent. The grain boundaries have eroded, and the previously uniform structure now displays uneven texture, indicating the impact of the corrosive environment.

4.2.2.2 MS Grade A (Welded)

The welded MS Grade A sample (Fig. 4.2(b)) before corrosion shows a more distinct grain structure compared to the seamless sample, with some grain refinement due to welding. Post-corrosion (Fig. 4.2(d)), the surface demonstrates noticeable degradation, though less severe than its seamless counterpart. The welded sample exhibits some localized pitting and roughened areas, but the structural changes appear slightly mitigated, suggesting better corrosion resistance in welded regions.

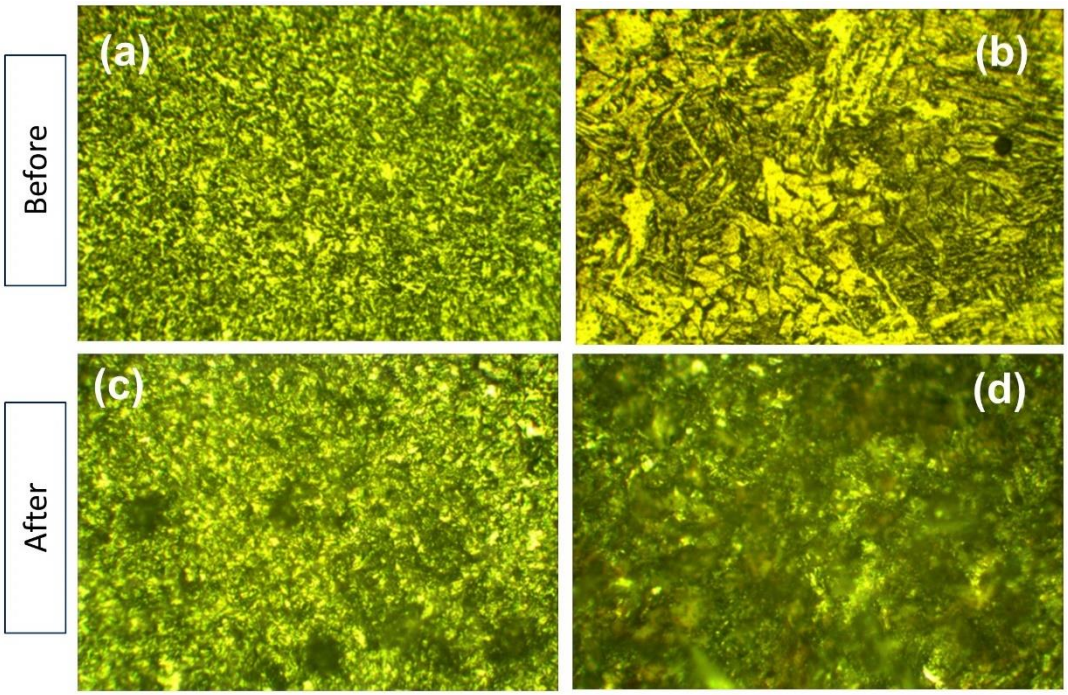

Figure 4.2: Optical micrographs of MS Grade A samples for both before and after corrosion at maginificaiton of 320X after 48 days immersion in seawater: (a) MS Grade A (Before Corrosion), (b) MS Grade A Welded (Before Corrosion), (c) MS Grade A (After Corrosion), (d) MS Grade A Welded (After Corrosion)

4.2.2.3 MS Grade 907 (Seamless)

The seamless MS Grade 907 sample (Fig. 4.3(a)) displays a uniform and tightly packed grain structure prior to corrosion, characteristic of its higher microhardness as observed in Vickers tests. Following exposure to corrosion (Fig. 4.3(c)), the sample undergoes significant structural degradation, with visible pitting, grain boundary dissolution, and a roughened surface texture. The impact of corrosion is more pronounced compared to MS Grade A, as seen in localized structural changes and pitting.

4.2.2.4 MS Grade 907 (Welded)

Before corrosion, the welded MS Grade 907 sample (Fig. 4.3(b)) exhibits a refined grain structure in the welded zones, with sharp, clear boundaries indicative of localized modifications. After corrosion (Fig. 4.3(d)), the microstructure shows visible surface damage, including pitting and uneven textures. However, the degradation appears slightly less intense compared to its seamless counterpart, reinforcing the understanding that welding provides modest resistance against corrosion-induced mechanical deterioration.

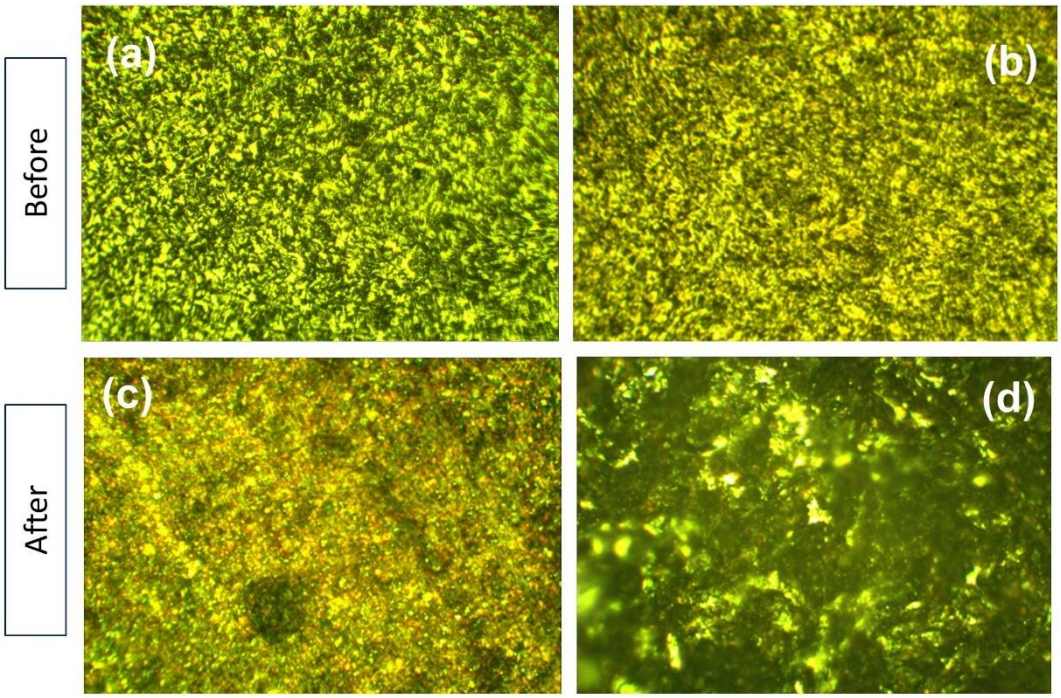

Figure 4.3: Optical micrographs of MS Grade 907 samples for both before and after corrosion at maginificaiton of 320X after 48 days immersion in seawater: (a) MS Grade 907 (Before Corrosion),(b) MS Grade 907 Welded (Before Corrosion), (c) MS Grade 907 (After Corrosion), (d) MS Grade 907 Welded (After Corrosion)

4.2.2.5 Summary of OEM Observations

Upon exposure to the corrosive marine environment, the "after" OEM images reveal notable changes. Across all samples, there is a visible degradation in the grain structure, with roughening and distortion becoming apparent. The microstructures lose their sharpness, displaying evidence of surface degradation, and some areas exhibit the early stages of corrosion-related damage, such as uneven texture and partial grain boundary dissolution. The welded samples appear to have suffered slightly more pronounced

structural alterations, likely due to the inherent susceptibility of welded regions to corrosion attacks.

However, while the OEM images provide a broad understanding of the general impact of corrosion on the surface microstructure, their resolution and magnification limit the detection of more intricate and detailed corrosion effects. Surface irregularities and the extent of micro-cracks are somewhat visible but lack the depth and fine detail necessary for a more comprehensive analysis of corrosion mechanisms.

4.3 Microstructure Inspection: SEM

The Scanning Electron Microscope (SEM) images are vital for capturing subtle corrosion effects. SEM reveals the intricate structural changes that occur post-corrosion, which are less visible under OEM. The two methods together offer a comprehensive understanding, with the OEM capturing broader surface-level changes and SEM diving into the finer, more detailed aspects of corrosion. This advanced imaging technique produces a detailed image of a sample's surface by scanning it with a focused beam of electrons.

4.3.1 Experimental Setup for SEM

For the Scanning Electron Microscopy (SEM) analysis, a comprehensive setup was established to ensure accurate and detailed imaging of the mild steel samples before and after exposure to corrosive environments. The SEM process was conducted in two facilities: the Metallurgical Lab at the Military Institute of Science and Technology (MIST) and the Bangladesh Council of Scientific and Industrial Research (BCSIR). Specimens of 5mm x 5mm x 5mm in size were carefully prepared to meet SEM standards, ensuring they fit within the SEM’s sample chamber and allowed for clear, high-resolution imaging.

The samples were mounted on conductive stubs, cleaned thoroughly to remove contaminants. The SEM instrument employed for this investigation was equipped with secondary and backscattered electron detectors to provide a diverse range of imaging capabilities, such as observing surface morphology and topography, as well as compositional differences. (Fig 4.4)

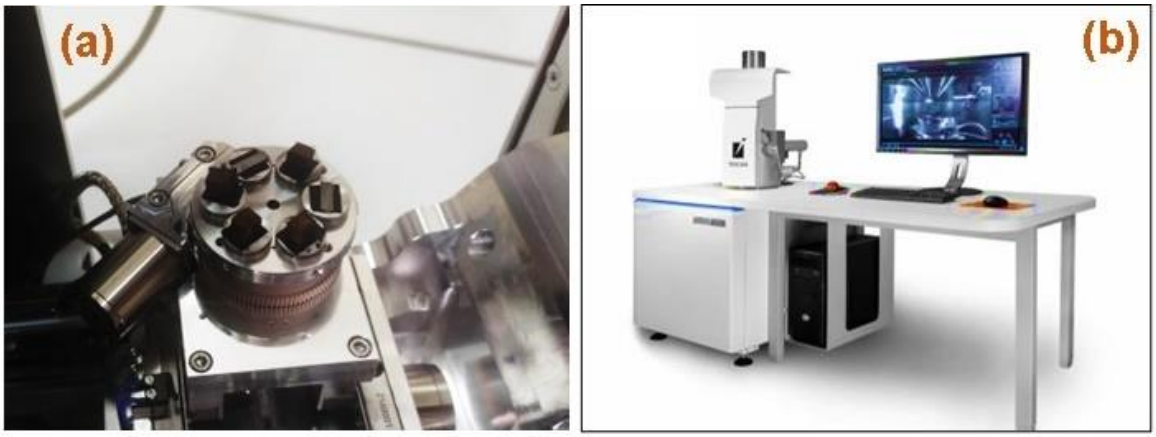

Figure 4.4: Scanning Electron Microscope (SEM) Setup: (a) Specimens placed in the holder inside the SEM chamber, (b) SEM workstation

SEM imaging was performed at various magnifications to observe both the general surface condition and finer details of the corrosion effects. The primary focus was on detecting and comparing pitting, cracks, and surface irregularities that developed as a result of corrosion exposure.

4.3.2 Results and Discussion for SEM

Before corrosion, the microstructures appear relatively uniform and well-ordered, characterized by smooth, elongated grains with minimal signs of degradation. This indicates the stability of the material's crystal structure in its unexposed state. However, after prolonged immersion in the corrosive seawater, the SEM images depict a definite contrast. The observed differences for the pre and post corrosion condition are discussed here separately for each type of sample.

4.3.2.1 MS Grade A (Seamless)

(i) **Before Corrosion.** The seamless MS Grade A sample, as seen in Figure 4.5(a), exhibits a relatively smooth and consistent surface texture prior to corrosion. The SEM micrograph highlights slight surface irregularities likely resulting from the manufacturing process, but no significant defects such as cracks or pits are visible. This uniformity reflects the material's pre-corrosion stability and mechanical integrity.

(ii) **After Corrosion.** Post-corrosion, the seamless sample, illustrated in Figure 4.5(c), shows considerable surface degradation. The SEM image reveals a

roughened surface, with visible pits and signs of grain boundary dissolution. These changes indicate the material's susceptibility to corrosion in the seawater environment, particularly in areas where the grain boundaries are more exposed to corrosive agents.

4.3.2.2 MS Grade A (Welded)

(i) **Before Corrosion.** The SEM micrograph of the welded MS Grade A sample before corrosion, presented in Figure 4.5(b), displays a surface dominated by elongated grooves and directional lines, likely resulting from mechanical finishing or rolling processes. There is no distinct evidence of structural variations that could directly identify the Heat-Affected Zone (HAZ) in this micrograph. The absence of significant surface irregularities suggests that the sample was in a relatively intact state before exposure to corrosive conditions.

(ii) **After Corrosion.** The welded MS Grade A sample of post-corrosion, depicted in Figure 4.5(d), shows a significantly altered surface morphology compared to its pre-corrosion state. The SEM image reveals a porous, sponge-like texture, with rounded protrusions indicating the accumulation of corrosion byproducts. Localized pitting and surface roughness are clearly evident, reflecting areas of strong corrosion attack. This observation shows the increased vulnerability of welded samples to localized corrosion, a trend supported by both static gravimetric and potentiostatic polarization analyses results.

4.3.2.3 MS Grade 907 (Seamless)

(i) **Before Corrosion.** The seamless MS Grade 907 sample, shown in Figure 4.6(a), demonstrates a smooth and uniform surface with minimal defects before corrosion. The SEM micrograph indicates that the grain boundaries are barely visible, reflecting the material's higher micro-hardness compared to MS Grade A. The surface appears compact and free from significant irregularities, indicative of its inherent resistance to environmental stresses in its original state.

(ii) **After Corrosion.** Post-corrosion, the seamless MS Grade 907 sample, visible in Figure 4.6(c), reveals significant surface degradation. The SEM image highlights extensive roughening and the presence of pitting, with regions of material loss

evident across the surface. These features indicate the progression of corrosion, with the material offering limited resistance to the aggressive marine environment.

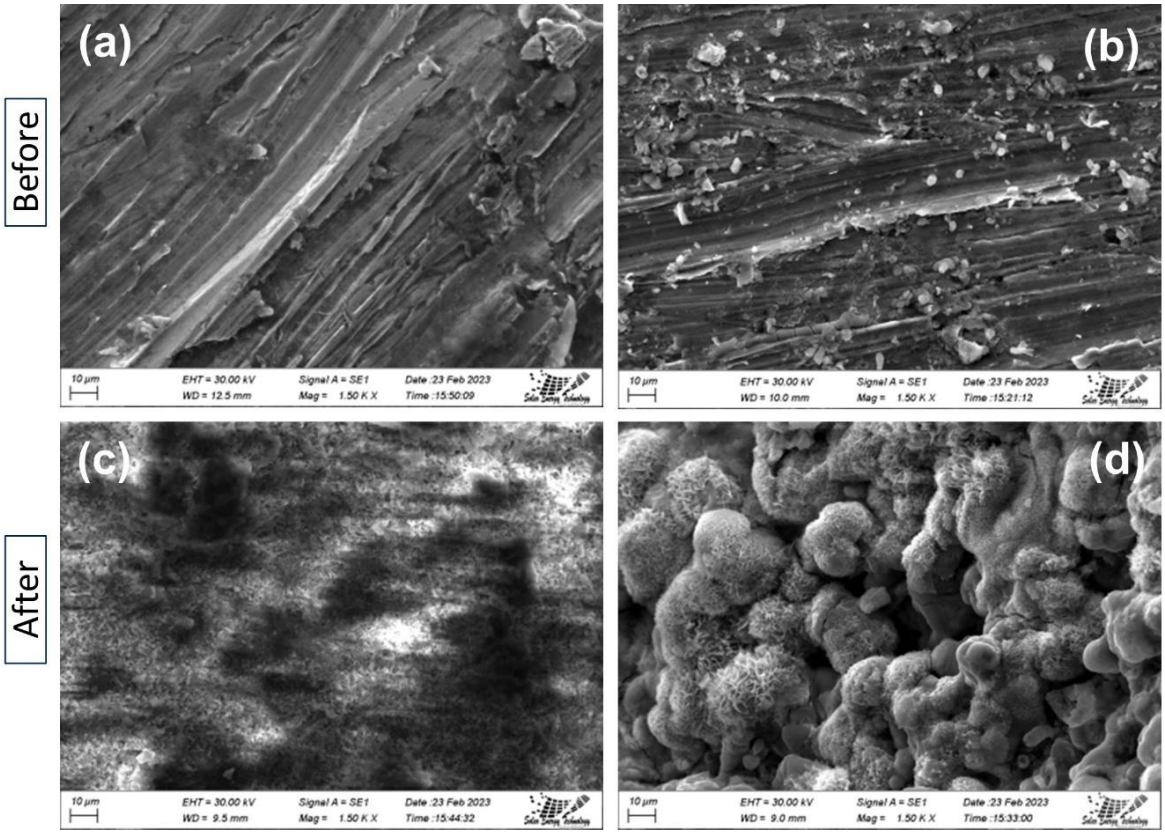

Figure 4.5: Sanning electron micrographs (SEM) of MS Grade A samples for both before and after corrosion at maginificaiton of 1500X after 48 days immersion in seawater: (a) Seamless (Before Corrosion), (b) Welded (Before Corrosion), (c) Seamless (After Corrosion), (d) Welded (After Corrosion)

4.3.2.4 MS Grade 907 (Welded)

(i) **Before Corrosion.** As observed in Figure 4.6(b), the welded MS Grade 907 sample prior to corrosion reveals a relatively smooth surface with very less number of imperfections. They are likely introduced during the welding process. Unlike seamless samples, the surface does not exhibit significant uniformity, and localized regions show slight undulations and debris, possibly residues from post-weld surface preparation.

(ii) **After Corrosion.** The SEM micrograph of the welded MS Grade 907 sample after corrosion, depicted in Figure 4.6(d), shows a significantly changed surface morphology. The previously smooth regions now appear roughened, with distinct, corrosion grooves. These indicate an advanced stage of material degradation. This is

likely driven by localized corrosion activity. The presence of layered structures and visible surface debris further suggests material loss and the deposition of corrosion products. The density of grooves and irregularities appears higher in this sample, emphasizing the vulnerability of welded regions to corrosion-induced surface damage.

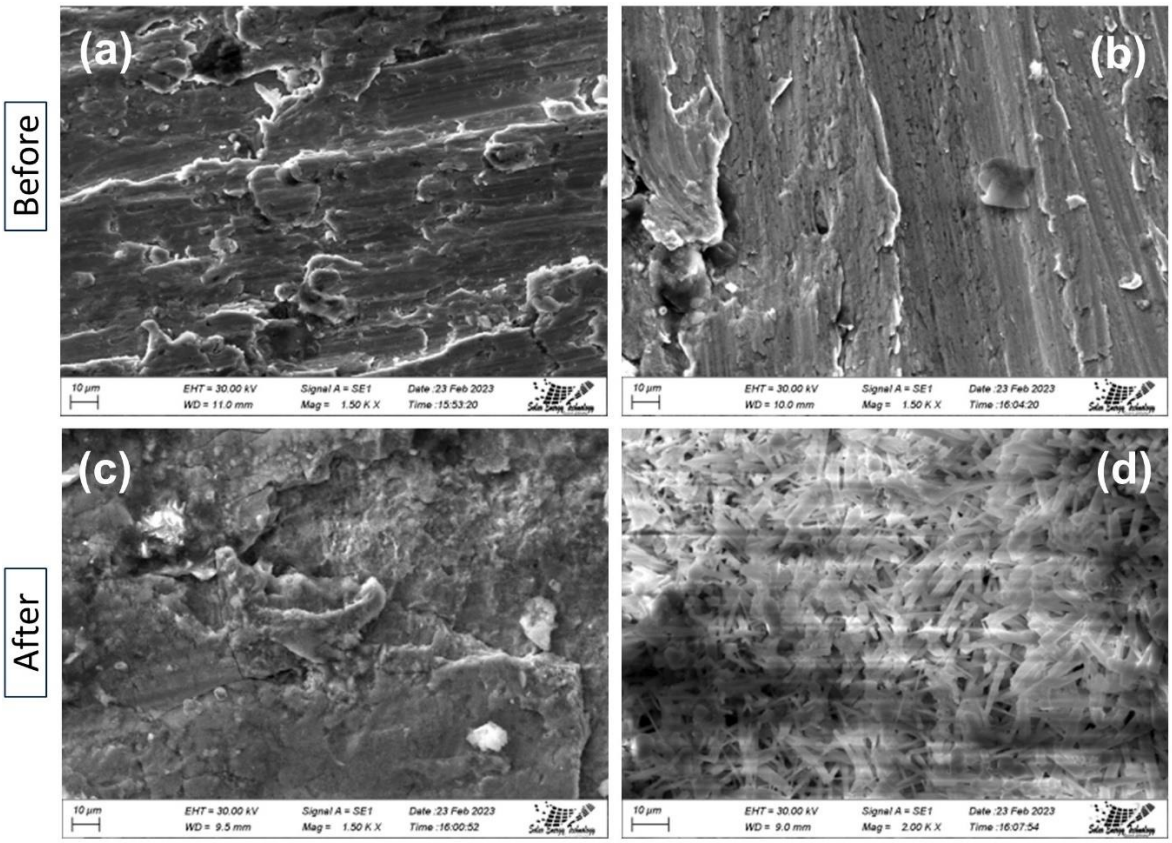

Figure 4.6: Sanning electron micrographs (SEM) of MS Grade 907 samples for both before and after corrosion at maginificaiton of 1500X after 48 days immersion in seawater: (a) Seamless (Before Corrosion), (b) Welded (Before Corrosion), (c) Seamless (After Corrosion), (d) Welded (After Corrosion)

4.4 EDX

Energy Dispersive X-ray Spectroscopy (EDX) is a versatile analytical technique. It is not a standalone corrosion test method, yet it provides invaluable insights into corrosion processes. By analyzing the characteristic X-rays emitted from a sample under electron bombardment, EDX can accurately determine the elemental composition of a material. This capability makes it a vital tool for understanding the formation of corrosion products

and evaluating the effects of corrosion on material properties. In the context of corrosion studies, EDX is particularly useful for:

(i) **Identifying Corrosion Products:** By analyzing the elemental composition of corrosion layers, EDX can help identify specific corrosion products, such as rust (iron oxide), green patina (copper carbonate), or other compounds. This information is essential for understanding the underlying corrosion mechanisms.

(ii) **Evaluating Material Degradation:** EDX can be used to assess the changes in elemental composition that occur within a material due to corrosion. This information can help determine the rate of corrosion, identify the factors influencing corrosion, and evaluate the potential for material failure.

(iii) **Investigating Corrosion Protection:** EDX can be employed to analyze the elemental composition of protective coatings or treatments. By comparing the composition of the coating to the underlying material, identification of effectiveness of the corrosion protection and any signs of degradation or failure can be done. EDX's ability to provide accurate elemental analysis makes it a valuable tool for understanding and investigating corrosion phenomena.

4.4.1 Experimental Setup for EDX

Energy Dispersive X-ray (EDX) analysis was conducted using the same scanning electron microscope (SEM) setup employed for the surface imaging. The SEM system was equipped with an EDX detector, which allowed for the simultaneous collection of elemental spectra alongside high-resolution electron microscopy images.

4.4.2 Results and Discussion for EDX

Based on the EDX results for the before and after corrosion conditions of MS Grade-A and MS Grade-907 (both welded and unwelded samples), several conclusions regarding the corrosion behavior can be drawn. The major elemental changes observed after conducting EDX is shown in Table 4.1:

Table 4.1 Results of EDX Before and After Corrosion

Elements	Weight %							
	MS Grade-A		MS Grade-A (Welded)		MS Grade-907		MS Grade-907 (Welded)	
	Before	After	Before	After	Before	After	Before	After
Fe	79.28	3.35	79.69	44.96	80.22	60.23	84.56	2.19
O	5.49	41.3	7.78	41.7	5.65	24.8	1.9	52.11
C	6.66	7.52	5.35	9.55	6.08	8.96	5.61	11.26

4.4.2.1 Iron (Fe) Content

(i) **Before corrosion:** All samples (MS Grade-A, MS Grade-A welded, MS Grade-907, and MS Grade-907 welded) show high percentages of iron (79.28%, 79.69%, 80.22%, and 84.56% respectively). This is expected, as iron is the primary constituent of mild steel.

(ii) **After corrosion:** After corrosion, the iron content dropped significantly in all cases. For MS Grade-A, it decreased drastically from 79.28% to 3.35%, while in the welded sample, it dropped from 79.69% to 44.96%. Similarly, in MS Grade-907, the iron content decreased from 80.22% to 60.23%, and in the welded sample, it dropped significantly from 84.56% to 2.19%. These reductions indicate substantial material degradation due to corrosion, with more severe losses observed in certain welded samples.

(iii) **Analysis:** The sharp decline in iron content suggests that corrosion has caused substantial oxidation of the surface. Iron atoms have reacted with oxygen in the environment, leading to the formation of corrosion products like iron oxides (Fe_2O_3 or Fe_3O_4). The particularly low Fe content in MS Grade-A and MS Grade-907 welded samples (3.35% and 2.19%, respectively) indicates severe surface degradation.

4.4.2.2 Oxygen (O) Content:

(i) **Before corrosion**: The oxygen content is relatively low, as expected, because the steel surface is not yet oxidized. For MS Grade-A, MS Grade-A welded, MS Grade-907, and MS Grade-907 welded, the oxygen levels are 5.49%, 7.78%, 5.65%, and 1.9%, respectively.

(ii) **After corrosion**: After corrosion, the oxygen content increased dramatically across all samples. In MS Grade-A, it rose from 5.49% to 41.3%, while in the welded sample, it increased from 7.78% to 41.7%. For MS Grade-907, the oxygen content increased from 5.65% to 24.8%, and in the welded sample, it showed the highest rise, from 1.9% to 52.11%. These substantial increases in oxygen content indicate significant oxidation processes occurring during corrosion, especially in the welded samples.

(iii) **Analysis**: The rise in oxygen content confirms the formation of oxides on the surface of the steel due to corrosion. The higher oxygen content in the welded samples (especially MS Grade-907 welded, with 52.11%) points to more aggressive oxidation processes, possibly due to the changes in the microstructure caused by welding. The significant presence of oxygen after corrosion suggests the creation of a thick oxide layer, which reduces the percentage of elemental iron detected.

4.4.2.3 Carbon (C) Content:

(i) **Before corrosion**: Carbon content was relatively stable across MS- Grade A and 907 for both welded and seamless types prior to immersion, ranging from 5.35% to 6.66%.

(ii) **After corrosion**: After corrosion, the carbon content showed slight variations across the samples. In MS Grade-A, it increased from 6.66% to 7.52%, while in the welded sample, it rose from 5.35% to 9.55%. For MS Grade-907, the carbon content increased from 6.08% to 8.96%, and in the welded sample, it showed the highest increase, from 5.61% to 11.26%. These variations suggest that corrosion may have led to the formation of carbon-rich compounds, especially in the welded samples.

(iii) **Analysis**: The modest rise in carbon content after corrosion may indicate the presence of carbon-rich corrosion products, such as carbonates or carbides, which form during the breakdown of steel in corrosive environments. In welded samples, the rise in carbon content is more pronounced, suggesting that the welding process may have influenced the steel's susceptibility to corrosion, possibly by altering the distribution of carbon in the heat-affected zones.

4.4.2.4 General Observations

(i) **Welded Samples**: For MS Grade-907, the welded sample showed more corrosion compared to the unwelded sample, as indicated by the drastic decrease in iron content and higher oxygen levels. However, for MS Grade-A, the unwelded sample experienced more severe corrosion than the welded sample, suggesting that the welding process had a lesser impact on corrosion in this grade. Welding can alter the microstructure of steel, making it more susceptible to localized corrosion, particularly around the weld joints, though this effect varies between steel grades.

(ii) **MS Grade-907 vs. MS Grade-A**: Although both steel grades show significant corrosion, MS Grade-907 retains more iron after corrosion than MS Grade-A. This suggests that MS Grade-907 may have better corrosion resistance, potentially due to differences in alloying elements or microstructure between the two grades.

(iii) **Summary:** The EDX analysis highlights that both grades of mild steel experienced substantial corrosion, with the welded samples showing more severe degradation. The significant reduction in iron content, coupled with the sharp rise in oxygen levels, confirms the formation of corrosion products, primarily iron oxides. The data suggests that MS Grade-907 offers slightly better corrosion resistance than MS Grade-A, but welding has a pronounced effect in accelerating corrosion. This information is crucial for assessing the long-term durability of these materials in marine environments.

4.5 Chemical Composition Test

A chemical composition test is an examination aimed at determining the specific constituents, components, or layers of a particular substance or specimen. This type of test is a significant procedure in materials science, chemistry, environmental science, and quality control, as it provides essential information about the sample taken for analysis.

4.5.1 Experimental Setup for Chemical Composition Test

To conduct the chemical composition test, the Arc/Spark Optical Emission Spectroscopy (OES) method was employed with the assistance of BN Dockyard, Chattogram. The experimental setup for chemical composition testing, employing the Arc/Spark Optical Emission Spectroscopy (OES) method, is displayed in Figure 4.7. This figure shows the equipment used for determining the elemental composition of the materials.The OES method, being destructive, causes the complete deformation or damage of the sample material after the test. Initially, the test was performed on the samples before corrosion. However, it was not continued for the post-corrosion analysis due to its destructive nature, which could alter the corroded metal's properties and state. Furthermore, this method would not be able to capture the surface condition of the corroded metal, thus failing to provide an accurate representation of the corrosion's effects. Nonetheless, it provided valuable insights into the chemical composition of the metals under study.

Figure 4.7: Experimental setup for chemical composition test

4.5.2 Results and Discussion for Chemical Composition Test

The result for Grade-A material is shown in Table 4.2, and Table 4.3 presents the result for Grade-907. In Tables 4.2 and 4.3, three samples of each material were tested, denoted as 1, 2, and 3, respectively. "Mean" indicates the average value of samples 1, 2, and 3, while "SD" stands for standard deviation. Finally, "RSD" represents the relative standard deviation. Calculating the mean, standard deviation (SD), and relative standard deviation (RSD) in the chemical composition test ensures the accuracy and reliability of the results. The mean provides an average value, offering a clear representation of the material's composition across different samples. The standard deviation (SD) highlights the consistency of these values by measuring how much the individual results deviate from the mean. A low SD indicates stability and precision in the measurements. The relative standard deviation (RSD), expressed as a percentage, further contextualizes this variation by comparing the degree of variability to the mean, helping to assess the reliability of the results. Together, these metrics offer a complete picture of both the overall trends and the variability in the material's composition.

Table 4.2 Chemical composition of Grade-A

	C Conc %	Si Conc %	Mn Conc %	P Conc %	S Conc %	Cr Conc %	Mo Conc %	NI Conc %	AI Conc %	Co Conc %	Cu Conc %	Nb Conc %	TI Conc %
1	0.15	0.16	0.26	0.019	0.012	0.028	0.17	0.057	0.034	0.14	0.038	0.026	0.004
2	0.16	0.16	0.26	0.019	0.012	0.028	0.17	0.056	0.033	0.13	0.038	0.027	0.004
3	0.15	0.16	0.26	0.019	0.011	0.028	0.17	0.056	0.033	0.13	0.037	0.026	0.004
Mean	0.15	0.16	0.26	0.019	0.012	0.028	0.17	0.056	0.034	0.13	0.038	0.026	0.004
SD	0.0009	0.0004	0.002	0.0003	0.0004	0.0000	0.0009	0.0006	0.0003	0.0009	0.0002	0.0006	0.000
RSD	0.57	0.25	0.68	1.77	3.25	0.023	0.5	0.98	0.81	0.64	0.43	2.36	0.94

	V Conc %	W Conc %	Pb Conc %	Sn Conc %	As Conc %	Zr Conc %	BI Conc %	Ca Conc %	Ce Conc %	Sb Conc %	Se Conc %	Te Conc %	Ta Conc %
1	0.040	0.089	>0.025	0.005	0.014	0.044	>0.036	0.0009	0.25	0.004	<0.002	0.012	>0.21
2	0.040	0.086	>0.025	0.005	0.011	0.044	>0.036	0.0009	0.25	0.004	<0.002	0.012	>0.21
3	0.041	0.088	>0.025	0.006	0.010	0.044	>0.036	0.001	0.24	0.002	<0.002	0.011	>0.21
Mean	0.040	0.087	>0.039	0.006	0.011	0.044	>0.94	0.0009	0.24	0.003	<0.002	0.012	>0.58
SD	0.0004	0.001	0.000	0.0001	0.002	0.0003	0.0000	0.0001	0.002	0.001	0.0000	0.0004	0.0000
RSD	1.030	1.55	0.000	2.55	16.87	0.63	0.0000	7.07	1.01	31.28	0.0000	3.24	0.0000

	B Conc %	Zn Conc %	La Conc %	N Conc %	Fe Conc %
1	0.001	>0.027	0.006	0.007	98.1
2	0.0009	>0.027	0.006	0.008	98.1
3	0.0008	>0.027	0.006	0.008	98.1
Mean	0.0009	>0.033	0.006	0.008	96.9
SD	0.0002	0.0000	0.0002	0.0003	0.017
RSD	17.12	0.0000	2.69	4.47	0.018

Table 4.3 Chemical composition of Grade-907

	C Cone %	Si Conc %	Mn Conc %	P Conc %	S Conc %	Cr Conc %	Mo Conc %	NI Conc %	AI Conc %	Co Conc %	Cu Conc %	Nb Conc %
1	0.071	0.34	0.43	0.015	0.007	0.33	0.18	0.28	0.038	0.18	0.54	0.04
2	0.071	0.34	0.43	0.016	0.008	0.34	0.18	0.29	0.038	0.18	0.54	0.038
3	0.072	0.34	0.43	0.016	0.008	0.34	0.18	0.29	0.038	0.18	0.54	0.040
Mean	0.071	0.34	0.43	0.016	0.008	0.34	0.18	0.29	0.038	0.18	0.54	0.039
SD	0.0003	0.0006	0.002	0.0004	0.0007	0.0010	0.001	0.0009	0.0001	0.0009	0.002	0.0008
RSD	0.41	0.17	0.45	2.5	9.14	0.4	0.54	0.3	0.32	0.53	0.29	2.03

	TI Conc %	V Conc %	W Conc %	Pb Conc %	Sn Conc %	As Conc %	Zr Conc %	BI Conc %	Ca Conc %	Ce Conc %	Sb Conc %	Se Conc %
1	0.009	0.13	0.087	>0.025	0.003	0.011	0.046	>0.036	0.0010	0.26	0.006	<0.002
2	0.009	0.13	0.086	>0.025	0.003	0.010	0.045	>0.036	0.0010	0.26	0.005	<0.002
3	0.010	0.13	0.086	>0.025	0.003	0.014	0.046	>0.036	0.0009	0.26	0.007	<0.002
Mean	0.009	0.13	0.086	>0.039	0.003	0.012	0.045	>0.96	0.0009	0.26	0.006	<0.001
SD	0.00010	0.0006	0.0007	0.0000	0.0001	0.002	0.0001	0.0000	0.0001	0.003	0.0010	0.0000
RSD	0.930	0.47	0.870	0.0000	1.88	16.48	0.2800	0.0000	6.84	0.99	17.5200	0.0000

	Te Conc %	Ta Conc %	B Conc %	Zn Conc %	La Conc %	N Conc %	Fe Conc %
1	0.013	>0.21	0.0008	>0.027	0.007	0.005	96.7
2	0.012	>0.21	0.0006	>0.027	0.007	0.005	96.7
3	0.013	>0.21	0.0007	>0.027	0.007	0.005	96.7
Mean	0.013	>0.8	0.0007	>0.032	0.007	0.005	95.1
SD	0.0002	0.0000	0.0001	0.0000	0.0003	0.0002	0.010
RSD	1.850	0.0000	12.780	0.0000	3.71	4.7	0.0110

4.6 Experimental Investigation of Hardness

Hardness measures a material's resistance to deformation, typically evaluated through indentation. Various methods are available to assess hardness, each suited to specific applications and materials. The most common hardness tests include Brinell, Rockwell, Vickers, and Knoop, each employing a unique indenter and load application technique. For this research, only the Vickers microhardness and Brinell hardness tests were conducted.

4.6.1 Experimental Setup for Hardness Test

Accurate hardness testing relies on proper setup and calibration, as these ensure the precision and reliability of results. Each hardness testing method requires specific equipment and procedures tailored to the material under evaluation. Adhering to these protocols is essential for obtaining consistent and repeatable measurements.

In this study, the hardness measurements were conducted using a Micro-Vickers Hardness Tester HV-100, with an applied load of 5 kgf for 10 seconds. For Brinell Hardness testing, a load of 187.5 kgf was applied for 20 seconds (Fig 4.8). Ten individual hardness readings were taken for each sample, and the average value was calculated for subsequent analysis.

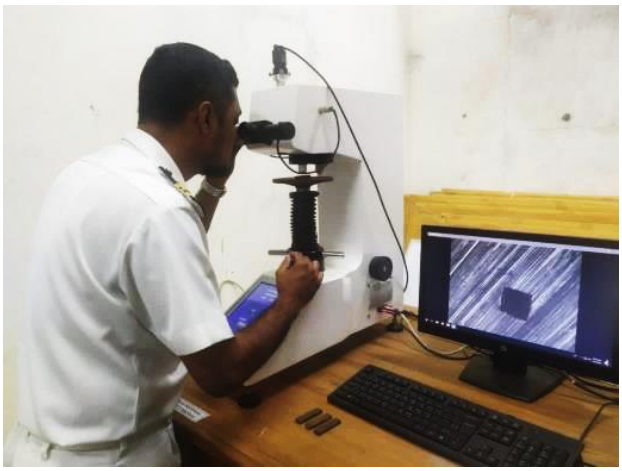

Figure 4.8: Micro-Vickers Hardness Testing

4.6.2 Result and Discussion for Viker’s micro hardness

Figure 4.9 illustrates the Vickers microhardness variations for all four samples, for before and after corrosion condition. The column chart is based on the average of the muliple data taken

for each sample. The average data are presented in a tabular form in table 4.4. In the chart significant reduction in hardness can be seen following exposure to the corrosive environment. There is a slight decrease in the microhardness of Grade-A samples, from 172.7 HV before corrosion to 170.48 HV in after corrosion state. A similar trend is observed in the Grade-A (Welded) coupons on corrosion, where microhardness declined from 186.08 HV to 169 HV. The reduction is more pronounced in Grade 907, where the microhardness decreases from 210.96 HV before corrosion to 192.65 HV, after the corrosion. Likewise, the Grade 907 (Welded) samples follow this trend, with hardness dropping from 214.27 HV to 200.22 HV.

Overall, the results indicate a consistent reduction in microhardness for all four samples after the corrosion process. Notably, the decrease is more significant in the Grade 907 coupons compared to the Grade-A ones. Welding does not appear to significantly alter the trend of decreasing microhardness after corrosion, although slight differences are observed between the welded and non-welded samples. In summary, corrosion led to a measurable reduction in microhardness across all samples tested.

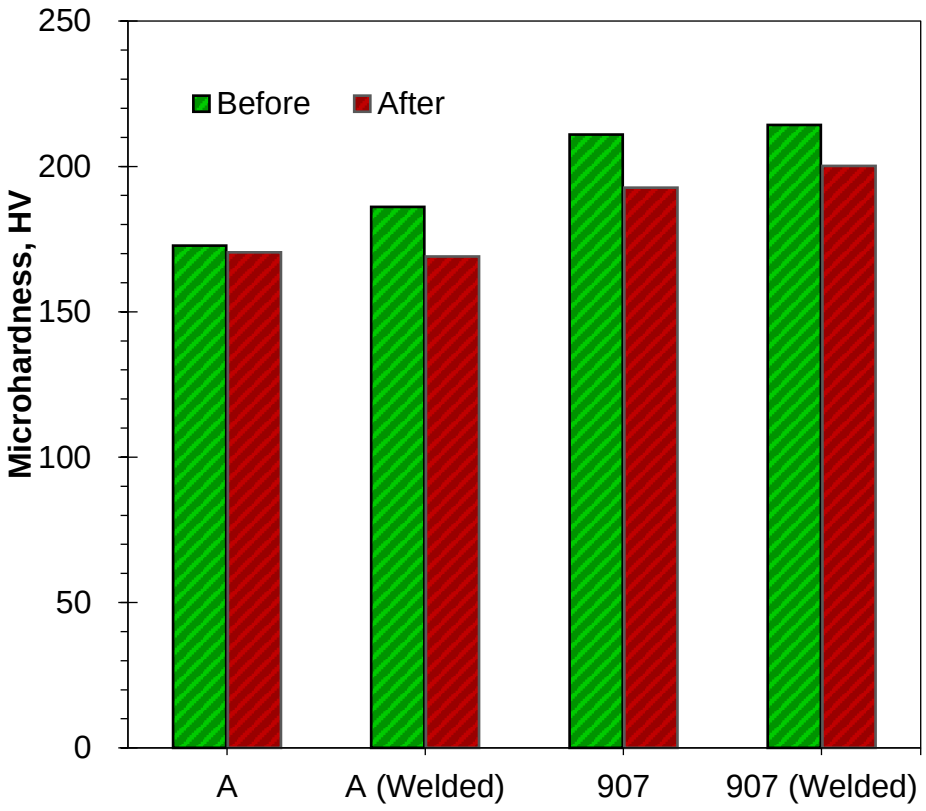

Figure 4.9 Viker's micro hardness for all four samples

Table 4.4 Viker's micro hardness for all four samples before and after corrosion

Material	Before Corrosion (HV)	After Corrosion (HV)	Percentage of Decrease
MS Grade- A	172.7	170.48	1.29%
MS Grade- A (Welded)	186.08	169.0	9.18%
MS Grade- 907	210.96	192.65	8.68%
MS Grade- 907 (Welded)	214.27	200.22	6.56%

Microhardness analysis revealed a significant decrease in hardness for all materials following corrosion. Grade A exhibited a modest 1.29% reduction in microhardness, but this value increased markedly to 9.18% for the welded Grade A sample. While Grade 907 experienced an 8.68% decrease in microhardness, the welded Grade 907 sample showed a slight reduction to 6.56%.

4.6.3 Result and Discussion for Brinell Hardness

Brinell hardness analysis revealed a significant reduction in hardness for all materials following corrosion. The average decrement in hardness after corrosion is summarized in Figure 4.10, providing a comparative analysis of the effects of corrosion on the different materials. MS Grade A experienced a 20.15% reduction in hardness, reflecting a considerable loss of material strength. Welded MS Grade A showed a smaller reduction of 11.94%, indicating that welding may provide some degree of enhanced resistance to corrosion-induced softening.

Similarly, MS Grade 907 exhibited a 29.63% reduction in hardness, with the welded sample showing a slightly lower decrease of 26.61%. These findings highlight that welded samples retained hardness better than seamless ones, suggesting greater mechanical stability under corrosive conditions.The collected data is shown in the chart below:

Figure 4.10 Brinell Hardness Number for all four samples

The table 4.5 presents the average of multiple hardness data set and percentage of deacrese in the materials following corrosion.

Table 4.5 Percentage of Decrement of Brinell Hardness Number after corrosion

Material	Before Corrosion (HV)	After Corrosion (HV)	Percentage of Decrease
MS Grade- A	161.43	128.9	20.15%
MS Grade- A (Welded)	173.73	153.0	11.94%
MS Grade- 907	137.86	97.01	29.63%
MS Grade- 907 (Welded)	147.16	108.0	26.61%

The results from Brinell hardness tests, as presented in Figure 4.7 and Table 4.6, align with the trends observed in micro-Vickers tests, confirming that exposure to the marine environment causes hardness degradation across all materials.

4.7 Tensile Testing

Tensile testing is a fundamental mechanical evaluation used to assess the behavior of metals under tensile (pulling) forces. It is a destructive test, as the tested specimen is subjected to stress until it fractures.

In this process, a specially prepared specimen is secured within a tensile testing machine, which applies a controlled pulling force at a constant rate until the specimen ultimately breaks. During the test, the machine generates a graph that correlates the applied force with the specimen’s elongation or strain, providing critical data on the material's mechanical properties.

4.7.1 Experimental Setup for Tensile Testing

For this research, tensile testing was conducted to assess the impact of corrosion on all four metal types. The tests followed the ASTM E8 standard, utilizing samples with dimensions of 200 mm x 12.5 mm and a gauge length (GL) of 50 mm. Tensile strength values were recorded for 10 samples of each metal type to ensure statistical validity and a comprehensive analysis of the corrosion effects. (Figure 4.11)

Figure 4.11 Experimental setup for Tensile Testing

Producing corroded tensile test specimens as per ASTM standard involves complexities. To overcome this, method of estimating Ultimate Tensile Strength (UTS) from Brinell Hardness Number (BHN) measurements was followed. This approach allowed for a more accurate assessment of the ultimate tensile strength of the corroded metal specimens.

4.7.2 Result and Discussion for Tensile Testing

The test result shown in the Figure 4.12 and Table 4.6 confirms that the UTS for all grades of mild steel decreases following corrosion, with the welded samples generally experiencing a greater reduction in strength compared to the non-welded samples. The reduction in UTS suggests a weakening of the material after exposure to corrosion. This may be attributed to factors such as increased porosity, microstructural alterations, and the presence of corrosion-induced defects that compromise the metal's integrity.

The results demonstrate a notable reduction in UTS after corrosion across all samples:

(i) For MS Grade-A, UTS decreased from approximately 500 MPa before corrosion to around 450 MPa afterward.

(ii) For MS Grade-A (Welded), the UTS exhibited a sharper decline, dropping from about 550 MPa to 400 MPa.

(iii) MS Grade-907 experienced a substantial reduction in UTS, from approximately 450 MPa to 300 MPa.

(iv) MS Grade-907 (Welded) also showed a significant decrease, with UTS reducing from about 500 MPa to 350 MPa.

This trend aligns with the findings from the hardness tests, where a reduction in hardness was observed after corrosion. Additionally, the results are consistent with the data obtained from the EDX analysis (Table 4.1), which showed an increase in carbon and oxygen content and a corresponding decrease in iron content after corrosion. The change in elemental composition, particularly the increase in carbon and oxygen, may have contributed to the reduction in tensile strength by altering the metal's microstructure and corrosion resistance.

Table 4.6 Percentage of Decrement of Ultimate tensile stress after corrosion

Material	% Decrement of UTS after corrosion
Grade A	15.32
Grade A (Welded)	8.11
Grade 907	26.24
Grade 907 (Welded)	20.72

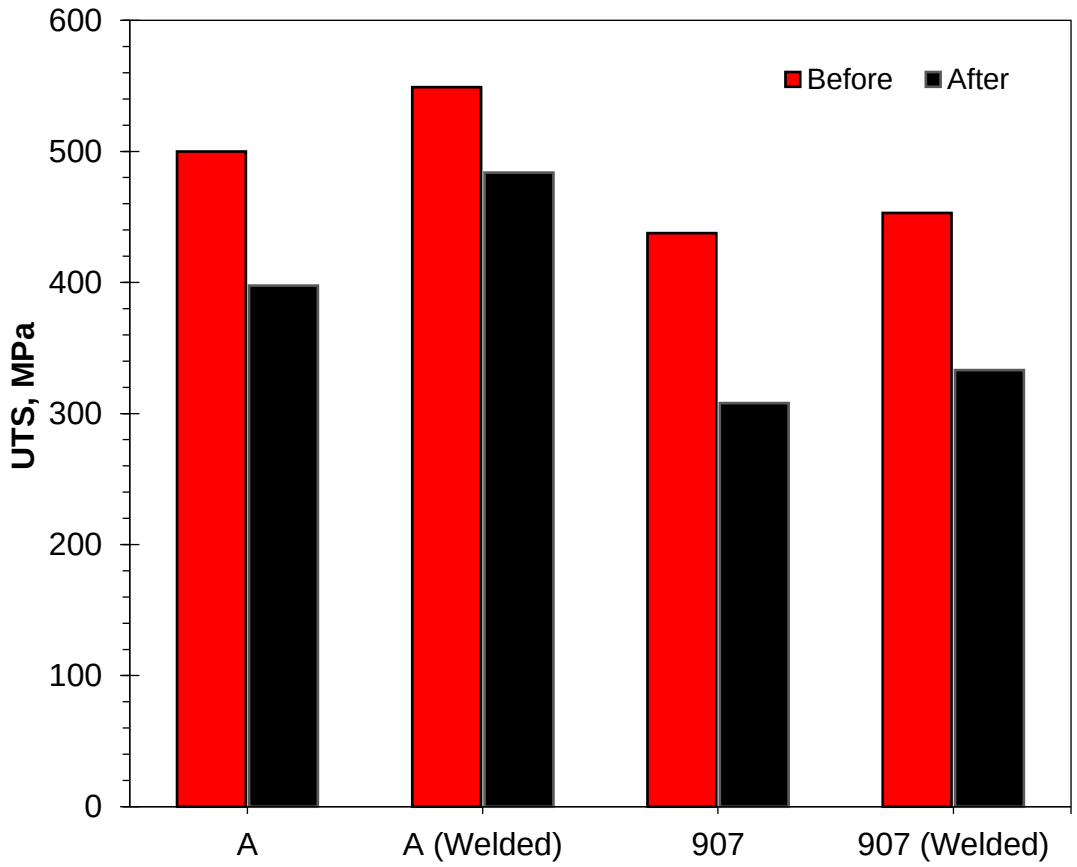

Figure 4.12 Ultimate tensile stress for all four samples before and after corrosion

Interestingly, both welded samples of Grade-A and Grade-907 exhibited a smaller percentage of UTS reduction compared to their non-welded counterparts. However, it is important to note that Grade 907 steels, both welded and non-welded, showed a higher rate of UTS reduction after corrosion compared to the Grade A steels. This suggests that Grade 907 steel may be more susceptible to corrosion-induced tensile strength degradation than Grade A, regardless of the welding process.

CHAPTER FIVE
EFFECT OF VARIATION IN ACIDIC AND ALKALINE MEDIUM IN CORROSION RATE

5.1 Preamble

By examining the effect of varying pH levels, this study aims to explore how pH impacts the corrosion rate of marine-grade mild steel. This chapter focuses on the pH-Varied Test, which evaluates the material's corrosion behavior under different pH conditions to provide insights into its performance in acidic, neutral, and alkaline environments, ultimately contributing to a broader understanding of its durability and potential applications in marine settings.

Overall, this study investigated the corrosion behavior of marine-grade mild steel in a pH-varied environment to assess how changes in pH affect corrosion rates. Corrosion is a complex electrochemical process influenced by factors like pH. This investigation aimed to observe how different pH levels impact corrosion rates and gain a deeper understanding of the material's performance across various pH environments.

5.2 Experimental Setup

Solutions of varying pH levels were prepared, including pH-1, pH-3, pH-5, pH-7, pH-9, pH-11, and pH-13. A pH meter was used to verify and monitor the pH of the solutions. The pH levels ranged from very acidic (e.g., pH-1) to very alkaline (e.g., pH-13). The sample materials were then exposed to these solutions (Fig 5.1).. The effects of the pH levels on the corrosion rate were investigated in the laboratory using the gravimetric method The pH levels shown in the Table 5.1 were applied to all types of samples in each test.

Table 5.1: pH levels used for testing all types of samples in each pH

pH	Distilled Water	HCl (1N)	HCl (1N)	NaOH (1N)	NaOH (1N)
	ml	ml	drop	ml	drop
1	1000	100	2000	-	-
3	1000	1	20	-	-
5	1000	0.01	0.2	-	-
7	1000	-	-	-	-
9	1000	-	-	0.01	0.2

pH	Distilled Water	HCl (1N)	HCl (1N)	NaOH (1N)	NaOH (1N)
	ml	ml	drop	ml	drop
11	1000	-	-	1	20
13	1000	-	-	100	2000

Figure 5.1: Experimental Setup for pH Varied Test

5.3 Results and Discussion

The results from the pH variation tests revealed distinct corrosion behaviors across different pH levels. The corrosion rates were found to vary significantly depending on the acidity or alkalinity of the solution.

5.3.1 Results and Discussion for pH-1 Solution

In the pH variation analysis, the samples exhibited highly reactive behavior in the pH-1 solution. The corrosion rate was highest during the initial period, then gradually decreased and eventually stabilized. Although the overall corrosion trend was similar for all materials, the sample of Grade 907 showed significantly higher corrosion rates in the pH-1 solution. The results are shown in Table 5.2 and Figure 5.2.

Table 5.2: Highest and lowest corrosion rate against materials for pH-1 solution

Material	Highest Corrosion Rate (mmpy)	Lowest Corrosion Rate (mmpy)
MS Grade A	3.66319	2.15292
MS Grade A (Welded)	4.43646	1.98546
MS Grade 907	5.00127	3.35555
MS Grade 907 (Welded)	5.15127	3.35676

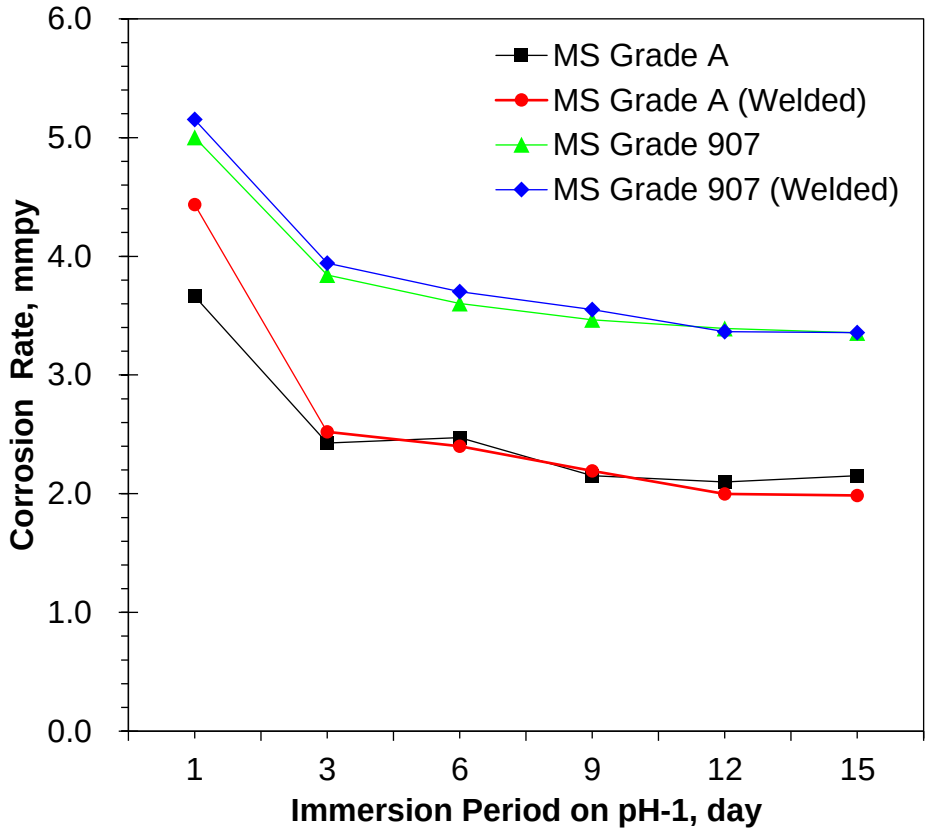

Figure 5.2: Corrosion rate vs Immersion period curve for pH-1 solution

5.3.2 Results and Discussion for pH-3 Solution

In the pH-3 solution, the corrosion rates for all samples were high in the initial period but decreased non-linearly over time, eventually stabilizing in the later stages. Table 5.3 and Figure 5.3 show that the corrosion rate curves for welded Grade A and Grade 907 are nearly identical, indicating that their corrosion rates became almost equal. In contrast to the results from the pH-1 solution, welded Grade 907 exhibited the lowest corrosion rate in the pH-3 solution.

Table 5.3: Highest and lowest corrosion rate against materials for pH-3 solution

Material	Highest Corrosion Rate (mmpy)	Lowest Corrosion Rate (mmpy)
MS Grade A	0.56928	0.12652
MS Grade A (Welded)	0.77178	0.13384
MS Grade 907	0.77165	0.12989
MS Grade 907 (Welded)	0.50774	0.12465

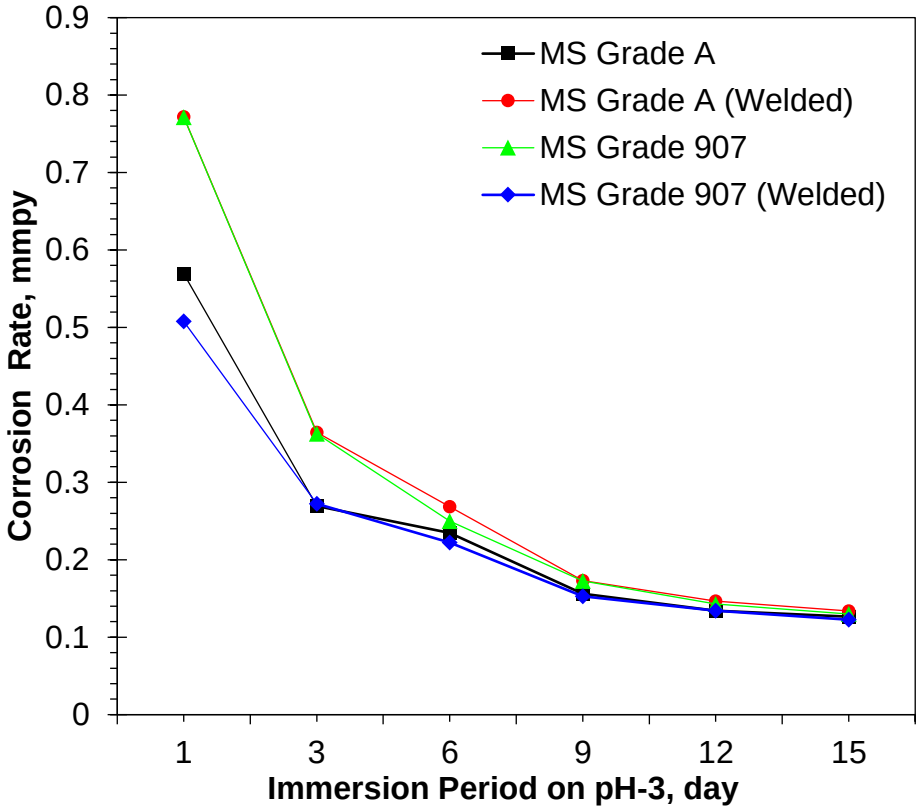

Figure 5.3: Corrosion rate vs Immersion period curve for pH-3 solution

5.3.3 Results and Discussion for pH-5 Solution

Similar to the previous case, in the pH-5 solution, the corrosion rates were highest during the initial period and then decreased, stabilizing after approximately 15 days (Table 5.4 and Figure 5.4). The overall pattern remained the same across all samples, though the corrosion rates differed.

Table 5.4: Highest and lowest corrosion rate against materials for pH-5 solution

Material	Highest Corrosion Rate (mmpy)	Lowest Corrosion Rate (mmpy)
MS Grade A	0.13503	0.07644
MS Grade A (Welded)	0.09721	0.07190
MS Grade 907	0.11206	0.07603
MS Grade 907 (Welded)	0.13776	0.07554

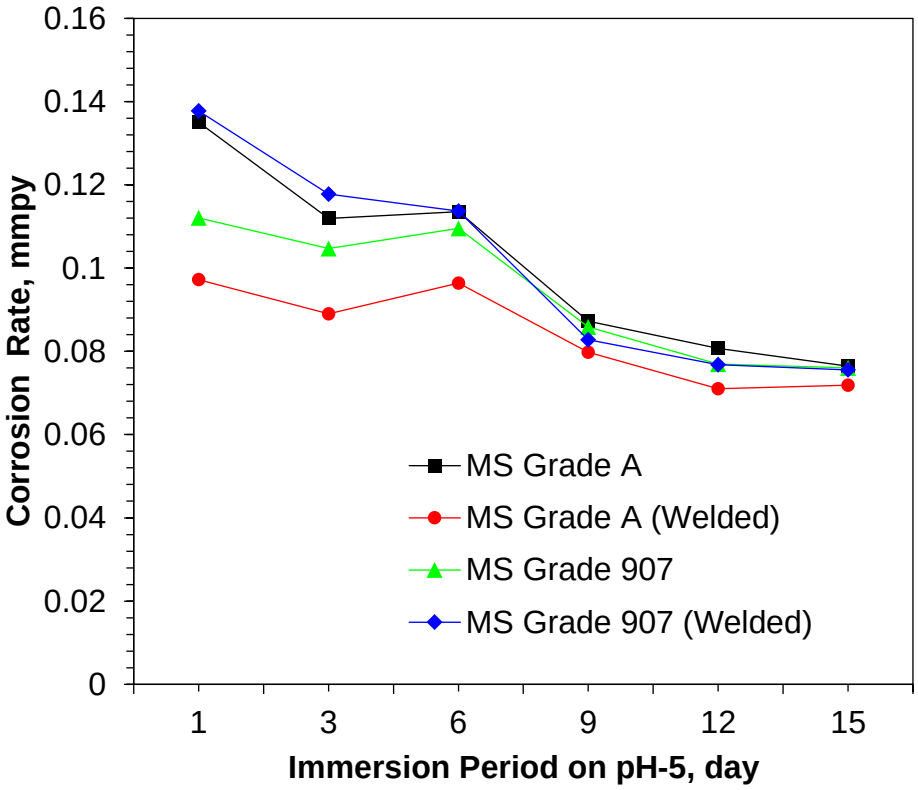

Figure 5.4: Corrosion rate vs Immersion period curve for pH-5 solution

5.3.4 Results and Discussion for pH-7 Solution

In the pH-7 solution, corrosion behavior followed a similar trend as seen in previous solutions (Table 5.5 and Figure 5.5). All samples experienced the highest corrosion rate at the beginning, followed by a sharp decline over time.

Table 5.5: Highest and lowest corrosion rate against materials for pH-7 solution

Material	Highest Corrosion Rate (mmpy)	Lowest Corrosion Rate (mmpy)
MS Grade A	0.29661	0.08553
MS Grade A (Welded)	0.33089	0.08047
MS Grade 907	0.33060	0.07828
MS Grade 907 (Welded)	0.24402	0.09127

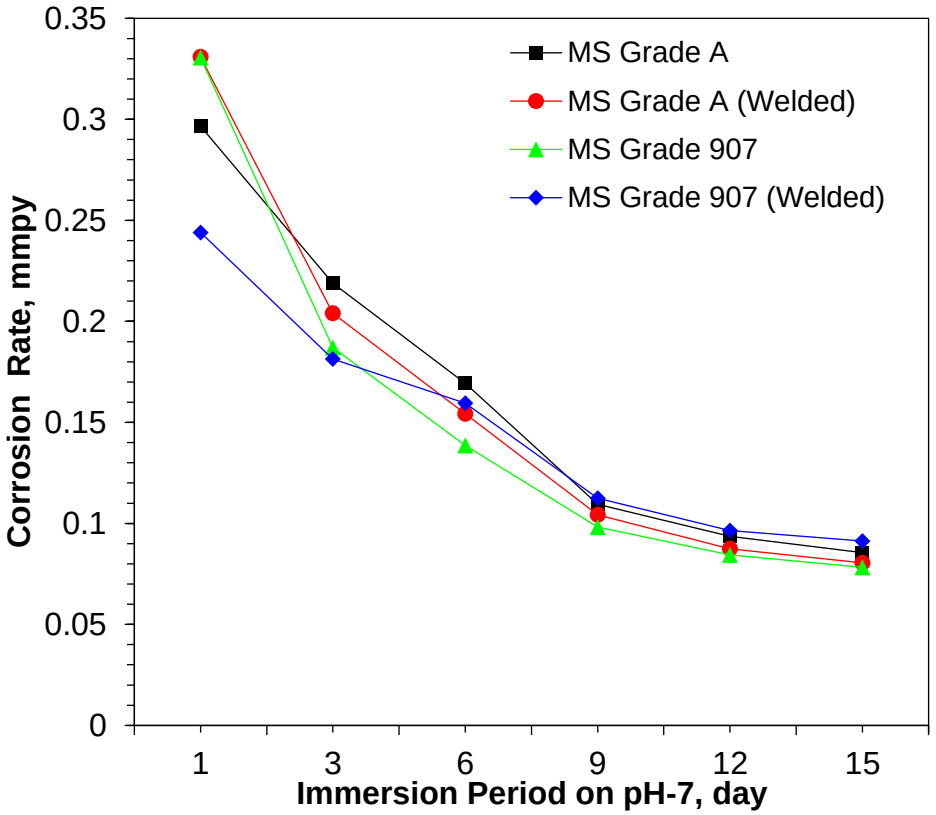

Figure 5.5: Corrosion Rate vs Immersion Period curve for pH-7 solution

5.3.5 Results and Discussion for pH-9 Solution

In the pH-9 solution, the corrosion patterns for all samples were consistent, but it took longer to observe significant corrosion compared to the previous pH levels. Although the highest rates were still observed in the initial stages, the decline in corrosion rate was slower, eventually becoming steady in the later stages (Table 5.6 and Figure 5.6).

Table 5.6: Highest and lowest corrosion rate against materials for pH-9 solution

Material	Highest Corrosion Rate (mmpy)	Lowest Corrosion Rate (mmpy)
MS Grade A	0.19610	0.14286
MS Grade A (Welded)	0.23393	0.15025
MS Grade 907	0.21281	0.14176
MS Grade 907 (Welded)	0.16032	0.13576

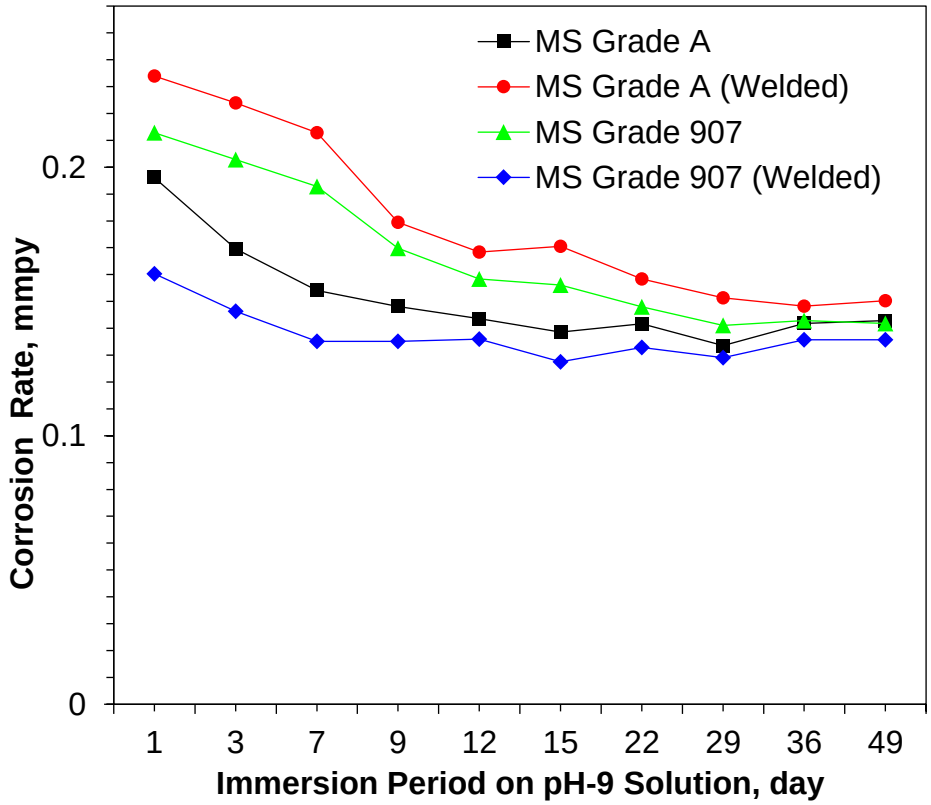

Figure 5.6: Corrosion Rate vs Immersion Period curve for pH-9 solution

Table 5.7: Highest and lowest corrosion rate against materials for pH-11 solution

Material	Highest Corrosion Rate (mmpy)	Lowest Corrosion Rate (mmpy)
MS Grade A	0.09987	0.06238
MS Grade A (Welded)	0.09814	0.06438
MS Grade 907	0.11998	0.06886
MS Grade 907 (Welded)	0.12187	0.07086

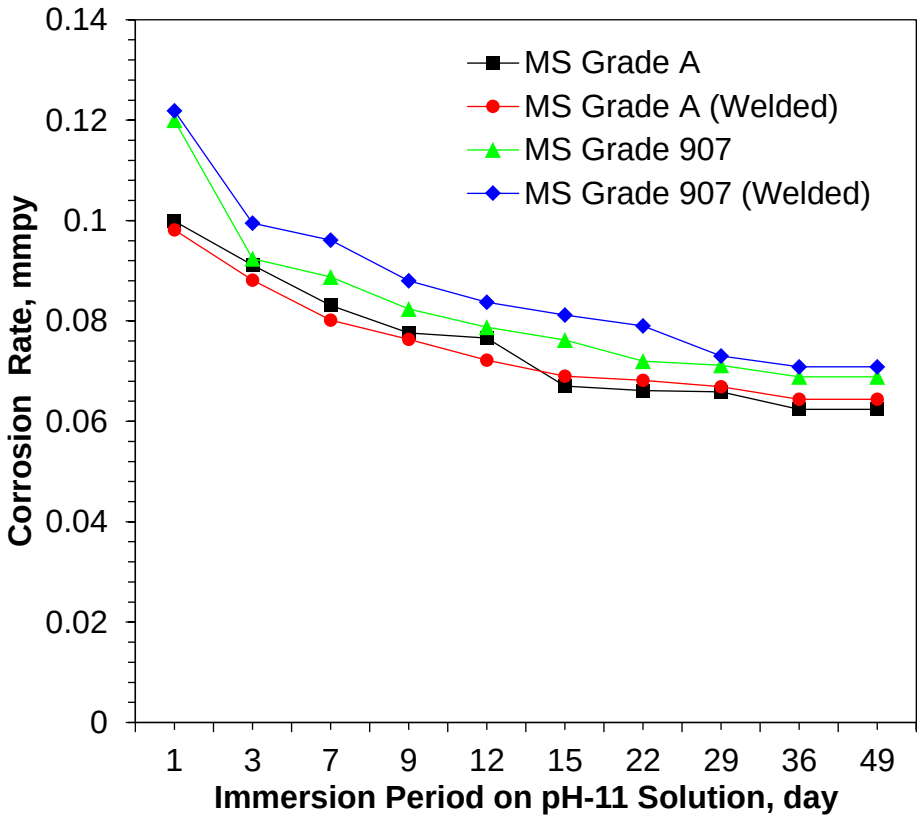

Figure 5.7: Corrosion Rate vs Immersion Period curve for pH-11 solution

5.3.6 Results and Discussion for pH-11 Solution

For pH-11 all the samples had similar trends of loss like the previous pH solutions. But the rate of corrosion is lower than the previous (Table 5.7 and Figure 5.7).

5.3.7 Results and Discussion for pH-13 Solution

No significant corrosion took place in pH-13 solution (Figure 5.8). The pH-13 solution represents a highly alkaline environment, which is typically less aggressive towards mild steel. This stability is reflected in the minimal corrosion rates observed throughout the immersion period.

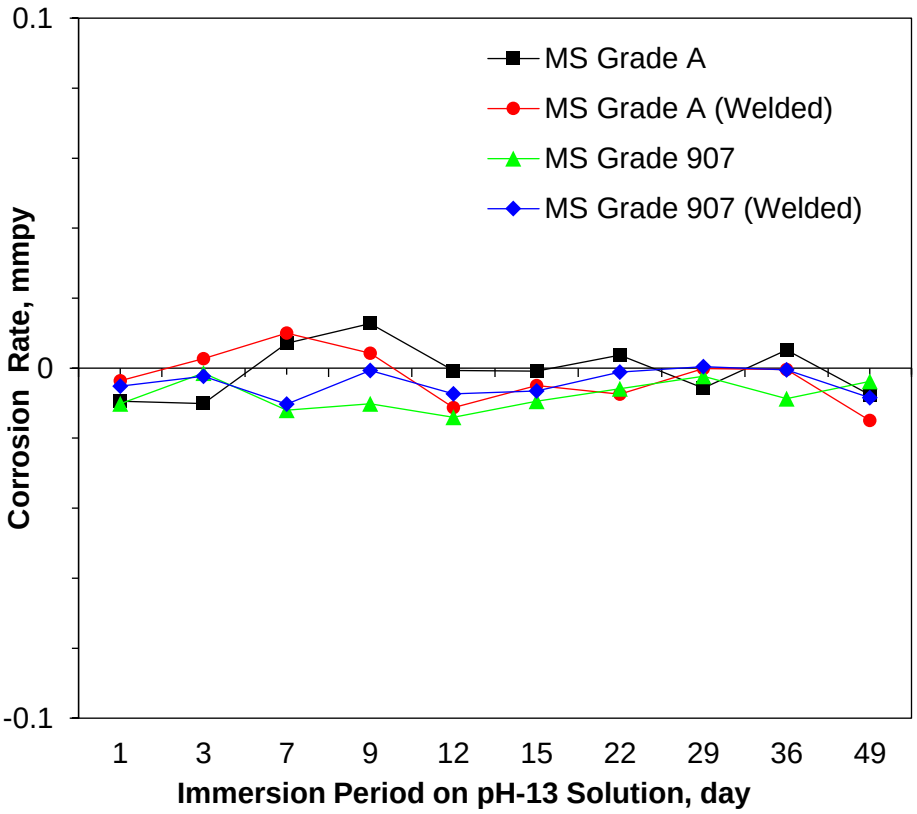

Figure 5.8: Corrosion Rate vs Immersion Period curve for pH-13 solution

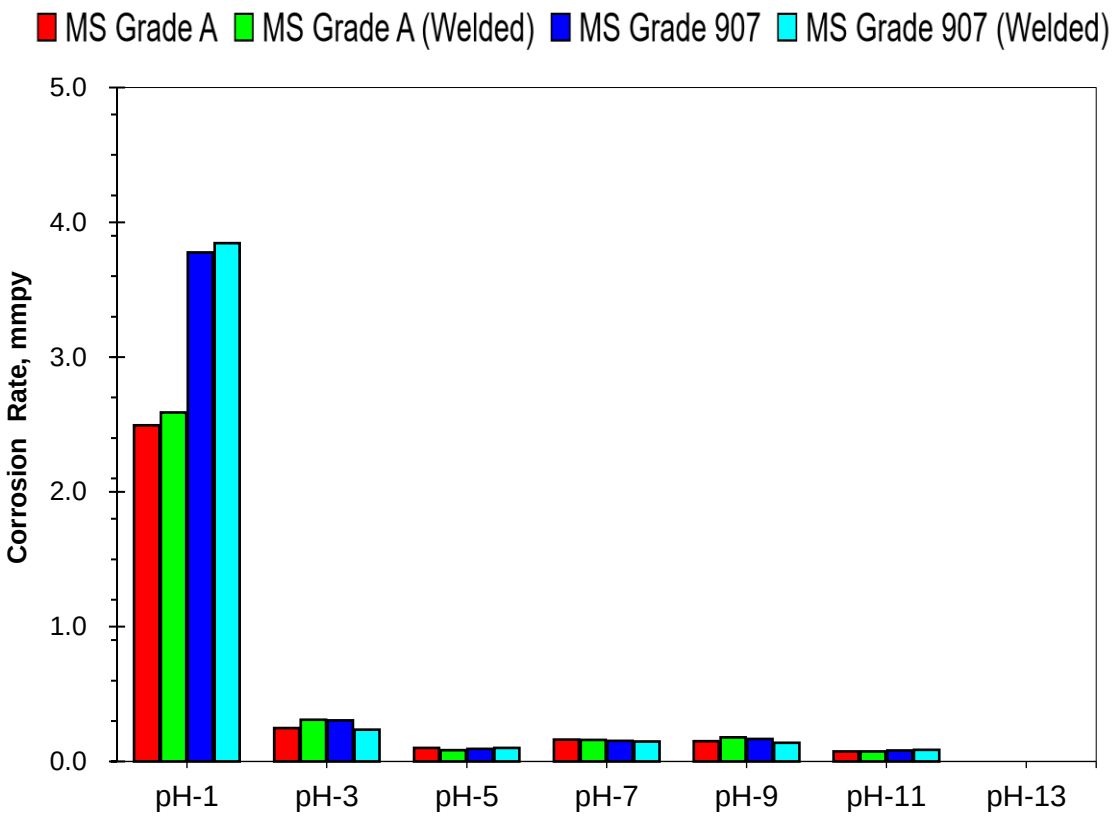

Figure 5.9: Comparison of Corrosion Rates for different pH solutions.

5.4 Summary of Results

The comparative graph of the pH variation analysis (Figure 5.9) clearly shows that the highest corrosion occurred in the pH-1 solution, while the lowest was observed in the pH-13 solution. Both in acidic and alkaline environments, the corrosion rate generally decreased as the pH level increased. In different pH environments, the corrosion rates varied likely due to how aggressive the solution was toward the metal surfaces.

Acidic Environments (Low pH). At lower pH levels, the solution is more corrosive, likely due to the high reactivity of the solution with the metal surface. The aggressive nature of acidic solutions, such as pH-1 or pH-3, might accelerate the breakdown of the metal's surface, leading to higher corrosion rates.

Neutral environment (pH-7). In neutral solutions, the corrosion rate tends to stabilize because the environment is less reactive compared to highly acidic or alkaline solutions. Here, the metal surface might not face such rapid degradation.

Alkaline environments (high pH). In highly alkaline solutions (e.g., pH-11 or pH-13), the metal's corrosion rate is typically lower. The less aggressive nature of alkaline solutions might slow down the interaction between the solution and the metal surface, leading to reduced material loss. In very high pH environments, corrosion can be quite slow, which explains the lowest rates or almost no corrosion at pH 13.

CHAPTER SIX
ELECTROCHEMICAL CORROSION BEHAVIOR

6.1. Introduction

Electrochemical corrosion testing is a fundamental and widely adopted method for assessing the corrosion behavior and durability of materials, particularly in harsh and aggressive environments such as marine settings. This type of test simulates real-world conditions by exposing materials to controlled electrochemical environments and measuring their response to various stimuli. This testing not only helps in estimating the corrosion rate but also plays a vital role in developing corrosion-resistant materials and coatings.

A commonly used electrochemical method in corrosion studies is Potentiostatic Polarization. This technique provides valuable information about corrosion mechanisms, material degradation, and protective behavior. Potentiostatic Polarization focuses mostly on identifying corrosion potentials and currents, offering direct measures of corrosion rate.

In this study, this mentioned method was employed to investigate the corrosion behavior of marine-grade mild steels in the Bay of Bengal water environment. This technique allowed for a comprehensive analysis of the electrochemical response of mild steels and provided a dataset for understanding their long-term corrosion resistance.

Data from 0-day, 1-day, and 3-day intervals were collected and analyzed to establish consistent and comparable data points under testing conditions. The earlier data points provide insights into the initial stages of corrosion initiation and acceleration, which are essential for understanding short-term material behavior.

6.2. Overview of Potentiostatic Polarization Test

6.2.1 Procedure

The test involves immersing three electrodes in an electrolyte. In this system, the working electrode’s potential is controlled relative to a reference electrode using a potentiostat. The resulting current flow is measured against a counter electrode. Then a dataset is created that characterizes the electrochemical behavior of the material.

This test relies on a three-electrode setup to ensure precision and reliability in measurements. In a two-electrode setup, the same electrode is responsible for both current delivery and potential measurement, leading to interference. The current flow can alter the electrode's potential, making it difficult to achieve precise control and accurate measurements. Introducing a third electrode separates these functions: one electrode accurately measures the potential, while another handles the current. This separation ensures precise control of the reactions occurring at the working electrode, resulting in more reliable and interpretable electrochemical measurements. Information on the three electrodes including their purposes is described in the below:

(i) Working Electrode (WE): The WE is the material being studied, where the electrochemical reactions occur. Depending on the potential applied, the WE acts as an anode during oxidation reactions, where material dissolution occurs. The WE serves as a cathode during reduction reactions, such as oxygen reduction or hydrogen evolution. Current density, a key parameter in corrosion analysis, is calculated by dividing the measured current by the surface area of the working electrode (WE). Current density, a key parameter in corrosion analysis, is calculated by dividing the measured current by the surface area of the working electrode (WE). This normalization eliminates the influence of sample size on the results, as larger samples naturally generate higher currents due to their greater exposed surface area. By expressing the current relative to the area, the corrosion behavior of materials can be evaluated and compared consistently, regardless of differences in sample dimensions.

(ii) Counter Electrode (CE): The CE completes the circuit and provides the surface for the reaction opposite to that occurring at the WE. For instance, if the WE is undergoing oxidation (anodic reaction), the CE supports reduction (cathodic reaction). Conversely, if the WE is undergoing reduction, the CE supports oxidation. The oxidation products from the Counter Electrode (CE) can sometimes interfere with the results or contaminate the electrolyte. The manage this issue two points are maintained. Firstly, CE made from inert materials like platinum or graphite are used. These materials are chosen because they produce minimal or non-reactive oxidation products. Secondly, often the CE is placed in a separate compartment connected to the main cell via a salt bridge or porous separator.

(iii) Reference Electrode (RE): The RE provides a stable and consistent reference potential for the WE and precisely controls the potential. A commonly used reference electrode is Silver/Silver Chloride (Ag/AgCl). The RE material is selected not to pass current, ensuring its potential remains constant throughout the test. Without this 3rd electrode, the RE, the potential measurement would depend on the CE. The CE is subject to potential shifts caused by current flow. This would lead to inaccurate results. Hence a RE is used to avoid the error.

To begin with the test using the potentiostat, the WE is initially stabilized at its open-circuit potential (OCP), or Ecorr, where no external current flows, and the rates of oxidation and reduction are naturally balanced. A potentiostat applies a controlled potential sweep to the WE, shifting it from cathodic (negative) to anodic (positive) regions or vice versa. The current flowing in response to the applied potential is measured and recorded. In corrosion testing, the currents are often very small (in microamps or nanoamps) because corrosion reactions are typically slow, and the surface area of the working electrode is usually small. The current reflects the rate of electron transfer from oxidation and reduction reactions, which proceed gradually under normal conditions.

6.2.2 Result Interpretation: Tafel Plot

To represent a wide range of current data applied in the plot logarithmic scale is used. The dataset of potential vs current is then plotted in a chart. In the Tafel plot, the x-axis represents potential (E), indicating voltage, while the y-axis represents current (in amperes). As the potential becomes more positive, represented by movement to the right on the x-axis, the current increases, corresponding to movement upward on the y-axis and vice-versa. By plotting the dataset of potential vs current two different branch or line is found. Where the slope upward to the right is an anodic Tafel slope (ba) and opposite downward is the cathodic tafel slope (bc).

6.2.2.1 Anodic Tafel Slope

The anodic branch, representing the oxidation reaction where the metal loses electrons and undergoes corrosion, slopes upward to the right. This behavior occurs because more positive potentials drive the oxidation process at an accelerated rate, resulting in an increase in

current. As the potential becomes increasingly positive, the metal corrodes faster, producing a higher current and causing the anodic branch to rise.

6.2.2.2 Cathodic Tafel Slope

The cathodic branch, representing the reduction reaction where the environment gains electrons, slopes downward to the left. At more negative potentials, the reduction process is driven at a faster rate, resulting in a larger negative current. This behavior is reflected in the downward slope, as the increased electron flow into the system at more negative potentials produces a greater magnitude of negative current.

6.2.2.3 Extrapolation and Finding Ecorr

The linear regions on the anodic and cathodic curves of the Tafel plot show where the reaction rates follow predictable patterns of behavior. Straight lines are drawn through the linear regions and extrapolated back to intersect at a point on the x-axis, representing Ecorr. This intersection point marks the balance between oxidation and reduction rates. A perpendicular line from Ecorr to the y-axis determines Icorr, the corrosion current, which is directly proportional to the corrosion rate. Near Ecorr, the current does not follow a linear trend due to the simultaneous occurrence of oxidation and reduction reactions, leading to a mixed-control region. Extrapolation eliminates this mixed behavior, ensuring accurate determination of Icorr. Without extrapolation, the results would be imprecise, undermining the reliability of the corrosion rate calculation.

6.2.2.4 Ecorr in Tafel Plots

Ecorr, or the corrosion potential, is the point on a Tafel plot where no net current flows in the system. It is a measure of the metal's tendency to corrode. A more negative Ecorr indicates a higher susceptibility to corrosion. This means the rate of metal dissolving (corrosion) is equal to the rate of protective reactions, like the formation of a surface layer. It represents the balance point where the metal and its environment establish a "natural agreement" on how the corrosion process will proceed under the given conditions.

6.2.2.5 Icorr in Tafel Plots

Icorr, or the corrosion current, is the point on a Tafel plot that indicates the rate of corrosion at the equilibrium potential (Ecorr). It represents the current associated with the natural corrosion process when the metal and its environment are in balance. The higher the Icorr value, the faster the metal is corroding. It is a key indicator of how quickly the metal is losing material to its environment, providing a measure of the severity of the corrosion process.

6.2.3 Formula Used for Corrosion Rate Calculation

The corrosion rate in potentiostatic polarization is calculated using the following formula:

$$CR = \frac{K \cdot Icorr \cdot EW}{A \,.\rho} \tag{6.1}$$

Where,

CR= Corrosion Rate (typically in mm/year or mils/year)

K= A constant that defines the unit for corrosion rate (for mm/year (mmpy), K= 3272

Icorr = Corrosion current in amperes

EW = Equivalent weight of the metal (in grams per equivalent)

A = Testing surface area in cm^2

ρ = Density of the metal (in g/cm^3)

6.3 Methodology

6.3.1 Experimental Setup

The mild steel samples were polished to a mirror-like finish using silicon carbide (SiC) emery paper. Wet polishing was performed to ensure the required smoothness for accurate testing. A controlled surface area of 6.5 mm x 4 mm of the mild steel sample was exposed to the electrolyte, with the remaining surface insulated using Teflon tape.

The test was controlled via a Gamry Framework™ Series G 300™ Potentiostat/Galvanostat/ZRA. The system interfaced with data acquisition software,

controlled test parameters and recorded real-time data. The test was conducted using a standard three-electrode setup:

a) Working Electrode: The mild steel sample.

b) Reference Electrode: A Silver/Silver Chloride Electrode (Ag/AgCl).

c) Counter Electrode: A platinum electrode.

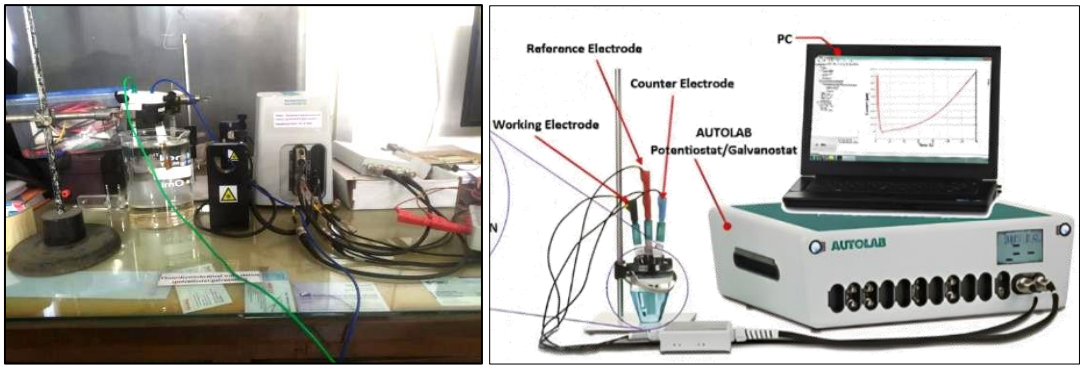

Figure 6.1: Gamry Framework™ Series G 300™ Potentiostat

Before each test, the Open Circuit Potential (OCP) of the sample was measured to establish a stable baseline. For the potentiostatic polarization test, polarization scans were performed from the OCP in both anodic and cathodic directions using a constant scan rate of 0.50 mV/s.Real seawater from the Bay of Bengal (St Martins Anchorage Point, Teknaf), was used as the electrolyte. The resulting polarization curves were analyzed to calculate corrosion potential (Ecorr), corrosion current (Icorr), and corrosion rate, following ASTM G102 standards.

6.3.2 Generation of Tafel Plots

The Tafel plots were generated (figure 5.1 to 5.12) by plotting the logarithm of the current (log(i)) against the applied potential (V). These plots were used to determine key corrosion parameters, such as the corrosion potential (Ecorr) and corrosion current (Icorr). These values were extracted from the intersection of the anodic and cathodic Tafel lines. The collected data provided crucial understandings into the corrosion rate of the samples.

6.4 Data and Analysis

6.4.1 Comparison among 0-Day Results

The corrosion behavior of MS Grade A and MS Grade 907, in both welded and unwelded forms, was analyzed through Tafel plots (Figures 6.2 to 6.5) and associated data summarized in Table 6.1. Among the samples, the welded MS Grade A exhibited the most positive Ecorr value of -0.592 V (Figure 6.3), indicating reduced anodic activity and slower initial oxidation tendency. In contrast, the unwelded MS Grade 907 showed the most negative Ecorr value of -0.664 V (Figure 6.4), suggesting higher susceptibility to corrosion due to its stronger anodic behavior. This difference highlights the role of material composition and structural integrity in influencing corrosion susceptibility.

Table 6.1: Potentiostatic Polarization Analysis Result for 0 day

Sample	Ecorr (V)	Icorr (A)	Corrosion Rate (mm/year)
MS Grade A	-0.655	1.8753E-5	0.82826
MS Grade A, welded	-0.592	2.467E-5	1.0471
MS Grade 907	-0.664	2.5711E-5	1.1204
MS Grade 907, welded	-0.645	4.5726E-5	1.9409

When examining the Icorr values, the welded MS Grade 907 displayed the highest current of 4.5726E-5 A (Figure 6.5), reflecting accelerated oxidation and the most rapid corrosion among all samples. Correspondingly, this sample also exhibited the highest corrosion rate of 1.9409 mm/year, confirming its lower corrosion resistance. On the other hand, the unwelded MS Grade A showed the lowest Icorr of 1.8753E-5 A (Figure 6.2), resulting in the slowest oxidation rate and the lowest overall corrosion rate of 0.82826 mm/year, demonstrating its superior performance in resisting corrosion. These trends suggest that while Ecorr indicates the tendency for anodic or cathodic behavior, Icorr more directly correlates with the actual rate of material degradation.

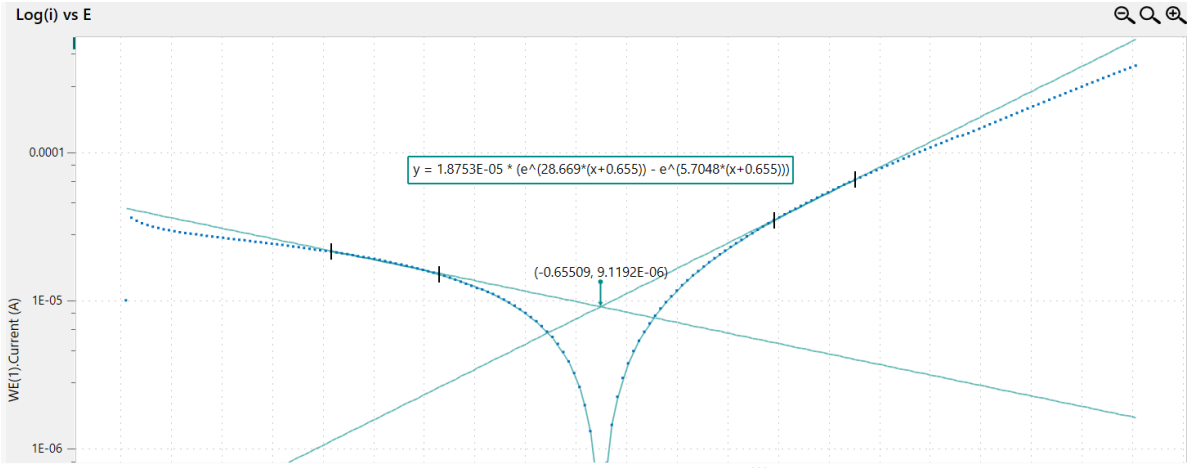

Figure 6.2: Tafel Plot of MS Grade A for 0 day

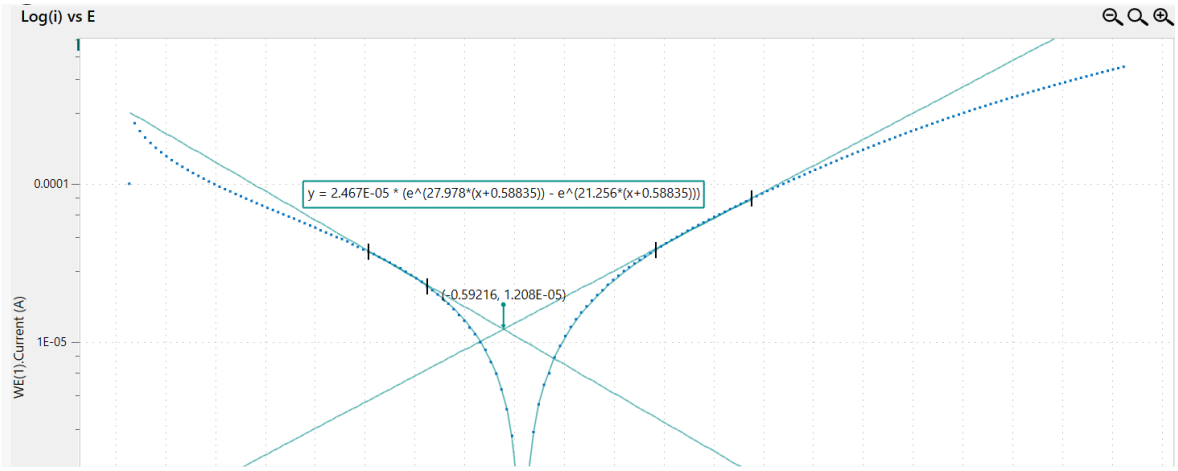

Figure 6.3: Tafel Plot of MS Grade A (Welded) for 0 day

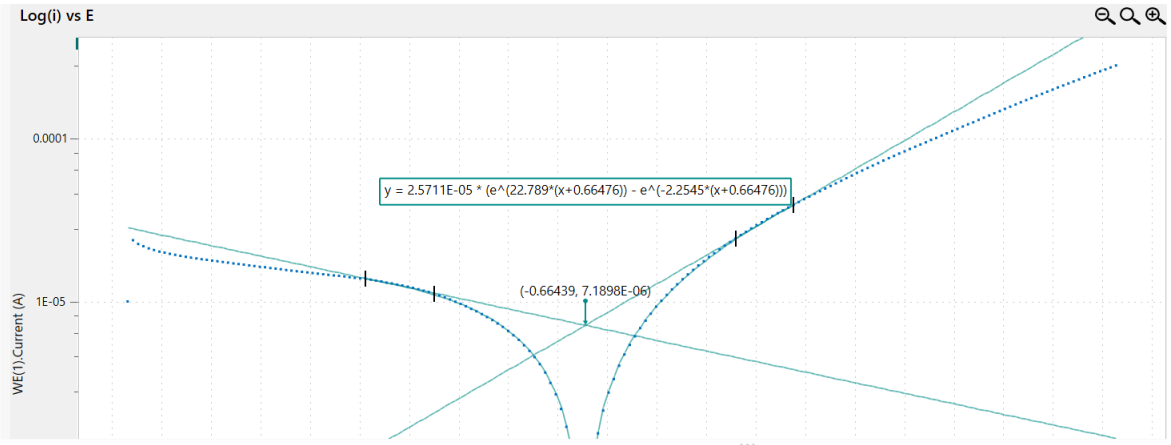

Figure 6.4: Tafel Plot of MS Grade 907 for 0 day

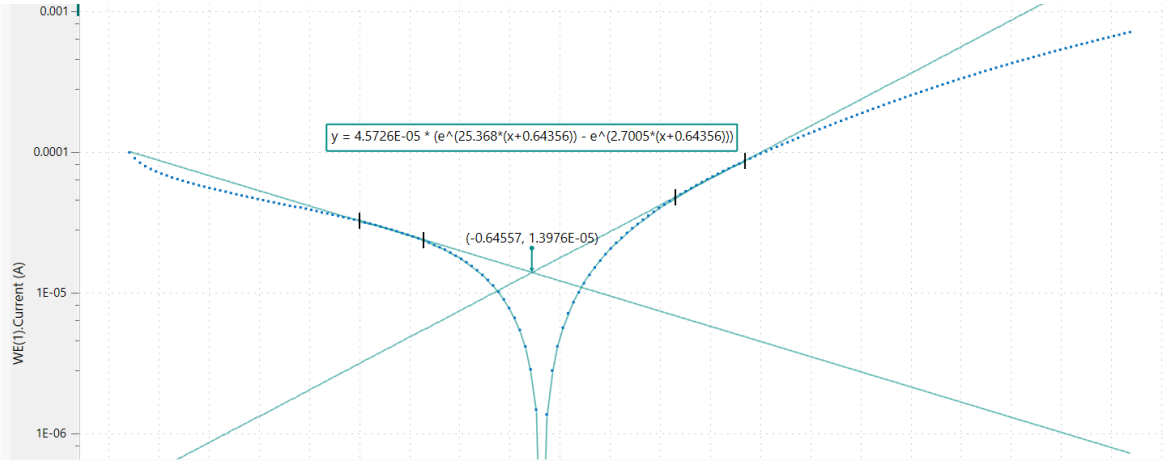

Figure 6.5: Tafel Plot of MS Grade 907 (Welded) for 0 day

The impact of welding was evident across both steel grades. The welded samples of both MS Grade A and MS Grade 907 consistently exhibited higher Icorr values and faster corrosion rates than their unwelded counterparts. For example, the welded MS Grade 907 sample (Figure 6.5), despite having a more positive Ecorr of -0.645 V than its unwelded counterpart (Figure 6.4), displayed significantly higher Icorr and corrosion rate, confirming the dominant role of current in driving corrosion. These findings emphasize the need for additional protective measures at welding lines to mitigate localized corrosion in marine environments.

6.4.2 Comparison among 1-Day Results

The corrosion behavior of MS Grade A and MS Grade 907, in both welded and unwelded forms, was analyzed after 1 day of exposure, based on the Tafel plots (Figures 6.6 to 6.9) and the data summarized in Table 6.2.

Table 6.2: Potentiostatic Polarization Analysis Result for 1 day

Sample	Ecorr (V)	Icorr (A)	Corrosion Rate (mm/year)
MS Grade A	-0.707	2.1846E-05	0.96486
MS Grade A, welded	-0.66079	0.00022549	9.5711
MS Grade 907	-0.70613	2.4128E-05	1.0514
MS Grade 907, welded	-0.71287	4.8063E-05	2.0401

The MS Grade A, welded sample exhibited the most positive Ecorr value of -0.66079 V (Figure 6.7), indicating reduced anodic activity and slower initial oxidation. In contrast, the unwelded MS Grade 907 showed the most negative Ecorr value of -0.70613 V (Figure 6.8),

highlighting higher susceptibility to corrosion due to its stronger anodic behavior. These trends were consistent with the observations from the 0-Day results, with welded samples tending toward more positive Ecorr values and unwelded samples showing greater susceptibility to anodic reactions.

In terms of Icorr, the welded MS Grade A displayed a significant increase to 0.00022549 A (Figure 6.7), reflecting accelerated oxidation and rapid corrosion, which was also confirmed by its intensely higher corrosion rate of 9.5711 mm/year. This corrosion rate was notably higher than any other sample, showing the pronounced impact of welding on corrosion susceptibility. On the other hand, the unwelded MS Grade A exhibited a much lower Icorr of 2.1846E-5 A(Figure 6.6), with a corresponding corrosion rate of 0.96486 mm/year, demonstrating significantly better corrosion resistance than its welded counterpart.

For MS Grade 907, welded sample exhibited the highest Icorr of 4.8063E-5 A(Figure 6.9) and a corrosion rate of 2.0401 mm/year, further confirming the trend of higher corrosion susceptibility in welded samples. Meanwhile, the unwelded MS Grade 907 displayed an Icorr of 2.4128E-5 A(Figure 6.8), with a corrosion rate of 1.0514 mm/year, showing a performance comparable to that of the unwelded MS Grade A sample but still inferior to the unwelded MS Grade A in terms of overall resistance.

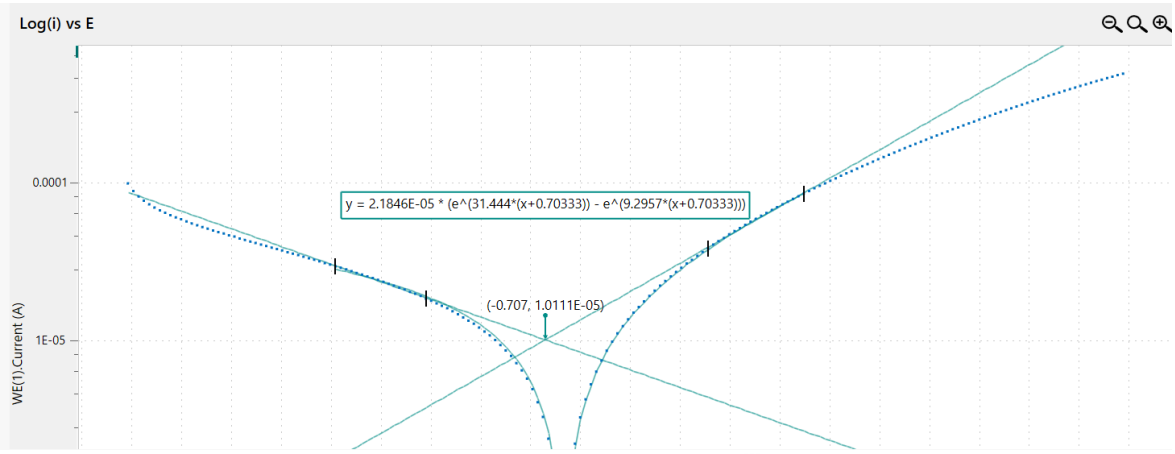

Figure 6.6: Tafel Plot of MS Grade A for 1 day

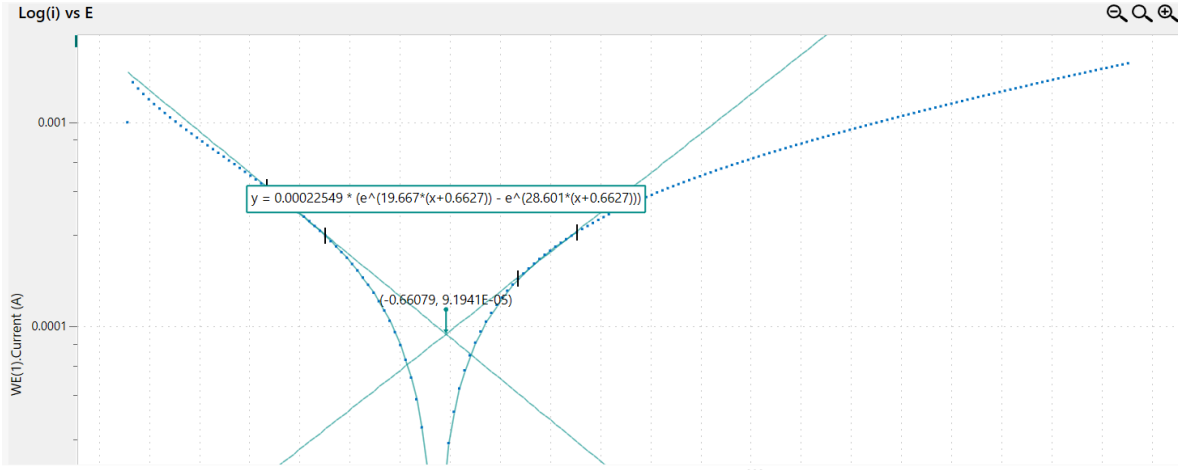

Figure 6.7: Tafel Plot of MS Grade A (Welded) for 1 day

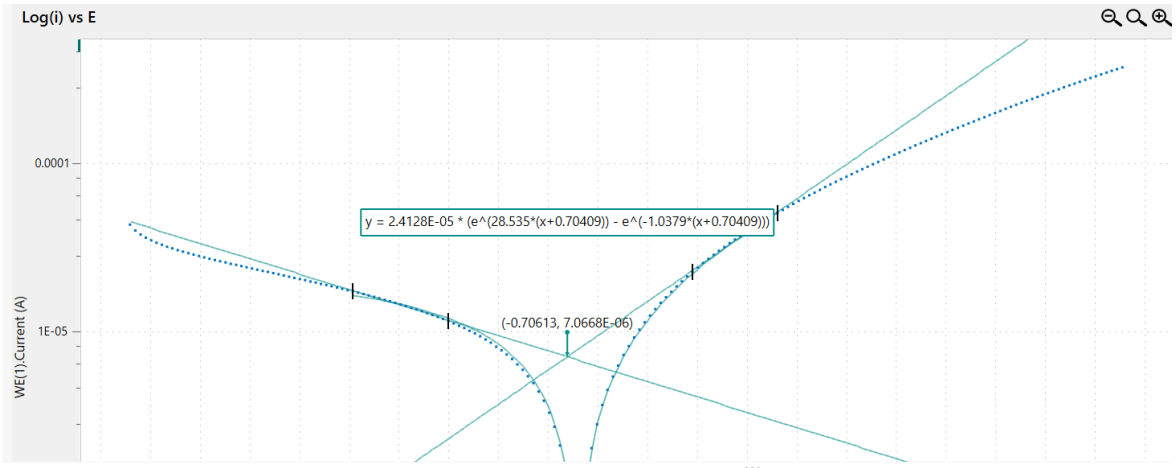

Figure 6.8: Tafel Plot of MS Grade 907 for 1 day

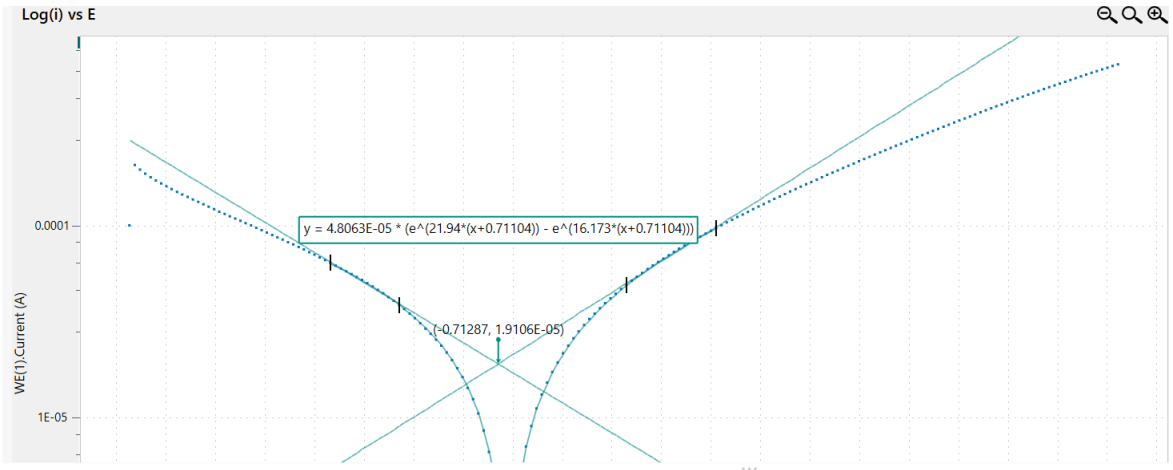

Figure 6.9: Tafel Plot of MS Grade 907 (Welded) for 1 day

The 1-Day results reaffirm that welding consistently increases the Icorr values and corrosion rates across both steel grades. The findings emphasize the need for protective measures at weld sites, as welding introduces structural vulnerabilities that accelerate material

degradation. The correlation between Icorr and corrosion rate was particularly evident, with the welded MS Grade A sample showing the highest current and correspondingly the highest corrosion rate among all samples.

6.4.3 Comparison among the 3rd Day Results

The corrosion behavior of MS Grade A and MS Grade 907, in both welded and unwelded forms, was analyzed after 3 days of exposure using the Tafel plots (Figures 6.10 to 6.13) and the data summarized in Table 6.3.

Table 6.3: Potentiostatic Polarization Analysis Result for 3 day

Sample	Ecorr (V)	Icorr (A)	Corrosion Rate (mm/year)
MS Grade A	-0.70582	2.3149E-05	1.0224
MS Grade A, welded	-0.70678	0.00014319	6.0778
MS Grade 907	-0.70999	2.0597E-05	0.89757
MS Grade 907, welded	-0.72666	3.096E-05	1.3141

Among the samples, the unwelded MS Grade A displayed the least negative Ecorr value of -0.70582 V (Figure 6.10), indicating better resistance to anodic reactions. On the other hand, the MS Grade 907, welded exhibited the most negative Ecorr of -0.72666 V (Figure 6.13), reflecting the highest susceptibility to corrosion among all samples. These results highlight that after 3 days of exposure, welded samples, especially MS Grade 907, showed a greater tendency for anodic activity compared to their unwelded counterparts.

The Icorr values further validated these observations. The welded MS Grade 907 displayed the highest Icorr of 3.096E-5 A(Figure 6.13), corresponding to the highest corrosion rate of 1.3141 mm/year. This reinforced the significant impact of welding on accelerating corrosion. In contrast, the unwelded MS Grade A showed the lowest Icorr of 2.3149E-5 A(Figure 6.10) and the lowest corrosion rate of 1.0224 mm/year, confirming its superior corrosion resistance.

The welded MS Grade A sample exhibited an Ecorr of -0.70678 V (Figure 6.11), slightly more negative than its unwelded counterpart, suggesting increased anodic susceptibility. Its Icorr was 0.00014319 A, with a corrosion rate of 6.0778 mm/year, showing a significant reduction compared to its 1-Day corrosion rate but still higher than that of the unwelded MS Grade A. For MS Grade 907, the unwelded sample exhibited an Icorr of 2.0597E-5 A(Figure

6.12), with a corrosion rate of 0.89757 mm/year, making it slightly more resistant than its welded form but still less resistant compared to the unwelded MS Grade A.

By the 3rd day, the corrosion rates showed a tendency to stabilize, reflecting the material's adjustment to the corrosive environment. However, welding remained a critical factor in accelerating corrosion across both grades, with welded samples consistently showing higher Icorr and corrosion rates compared to their unwelded counterparts. The correlation between Icorr and corrosion rate persisted, as samples with higher Icorr consistently exhibited faster material degradation. The data further underscores the importance of protective measures at weld sites, especially for MS Grade 907, which demonstrated the highest corrosion susceptibility under prolonged exposure.

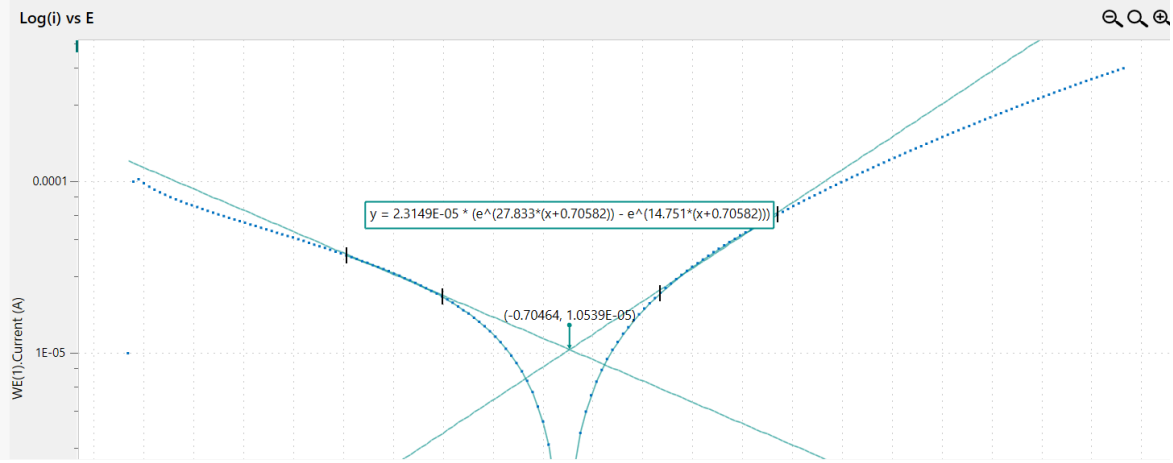

Figure 6.10: Tafel Plot of MS Grade A for 3 day

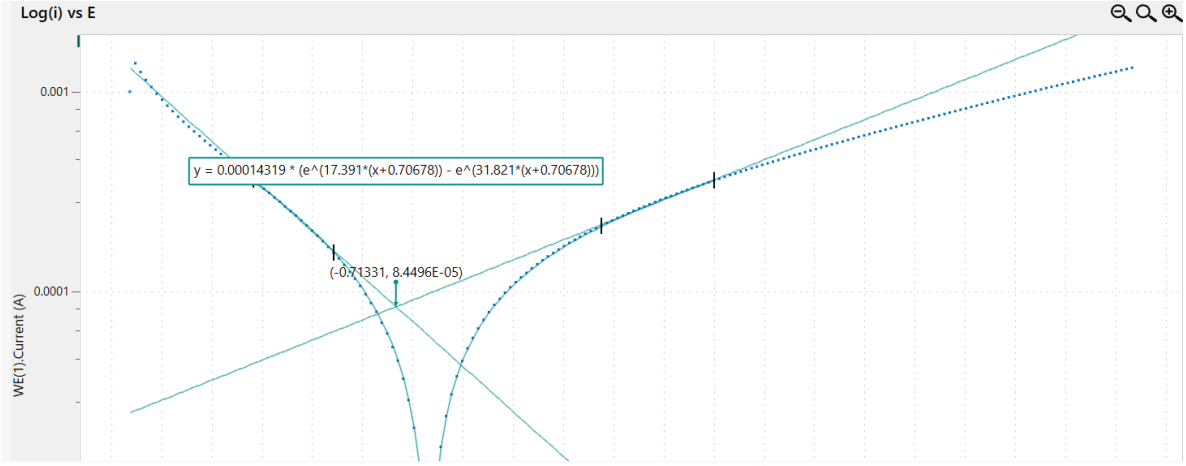

Figure 6.11: Tafel Plot of MS Grade A (Welded) for 3 day

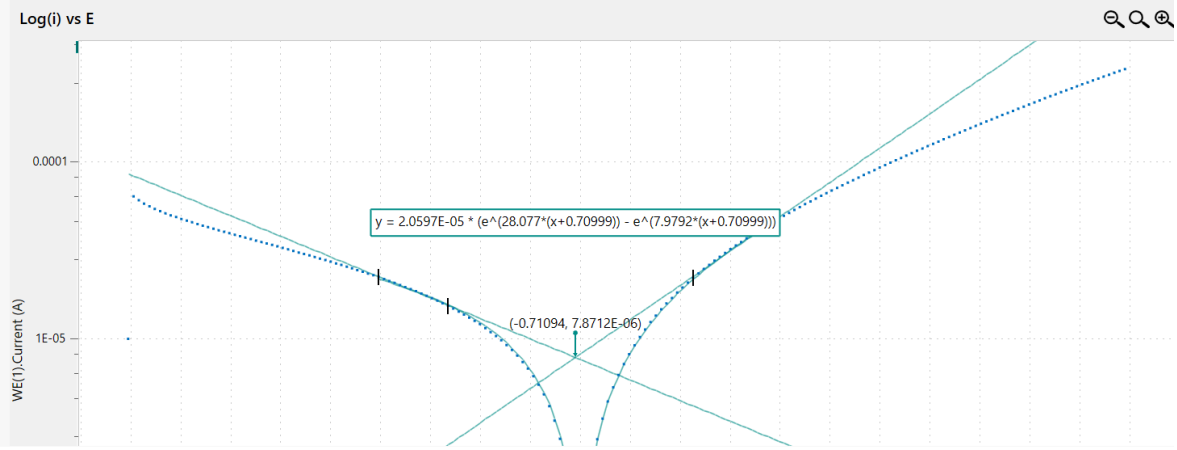

Figure 6.12: Tafel Plot of MS Grade 907 for 3 day

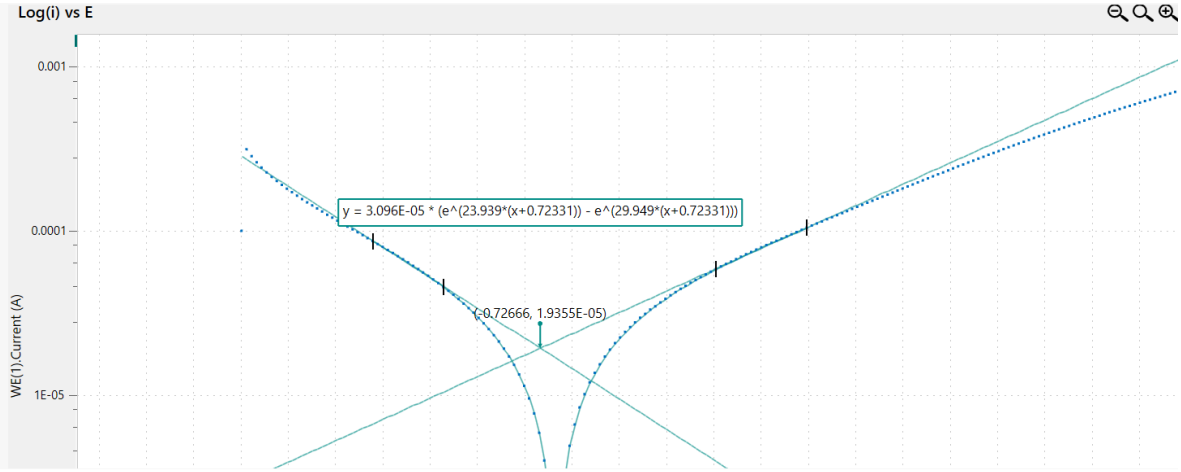

Figure 6.13: Tafel Plot of MS Grade 907 (Welded) for 3 day

6.4.4 Outcome of the Results

(i) **Welding Effects:** In both MS Grade A and MS Grade 907, the welded samples consistently exhibit higher corrosion rates (Icorr) across all three time points (0-day, 1-day, and 3-day). This indicates that the welding process weakens the corrosion resistance of the material, potentially due to microstructural changes or residual stresses induced during the welding process.

(ii) **Material Comparison**: MS Grade A demonstrates slightly better corrosion resistance across all time periods when compared to MS Grade 907, though the difference is not drastic. For MS Grade A, the unwelded sample shows the lowest corrosion rate and the least negative Ecorr, making it the best-performing sample overall.

(iii) **Time-Dependent Corrosion Trends:** The data reveals that the corrosion rate generally increases from 0-day to 1-day in all samples, indicating that the early exposure to the corrosive environment triggers a rapid corrosion process. By 3 days, the corrosion rates stabilize across all samples, suggesting that the material reaches a more stable corrosion state after prolonged exposure.

6.5 Summary

The experimental results align well with established knowledge about the corrosion behavior of marine-grade mild steels in seawater environments. The higher corrosion rates during the initial exposure period (0-day to 1-day) are consistent with expectations, as mild steel tends to exhibit more aggressive corrosion upon initial exposure to chloride-rich environments, such as the Bay of Bengal's seawater. The stabilization of corrosion rates by the 3rd day indicates that the material reaches a more stable corrosion state over time, which is typical as passive oxide films begin to form and slow the rate of corrosion.

The significant increase in corrosion rates for welded samples is also consistent with existing literature, which highlights how welding processes can introduce microstructural heterogeneities and residual stress, both of which can accelerate corrosion. The slightly better performance of MS Grade A compared to MS Grade 907 aligns with the expectation that lower-grade mild steels (like MS Grade A) tend to have slightly better corrosion resistance due to their simpler composition and fewer alloying elements that can create local galvanic cells. The findings from this study have direct implications for predicting the long-term performance of marine structures and vessels constructed with marine-grade mild steel in the Bay of Bengal environment.

CHAPTER SEVEN
CASE STUDY: STUDY OF SHELL EXPANSION REPORT OF THE SHIP MADE OF THE MATERIALS UNDER STUDY

7.1 Significance of the Study

A shell expansion drawing is an essential naval architectural drawing that provides a detailed layout of a ship's hull plates, organized according to their size, shape, and thickness. These drawings are essential during both the construction and maintenance phases of a vessel's lifecycle. During the docking period, the actual thickness of the hull plates is measured and the drawing is revised. The revised drawing is compared with the original shell expansion drawing. As such, any loss in thickness due to corrosion can be noted.

By studying the changes in plate thickness over time, it becomes possible to evaluate the severity of corrosion and identify specific areas where material degradation is most pronounced. Such data not only helps understand the impact of corrosion on the hull's structural health but also inform decisions regarding necessary repairs, plate replacement, or protective treatments. Moreover, by providing information on corrosion trends, this study aids in developing preventive strategies, ensuring that the ship remains seaworthy and compliant with classification society standards.

7.2 Shell Expansion Report for MS Grade-A

The ship discussed in the following case report was constructed from Grade-A material in 2011, with shell expansion reports compiled in both 2016 and 2020. BNS Bijoy is a vessel of the Bangladesh Navy, constructed with MS Grade A. The ship operates extensively in the Bay of Bengal. With a principal dimension of 81 meters in length and a beam of 11.5 meters, BNS Bijoy provides valuable real-world data on how these materials perform under prolonged exposure to seawater. This data is important for comparing with laboratory corrosion tests, helping to understand the corrosion rates and overall durability of marine-grade steel in actual sea conditions. Table 7.1 shows plate thickness data extracted from 3 docking periods's shell expansion report, for around 9 years duration:

Table 7.1: ‘A’ Grade Plate Thickness Comparison

Frame No	**Plate thick- 2011 (mm)**		**Plate thick-2016 (mm)**		**Plate thick-2020 (mm)**		**Strake**
	(P)	(S)	(P)	(S)	(P)	(S)	
0-6	16	16	15.6	15.8	15.6	15.7	A
	16	16	15.5	15.7	15.7	15.7	C
	9.5	9.5	9.5	9.5	9.4	9.3	E
	9.5	9.5	9.5	9.5	9.2	9.2	F
	9.5	9.5	9.5	9.5	9.5	9.5	G
	9.5	9.5	9.5	9.5	9.5	9.5	H
6-8	16	16	5.5	5.7	15.6	15.4	A
8-13	10	10	10	10	10.7	9.7	A
	10	10	10	9.8	9.8	9.7	C
13-22	14	14	14	14	13.6	13.6	A
	14	14	14	14	13.7	13.6	B
	10.5	10.5	10.5	10	10.1	10.1	C
	10.5	10.5	10.5	10.4	9.8	9.8	E
22-29	16	16	15.5	15.6	15.7	13.9	A
	16	16	15.5	15.6	13.7	13.5	B
	11.5	11.5	11.5	11	11.5	11.4	C
	11.5	11.5	11	11.5	11.3	11.4	D
29-37	19	19	19	19	18.4	18.4	A
	19	19	19	18.9	18.4	18.4	B
	16	16	15.5	16	15.7	15.6	C
	12	12	12	11.8	11.6	11.7	D
37-45	19	19	19	19	18.4	18.5	A
	19	19	19	19	18.3	18.7	B
	16	16	16	16	15.4	15.7	C
	12	12	12	11.7	11.8	11.8	D
45-55	19	19	19	18.6	18.3	18.5	A
	19	19	19	19	18.0	18.1	B
	16	16	16	16	15.6	15.6	C

Frame No	**Plate thick- 2011 (mm)**		**Plate thick-2016 (mm)**		**Plate thick-2020 (mm)**		**Strake**
	(P)	(S)	(P)	(S)	(P)	(S)	
	12	12	-	11.6	11.6	11.7	D
55-63	19	19	18.7	19	18.3	18.4	A
	19	19	18.8	19	18.3	18.4	B
	16	16	15.5	15.7	15.6	15.7	C
	12	12	12	11.5	11.7	11.5	D, E/12.5, 11.7, 11.6
63-71	19	19	18.7	19	18.3	18.5	A
	19	19	18.7	19	18.7	18.4	B
	16	16	15.5	16	15.6	15.5	C
	12	12	11.3	12	11.6	11.5	D
	12	12	11.6	11.6	11.6	11.7	E
71-78							A
	19	19	19	19	18.4	18.3	B
	16	16	15.7	15.7	15.2	15.7	C
	12	12	11.8	11.8	11.7	11.6	D
78-86	19	19	19	19	18.6	18.3	A
	16	16	15.8	15.7	15.6	15.7	B
	12	12	11.5	12	11.5	11.8	C
	12	12	11.5	12	11.5	11.7	E
86-94	19	19	11.5	19	18.2	18.3	A
	16	16	11.5	15.7	11.5	18.5	B
	12	12	11.5	19	11.4	11.6	C
	12	12	11.5	11.5	11.4	11.6	E
94-102	16	16	15.6	15.8	15.2	15.6	A
	16	16	15.7	15	15.6	15.4	B
	12	12	12	12	11.4	11.5	C
	11.5	11.5	11.5	11.5	11.4	11.3	E

Frame No	Plate thick- 2011 (mm)		Plate thick-2016 (mm)		Plate thick-2020 (mm)		Strake
	(P)	(S)	(P)	(S)	(P)	(S)	
102-114	14.5	14.5	14.5	14.5	12.4	12.3	A
	12	12	10.7	11.8	11.5	11.4	C
	10	10	10	10	9.5	9.6	E
114-122	9.5	9.5	9.4	9.4	9.3	9.3	A
	9.5	9.5	9.5	9.4	9.4	9.2	C

7.3 Shell Expansion Report Analysis for MS Grade-A

After averaging the report data, it was found that the average corrosion rate over 5 years (2016) is significantly higher than the average corrosion rate over 9 years (2020) on the port side. However, on the starboard side, the average corrosion rate over 5 years (2016) is slightly lower than the average corrosion rate over 9 years (2020). Furthermore, the difference in corrosion rates between the port and starboard sides is also significantly higher. (Figure 7.1)

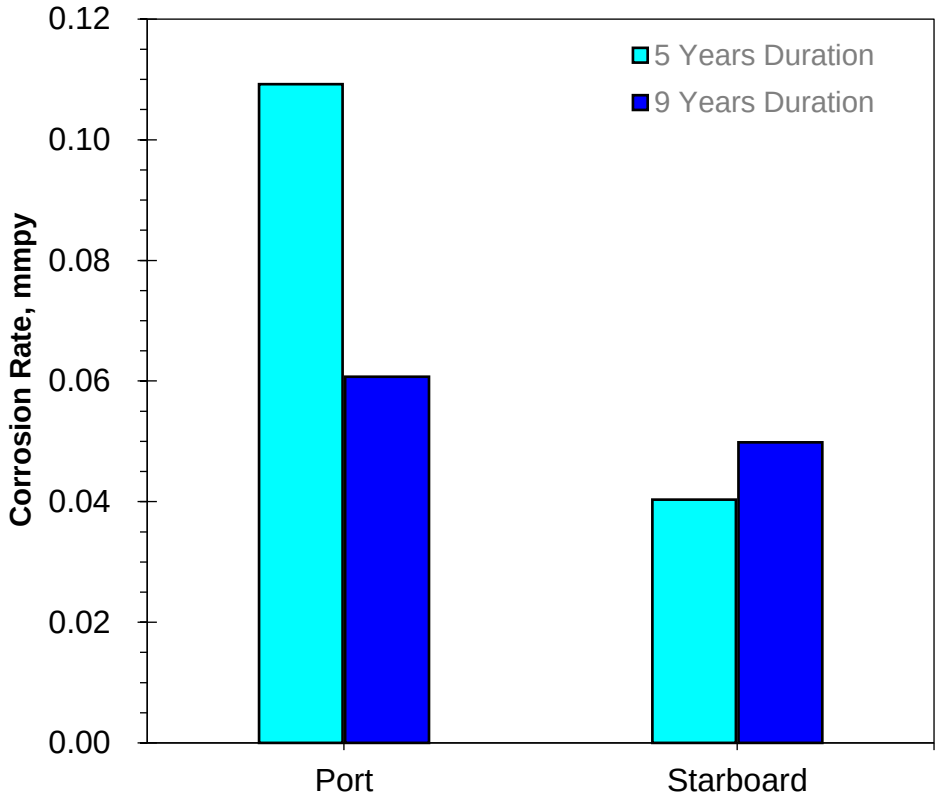

Figure 7.1: Shell expansion report analysis for Grade-A

7.4 Shell Expansion Report for MS Grade-907

The following case report is based on a ship constructed with Grade-907 material. The ship was built in 2011, and shell expansion reports were collected in 2016 (after five years) and 2020 (after nine years), which are shown in Table 7.2. BNS Nirmul, another vessel of the Bangladesh Navy, is built with MS Grade 907. The ship operates under the same environmental conditions in the Bay of Bengal, offering further data on the effects of marine corrosion. BNS Nirmul has a length of 64.2 meters and a beam of 9 meters, making it equally important source of data for corrosion studies. The structural performance data from this ship in the Bay of Bengal provides a practical comparison to the laboratory tests conducted on marine-grade steels, ensuring the lab results are applicable in real-world maritime conditions.

Table 7.2: ‘907’ Grade Plate Thickness Comparison

Frame No	**Plate thick- 2011 (mm)**		**Plate thick-2016 (mm)**		**Plate thick-2020 (mm)**		**Strake No**
	(P)	(S)	(P)	(S)	(P)	(S)	
1 to 8	10	10	9.9	9.8	9.9	9.8	K
	10	10	9.9	9.8	9.9	9.8	A
	10	10	9.9	9.85	9.9	9.85	C
	8	8	7.9	7.85	7.9	7.85	D
	8	8	7.85	7.85	7.85	7.85	E
8 to 16	10	10	9.9	9.8	9.9	9.8	K
	8	8	7.9	7.9	7.9	7.85	A
	8	8	7.85	7.85	7.85	7.85	C
	8	8	7.9	7.85	7.9	7.85	D
	8	8	7.85	7.85	7.9	7.85	E
16-26	10	10	9.9	9.9	9.9	9.9	K
	8	8	7.85	7.8	7.85	7.85	A
	8	8	7.85	7.85	7.8	7.85	C
	8	8	7.85	7.85	7.85	7.85	D
	8	8	7.85	7.85	7.8	7.85	E
26-37	10	10	9.9	9.85	9.9	9.85	K
	8	8	7.9	7.85	7.9	7.85	A
	8	8	7.85	7.85	7.85	7.85	C
	8	8	7.85	7.85	7.85	7.85	D
	8	8	7.85	7.85	7.85	7.85	E
37-48	10	10	9.9	9.8	9.9	9.8	K
	8	8	7.9	7.8	7.9	7.8	A
	8	8	7.9	7.8	7.9	7.8	C
	8	8	7.9	7.8	7.9	7.8	D

Frame No	**Plate thick- 2011 (mm)**		**Plate thick-2016 (mm)**		**Plate thick-2020 (mm)**		**Strake No**
	(P)	(S)	(P)	(S)	(P)	(S)	
	8	8	7.9	7.8	7.8	7.8	E
48-60	10	10	9.85	9.85	9.85	9.85	K
	7	7	6.85	6.85	6.85	6.85	A
	7	7	6.9	6.85	6.85	6.85	C
	7	7	6.9	6.85	6.85	6.85	D
	6	6	5.9	-	5.9	5.85	E
60-75	10	10	9.85	9.85	9.85	9.85	K
	7	7	6.9	6.85	6.9	6.85	A
	7	7	6.85	6.85	6.85	6.85	B
	7	7	6.85	6.85	6.85	6.85	C
	7	7	6.85	6.85	6.85	6.85	D
	6	6	5.85	5.9	5.85	5.9	E
75-87	10	10	9.9	9.8	9.9	9.85	K
	7	7	6.85	6.8	6.85	6.8	A
	7	7	6.9	6.85	6.9	6.85	B
	7	7	6.85	6.85	6.85	6.85	C
	7	7	6.9	6.85	6.85	6.85	D
	6	6	5.9	5.9	5.9	5.9	E
87-100	10	10	9.85	9.9	9.85	9.9	K
	7	7	6.9	6.8	6.85	6.85	A
	7	7	6.85	6.85	6.85	6.85	B
	7	7	6.85	6.85	6.85	6.85	C
	7	7	6.9	6.85	6.9	6.85	D
	6	6	5.9	5.9	5.9	5.85	E

Frame No	**Plate thick- 2011 (mm)**		**Plate thick-2016 (mm)**		**Plate thick-2020 (mm)**		**Strake No**
	(P)	(S)	(P)	(S)	(P)	(S)	
100-113	10	10	9.85	9.8	9.85	9.8	K
	7	7	6.85	6.8	6.85	6.85	A
	7	7	6.9	6.8	6.9	6.8	B
	7	7	6.9	6.85	6.9	6.85	C
	7	7	6.75	6.85	6.8	6.85	D
	6	6	5.85	5.85	5.85	5.85	E
113-122	10	10	9.85	9.85	9.85	9.85	K
	7	7	6.85	6.8	6.85	6.85	A
	7	7	6.85	6.8	6.85	6.85	B
	7	7	6.9	6.85	6.85	6.85	C
	7	7	6.9	6.85	6.85	6.85	D
	6	6	5.85	5.85	5.85	5.85	E
122-132	10	10	9.85	9.8	9.85	9.85	K
	7	7	6.9	6.9	6.9	6.9	A
	7	7	6.85	6.85	6.85	6.85	B
	7	7	6.85	6.85	6.85	6.85	C
	7	7	6.85	6.85	6.85	6.85	D
	6	6	5.85	5.85	5.85	5.85	E
132-141	10	10	9.9	9.9	9.9	9.9	K
	7	7	6.9	6.85	6.85	6.85	A
	7	7	6.85	6.85	6.85	6.85	B
	7	7	6.9	6.85	6.9	6.85	C
	7	7	6.85	6.85	6.85	6.85	D
	6	6	5.85	5.85	5.85	5.85	E
141-151	10	10	9.9	9.9	9.9	9.85	K

Frame No	Plate thick- 2011 (mm)		Plate thick-2016 (mm)		Plate thick-2020 (mm)		Strake No
	(P)	(S)	(P)	(S)	(P)	(S)	
	7	7	6.9	6.85	6.85	6.85	A
	7	7	6.9	6.8	6.9	6.85	B
	7	7	6.9	6.85	6.85	6.85	C
	7	7	6.85	6.85	6.85	6.85	D
	7	7	6.85	6.9	6.85	6.9	E
151-160	10	10	9.9	9.85	9.85	9.9	K
	10	10	9.8	9.85	9.8	9.85	A
	10	10	9.85	9.85	9.85	9.85	B
	10	10	9.9	9.8	9.85	9.85	C
	8	8	7.85	7.85	7.85	7.85	D
	8	8	7.85	8	7.85	7.9	E
160-170	10	10	9.85	9.85	9.85	9.85	K
	10	10	9.8	9.85	9.85	9.85	A
	10	10	9.9	9.9	9.9	9.85	B
	10	10	9.85	9.85	9.85	9.85	C
	8	8	7.85	7.85	7.85	7.85	D
	8	8	7.85	7.9	7.85	7.85	E

7.5 Shell Expansion Report Analysis for MS Grade 907

After analyzing the report, it was found that the average corrosion rate after 5 years (2016) is significantly higher than the average corrosion rate after 9 years (2020) for both the port and starboard sides. The difference in average corrosion rates between the port and starboard sides is minimal, with the rates being nearly equal. (Figure 7.2)

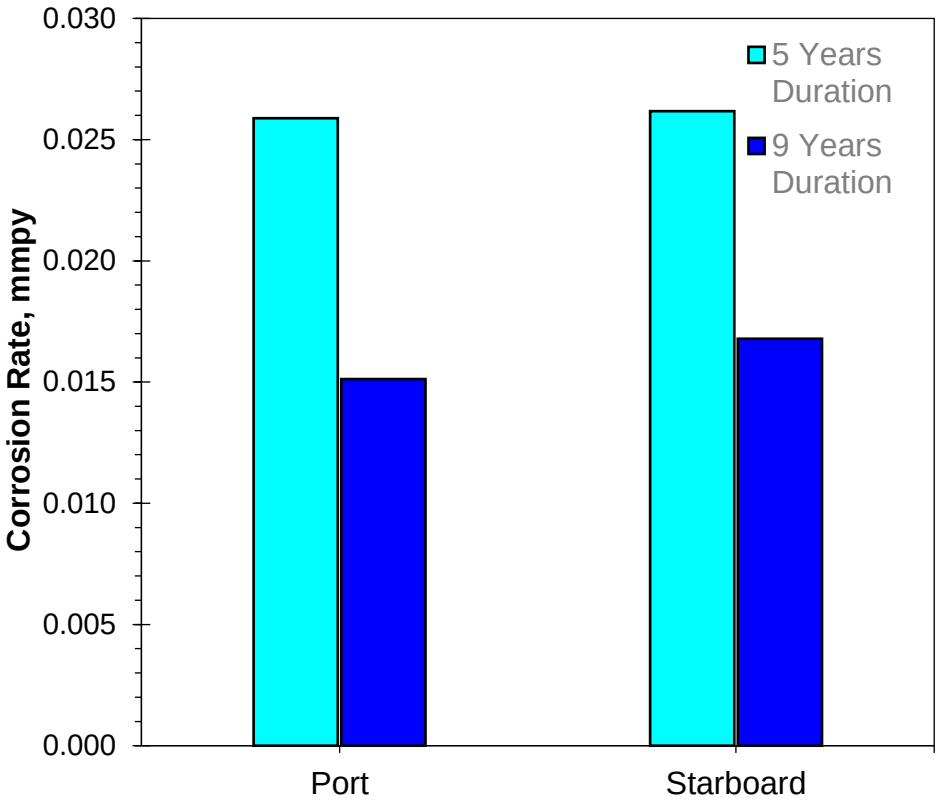

Figure 7.2 Shell expansion report analysis for Grade-907

7.6 Comparison of the Two Ships' Findings

The corrosion behavior of the two ships constructed from Mild Steel (MS) Grade A and MS Grade 907 materials under the same environmental conditions has shown noticeable differences. According to the chemical composition data, MS Grade 907 contains a higher proportion of alloying elements such as Si, Mn, Ta, and Mo compared to MS Grade A. These elements, particularly manganese (Mn), silicon (Si), and molybdenum (Mo), are known to enhance the corrosion resistance of steel, which is reflected in the lower overall corrosion rates for MS Grade 907 compared to MS Grade A. This result is in agreement with lab based static gravimetric test results.

The shell expansion report for MS Grade A indicates a significantly higher corrosion rate after five years, particularly on the port side. Although this rate decreases after nine years, it remains elevated compared to that of MS Grade 907. In contrast, MS Grade 907 displays a more stable corrosion pattern, with only a slight decrease in corrosion rate over the same period.

Remarkably, the difference in corrosion rates between the port and starboard sides is minimal for MS Grade 907, suggesting uniform corrosion behavior across both sides. For MS Grade A, while the port side shows a higher initial corrosion rate, the rates between both sides converge over time, indicating that while the material undergoes a higher initial corrosion rate, it stabilizes somewhat with age.

The asymmetric corrosion observed between the port and starboard sides likely resulted from localized environmental conditions at the berthing area. The Chittagong and Mongla Port are near cement and chemical factories that discharge particles and potentially corrosive chemicals into the berthing area, which could increase sediment and aggressive ions, accelerating corrosion.

In summary, MS Grade 907's increased corrosion resistance, attributed to its higher content of alloying elements, makes it a more suitable choice for ships operating in highly corrosive marine environments, such as the Bay of Bengal. The significant difference in corrosion rates between the two grades of mild steel highlights the importance of selecting the appropriate material to enhance the longevity and durability of marine vessels.

CHAPTER EIGHT
CONCLUSION

8.1 General

The primary objective of the research was to investigate the corrosion rate (CR) of marine-grade steels in the Bay of Bengal water environment. Additionally, the study evaluated the effect of arc welding joints on the corrosion resistance of MS Grade A and MS Grade 907, and it also aimed to analyze the physical and mechanical behavior changes in marine-grade mild steels after prolonged immersion in seawater.

To reach these objectives, this research investigated the corrosion behavior of marine-grade mild steels exposed to the Bay of Bengal environment. Mild steels of Grades A and 907, both seamless and welded, were evaluated under varying environmental conditions. The study integrated gravimetric, electrochemical tests and mechnical analyses to comprehensively assess the corrosion performance, surface degradation and mechanical properties of the selected materials.

8.2 Summary of Major Findings

From the experimental analysis and observations, the following key findings were drawn:

(i) The average corrosion rate at dynamic condition (with a relative velocity of about 2 m/s) is found to be four times higher than that the stagnant condition. This demonstrates the substantial influence of environmental motion on accelerating corrosion rates.

(ii) Among the selected locations of Bay of Bengal, seawater from St. Martin’s Anchorage exhibited the highest corrosive behavior at stagnant water condition in the laboratory test. The behavior is primarily attributed to elevated salinity and dissolved oxygen levels in that location.

(iii) In the static gravimetric analysis, MS Grade 907 demonstrated a lower corrosion rate than MS Grade A, indicating better resistance to corrosion. This indicates that the lower carbon and manganese levels in MS Grade A's composition directly reduce its corrosion resistance.

(iv) Corrosion data of real ships operating in Bay of Bengal water for the duration of 9 years have showed that the corrosion rate was higher in the first 5 years than the later part. Besides, MS Grade-A has been found to be more prone to corrosion than MS Grade-907. This data verifies the test result of the gravimetric analysis.

(v) In pH varied analysis, pH1 has been found to be the highest corrosive environment and pH13 the lowest for all the samples. This highlights the significant effect of pH on corrosion rates.

(vi) In all environments, corrosion rates of all four types of materials have been found to be the highest at the initial attack after immersion, and gradually, the rates are getting decreased to a steady value. This suggests a time-dependent stabilization of corrosion rates.

(vii) On-site corrosion tests conducted in deep sea and coastal region of Bay of Bengal have revealed that the corrosion rate is 1.8 times higher in the deep sea than that of inner region.

(viii) In the laboratory static gravimetric analysis, Welded samples exhibited higher corrosion rates than seamless samples, reflecting the increased vulnerability introduced by welding processes. The localized crystalline modifications during welding may contribute to the observed corrosion behavior.

(ix) Localized corrosion investigated through the potentiostatic polarization method has indicated that welded samples of both steel grades are more corrosive than the seamless samples. So, the welding lines of ship need more attention on the aspect of protective measures. The behavior observed in the potentiostatic polarization method aligns with the results of the laboratory-based static gravimetric analysis.

(x) Both micro-Vickers and Brinell hardness tests have affirmed that the hardness is decreased after the corrosion. Post-corrosion tests confirmed a reduction in hardness across all samples, reflecting the mechanical degradation caused by exposure to the marine environment.

(xi) Microstructures observed by OEM and SEM have clearly noticed the crystalline change due to corrosion. EDX test results of the samples concur with the change by

showing higher oxygen and carbon content on the surfaces after corrosion. Corrosion-induced changes in microstructure were evident from SEM and OEM observations, with EDX analysis confirming increased oxygen and carbon levels on the surfaces.in corroded samples confirm the role of elemental composition in material degradation.

8.3 Significance of the Results

This study's findings shed light on the challenges of marine-grade mild steel corrosion in the Bay of Bengal. The faster corrosion in dynamic, highly saline, and oxygen-rich waters like St. Martin's Anchorage emphasizes the need for environment-specific design and maintenance. Additionally, the improved hardness of welded samples highlights the importance of optimized welding techniques for better performance in corrosive conditions. The analysis of mechanical and microstructural changes due to corrosion, such as reduced hardness and surface alterations, helps us choose and treat materials for long-term durability. These insights can lead to more cost-effective and sustainable marine infrastructure solutions in similar environments.

8.4 Implications for Practical Applications

The findings of this study offer valuable guidance for practical applications in marine environments. These implications highlight opportunities to enhance material performance, optimize maintenance strategies, and improve the design of corrosion-resistant marine structures.The possible areas of implications for practical applications are appended below:

(i) Material Selection and Optimization: Insights into the microstructural changes induced by corrosion can guide the development of advanced steel alloys with superior corrosion resistance and mechanical properties.

(ii) Improved Welding Techniques and Joint Design: Optimized Welding Parameters: The study highlights the critical role of welding parameters in influencing the corrosion behavior of joints. By carefully controlling welding techniques including the selection of suitable welding rods, it is possible to minimize reduce welding induced weaknesses observed in this study.

(iii) Enhanced Maintenance and Protection Strategies: Predictive Maintenance: The insights gained from this research can be used to develop predictive maintenance models that anticipate and prevent corrosion-related failures. By monitoring critical parameters such as corrosion rates and environmental conditions, maintenance schedules can be optimized to minimize downtime and costs.

(iv) Advanced Corrosion Protection Systems: The findings support the development of advanced corrosion protection systems, such as high-performance coatings and cathodic protection techniques, that are tailored to counter the corrosion trend observed in this study.

8.5 Limitations of the Thesis

Acknowledging the limitations is crucial for research studies. The following limitations were identified during this research:

(i) This study focused on two grades of mild steel (MS Grade A and MS Grade 907) commonly used in marine applications. While these materials provide valuable insights, the inclusion of additional grades could further broaden the understanding of corrosion behavior under similar conditions.

(ii) Dynamic conditions were simulated using a fixed flow rate to maintain experimental consistency. While this approach effectively analyzed flow-induced corrosion, variable flow rates typical of natural marine environments could provide a more comprehensive understanding of the effect of environmental motion.

(iii) The research was limited to specific locations within the Bay of Bengal, which were selected based on their environmental significance. Testing seawater from additional regions could offer a more representative understanding of corrosion behavior across diverse marine conditions.

(iv) The study primarily focused on hardness changes and ultimate tensile strength as key indicators of mechanical degradation. While this provides critical insights, analyzing other properties such as fatigue resistance or elongation could offer a more complete picture of the mechanical impact of corrosion.

(v) While natural environment tests were conducted to reflect real-world conditions, weight measurements could only be taken before and after immersion due to the unavailability of precision weighing equipment on-site. However, laboratory-based gravimetric tests served as the primary focus of this study, providing detailed and consistent measurements of corrosion behavior.

(vi) The UTS for post-corrosion samples was obtained by converting Brinell Hardness Numbers (BHN) using established correlation factors, rather than conducting direct tensile strength tests. This approach ensured consistency while addressing the dimensional constraints of ASTM guidelines. However, direct UTS testing could provide more precise results and eliminate potential uncertainties associated with conversion factors.

(vii) During hardness testing of the corroded samples, the cleaning process followed ASTM guidelines, which involved removing only the top corroded layer. While this method ensured standardization, performing hardness tests after completely removing all corrosion products could provide additional insights into the material's true mechanical behavior.

(viii) The study did not account for the influence of temperature on corrosion and mechanical properties. Incorporating temperature as a variable in future tests could help establish a more comprehensive understanding of environmental effects on corrosion behavior.

(ix) In laboratory tests lasting up to 48 days, the test water was not replaced but used continuously for the entire period. Although this approach maintained experimental consistency, periodic replacement of water could better replicate natural marine conditions

(x) The study evaluated welded joints using a single type of welding rod, without exploring the effects of varying welding rod materials or compositions. Investigating the influence of different welding rods could provide a deeper understanding of how welding practices affect corrosion resistance and mechanical properties.

8.6 Future Study

Future research can expand upon the findings of this study by addressing its limitations and exploring new areas. One important direction is the inclusion of additional grades of mild steel and other marine-grade materials to broaden the understanding of corrosion behavior and improve material selection for diverse marine applications. Expanding the geographical scope to include seawater from more regions of the Bay of Bengal and other global marine environments would also capture regional variations in corrosion rates. Additionally, investigating variable flow rates in dynamic conditions could better replicate natural fluctuations and provide a deeper understanding of how environmental motion affects material performance.

Further studies could also focus on mechanical properties beyond hardness and ultimate tensile strength. Including analyses of fatigue resistance, elongation, and fracture toughness would provide a more complete picture of the mechanical impact of corrosion on marine-grade mild steels. For natural environment tests, incorporating more frequent weight measurements during immersion would increase the accuracy of corrosion rate calculations and improve the understanding of material degradation over time. Additionally, performing direct tensile strength tests on post-corrosion samples, instead of relying on conversion factors, would yield more precise data and reduce potential uncertainties.

Temperature, as a critical factor influencing corrosion, warrants further investigation to understand its effects on marine environments. Similarly, future studies could enhance laboratory tests by periodically replacing test water to simulate the replenishment of dissolved oxygen and salinity in real-world conditions. Conducting hardness tests after completely removing all corrosion products would provide clearer insights into the intrinsic mechanical properties of corroded samples. By addressing these areas, future research can build on the findings of this study to advance more durable and cost-effective solutions for marine infrastructure.

REFERENCES

Abbas., M., Simms, N. J., Sumner, J., Sarfaraz S. A., and Malik, O. A. K. (2019), Evaluation of the effects of highly saline and warm seawaters on corrosivity of marine assets, Int Conference EUROCORR 2019.

Adetoro, K. (2011). Effect of environment on the mechanical properties of mild steel. ARPN Journal of Science and Technology, 3(9), pp. 915-918.

Alcántara, J., Fuente, D., Chico, B., Simancas, J., Díaz, I. and Morcillo, M. (2017) Marine atmospheric corrosion of carbon steel: a review. J. Materials, 10(4), 406.

Al-Moubaraki, A. H., Al-Judaibi, A. and Asiri, M. (2015), Corrosion of C-steel in the Red Sea: effect of immersion time and inhibitor concentration. Int. J. Electrochem. Sci., 10, pp 4252-4278.

ASM. (1987), ASM metals handbook, Vol. 13: Corrosion (9th ed.). ASM International.

Chuka, C. E., Betancourt Odio, J. L. C., Chukwuneke, J. E., & Sinebe, J. E. (2014), Investigation of the effect of corrosion on mild steel in five different environments. International Journal of Scientific & Technology Research, 3, pp. 306-310.

Dorothy, R. and Thankappan, S. (2021), Corrosion resistance of mild steel (hull plate) in sea water in the presence of a coating of an oil extract of plant materials, International Journal of Corrosion and Scale Inhibition, 10(2), pp 676-699.

Durodola, B. M., Olugbuyiro, J. A. O., Moshood, S. A., Fayomi, O. S. and Popoola, A. P. I. (2011), Study of influence of zinc plated mild steel deterioration in seawater environment. Int. J. Electrochem. Sci., 6, pp 5605-5616.

Dyczko, A. (2023), Production management system in a modern coal and coke company based on the demand and quality of the exploited raw material in the aspect of building a service-oriented architecture. Journal of Sustainable Mining, 22(1), pp. 2-19.

Eddy, N. O., Odoemelam, S. A. and Mbaba, A. N. (2008), Inhibition of the corrosion of mild steel in HCl by sparfloxacin, African Journal of Pure and Applied Chemistry Vol. 2 (12), pp. 132-138.

Fink, F. W. (1960), Corrosion of Metals in Sea Water. PB 171344, Battelle Memorial Institute, Columbus, OH.

Fujiwara, K., et al. (2020), Corrosion Behavior of Carbon Steel Piping in Flowing Diluted Seawater. Corrosion, 77(1), pp. 62-71.

Hao, X., Wang, C., Guo, S., Ma, J., Chen, H., Zhao, X. (2023), The microstructure and corrosion behavior of Cr-containing ferrite-pearlite steels in an acidic environment. J. Anti-Corrosion Methods and Materials, 70(4), pp 218-226.

Hillstrom, K. and Hillstrom, L. C. (2005), Industrial revolution in america: iron and steel, ABC-CLIO, Santa Barbara, California , USA.

Khan, S. A. R., Hossain, M. A., Nur, M., & Kaiser, M. (2021), Electrochemical corrosion properties of ternary Al and quaternary Zr added bell metal in 0.1M NaCl solution, Journal of Mechanical Engineering Science and Technology, 5(1), pp 1-16.

Larrabee, C. P. (1958), Corrosion-resistant experimental steels for marine applications. Corrosion, 14(11), pp. 21-24.

Li, Q. S., Luo, S. Z., Xing, X. T., et al. (2019), Effect of deep sea pressures on the corrosion behavior of x65 steel in the artificial seawater. Acta Metall. Sin. (Engl. Lett.), 32, pp. 972-980.

Li, Y. and Li, Y. (2000), Effect of different offshore seabed sediment on steel corrosion. J. Materials and Corrosion, 51(8), pp 570-573.

Li, Z., Long, Z., Lei, S., Liu, X., Li, Y., Zhang, W., et al. (2022), Evaluating the corrosion resistance of marine steels under different exposure environments via machine learning. J. Physica Scripta, 98(1), 015402.

Malik, A. U., Ahmda, S., Andijani, I., Al-Fouzan, S., (1999) Corrosion behavior of steels in Gulf Seawater environment, J. Desalination, 123(2-3), pp 205-213.

Natesan, M., Selvaraj, S., Manickam, T. and Venkatachari, G. (2008), Corrosion behavior of metals and alloys in marine-industrial environment. J. Science and technology of advanced materials, 9(4), pp. 045002-045002.

Oluwaseun, A. A. and Ibitoye, S. A. (2015), Effect of induced stress on the corrosion rate of medium Carbon Steel in saline environment. Journal of Chemical Engineering and Materials Science, 6(4), pp 52-59.

Ong, S. T., Potty, N. S. and Liew, M. S. (2012), Marine corrosion of mild steel at Lumut, Perak. AIP conference proceedings, pp 96–102.

Okpaga, D. M. (2021), Investigating the inhibitive characteristics of Moringa Oleifera on the corrosion of mild steel, International Journal for Research in Applied Science and Engineering Technology, 9, pp. 595-602.

Paul, S., (2010) Estimation of corrosion rate of mild steel in sea water and application of genetic algorithms to find minimum corrosion rate, J. The Canadian Met. And Mat. Sc., 49(1), pp 99-106.

Priyotomo, G., Nuraini, L., and Prifiharni , S., (2019) Corrosion behavior of mild steels in seawater from Karangsong & Eretan of West Java Region, Indonesia, J. of Mar. Sc. and Tech. 11(2), pp 184-191.

Rahman, M. M., Prova, M., Halim, M., & Ahmed, S. (2022). Investigation of Arc Welding Joining Effects on Tensile Behavior of Marine Grade-A Mild Steel, Conference: International Conference on Mechanical, Manufacturing and Process Engineering (ICMMPE 2022), Bangladesh, pid 5710.

Rahman, M. M., Ahmed, S. R. and Kaiser, M. S. (2022), Corrosion behavior of work hardened SnPb-solder affected copper in the Bay of Bengal water environment. J. Advances in Materials Science and Engineering, 2022 (7) pp 1-14.

Rahman, M. M., Ahmed, S. R. and Kaiser, M. S. (2020a), Corrosion behavior of work hardened commercial copper alloys in the Bay of Bengal water environment, the 6th ICMIEE proceedings.

Rahman, M. M., Ahmed, S. R. and Kaiser, M.S. (2020b), Corrosion Behavior of Copper Based Heat Exchanger Tube in Waters of Bangladesh Region at Varied Temperature and Flow Velocity. MIST Journal (DHAKA), 8(2), pp 15-23.

Rajendran, D., Thankappan, S., Rajendran, S., Al-Hashem, A., Lačnjevac, Č., & Singh, G. (2022), Inhibition of corrosion of mild steel hull plates immersed in natural sea water

by sandalwood oil extract of some natural products. Zastita Materijala, 63, pp. 23-36.

Sarma, V., Krishna, M., Rao, V., Viswanadham, R., Kumar, N., Kumari, T., et al (2012), Sources and sinks of CO_2 in the west coast of Bay of Bengal. J. Tellus B, 64(1), 10961.

Sawant S. S., Venkat, K. and Wagh, A. B. (1993), Corrosion of metals and alloys in the coastal and deep waters of the Arabian Sea and the Bay of Bengal, Indian J. of Tech., 31, pp 862-866.

Shikshak, A. A. A., Mansour A. A. and Taher, A. (2015), Effect of flow velocity of sea water on corrosion rate of low carbon steel, J. Applied Mechanics and Materials, 799-800, pp 232-236.

Sundjono, S., Priyotomo, G., Nuraini, L., and Prifiharni, S. (2018), Corrosion behavior of mild steel in seawater from northern coast of Java and Southern Coast of Bali, Indonesia. J. of Engineering and Technological Sciences, 49(6), pp 770-784.

Świątkowski, A., Kuśmierek, E., Kuśmierek, K., & Błażewicz, S. (2024), The influence of thermal treatment of activated carbon on its electrochemical, corrosion, and adsorption characteristics. Molecules, 29(20), pp. 4930.

Usman, N. A., Tukur, U. M., and Usman, B., (2019) Comparative study on the corrosion behavior of mild steel in effluents, sea and fresh water, J. of Pure and Applied Sc., 12(1), pp 280-284

Valdez, B., Hernandez, J. R., Eliezer, A., Wiener, M. S., Ramos R. and Salinas, R., (2016), Corrosion assessment of infrastructure assets in coastal seas, J. Mar. Eng. & Tech., 15(3), pp 124-134.

Venkatesh, B., Shiva, M., Reddy, C. A. K., Hrishikesh, M., & Chaitnaya, U. (2022), Corrosive behavior of 440C and M50 steels for marine applications. Proceedings Aistsse Conference 2648(1), pp. 030010.

Vinayachandran, P., Shankar, D., Vernekar, S., Sandeep, K., Amol, P., Neema, C.,et al. (2013), A summer monsoon pump to keep the bay of bengal salty. J. Geophysical Research Letters, 40(9), pp 1777-1782.

Wan Nik, W. B. Z., Rahman, F. M. M., & Rosliza, R. (2011), Corrosion behavior of mild steel in seawater from two different sites of Kuala Terengganu coastal area, International Journal of Basic & Applied Sciences, 11(6), pp 75-80.

Warren, K. (1998), Steel, Ships and Men: Cammell Laird, 1824–1993, Liverpool University Press, Liverpool, UK.

Yuan, J., Li, P., Zhang, H., Yin, S. and Xu, M. (2024), Electrochemical characteristics and corrosion mechanisms of high-strength corrosion-resistant steel reinforcement under simulated service conditions. J. Metals, 14(8), pp. 876.

Zhu, X., Huang, G., Lin, L., and Liu, D. (2008), Long term corrosion characteristics of metallic materials in marine environments. J. of Corrosion Processes and Corrosion Control, 43(4), pp 328-334.